UNIVERSITY OF GAZİANTEP
GRADUATE SCHOOL OF
NATURAL & APPLIED SCIENCES

IMPROVEMENT OF BACKHOE-LOADER BACK AND FRONT ARMS

M. Sc. THESIS
IN
MECHANICAL ENGINEERING

BY
EYÜP YETER
DECEMBER 2009

Improvement of Backhoe-Loader Back and Front Arms

M.Sc. Thesis
in
Mechanical Engineering
University of Gaziantep

Supervisor
Assist. Prof. Dr.Ahmet ERKLİĞ

by

EYÜP YETER

December 2009

T.C.
UNIVERSITY OF GAZİANTEP
GRADUATE SCHOOL OF
NATURAL & APPLIED SCIENCES
MECHANICAL ENGINEERING

Name of the thesis: Improvement of Backhoe-Loader Back and Front Arms
Name of the student: Eyüp YETER
Exam date: 12.01.2010

Approval of the Graduate School of Natural and Applied Sciences

Prof. Dr Ramazan KOÇ

Director

I certify that this thesis satisfies all the requirements as a thesis for the degree of Master of Science.

Prof. Dr. Sedat BAYSEÇ

Head of Department

This is to certify that we have read this thesis and that in our opinion it is fully adequate, in scope and quality, as a thesis for the degree of Master of Science.

Assist. Prof. Dr. Ahmet ERKLİĞ
Supervisor

Examining Committee Members   signature

1. Prof. Dr. İ. Hüseyin FİLİZ   ————————————

2. Prof. Dr. İbrahim H. GÜZELBEY   ————————————

3. Assoc. Prof. Dr. Bahattin KANBER   ————————————

4. Assist. Prof. Dr. Abdulkadir ÇEVİK   ————————————

5. Assist. Prof. Dr. Ahmet ERKLİĞ   ————————————

ABSTRACT

IMPROVEMENT OF BACKHOE-LOADER BACK AND FRONT ARMS

YETER, Eyüp
M. Sc. in Mechanical Eng.
Supervisor: Assist. Prof. Dr. Ahmet ERKLİĞ
December 2009, 95 pages

This study aims to analyze back and front arms of Backhoe-Loader and improve them with respect to analysis results. Firstly, reaction forces of arm joints calculated according to maximum piston forces. Then, finite element analysis was performed according to the calculated maximum loads and symmetrical and unsymmetrical boundary conditions. Reinforcements were performed in the zones of stress intensity to reduce stress and again finite element analysis was performed. ANSYS Workbench finite element package program is used in finite element analysis.

ÖZET

KAZICI-YÜKLEYICININ ARKA VE ÖN KOLLARININ TASARIMININ IYILEŞTIRILMESI

YETER, Eyüp
Yüksek Lisans Tezi, Makine Müh. Bölümü
Tez Yöneticisi: Assist. Prof. Dr. Ahmet ERKLİĞ
Aralık 2009, 95 sayfa

Bu çalışma Kazıcı-Yükleyicinin ön ve arka kollarının analizleri ve analiz sonuçlarına göre güçlendirilmesi hedeflenmektedir. Öncelikle maksimum piston gücüne göre kolların bağlantı noktalarında tepki kuvvetleri hesaplandı. Daha sonra hesaplanan maksimum yüklere ve simetri ve simetri olmayan sınır şartlarına göre sonlu eleman analizleri gerçekleştirildi. Gerilim yoğunluğu olan bölgelerde gerilim değerlerini azaltacak şekilde güçlendirmeler yapıldı ve tekrar sonlu eleman analizleri gerçekleştirildi. Sonlu eleman analizleri ANSYS Workbench paket programı ile yapıldı.

Anahtar Kelimeler: Kazıcı-Yükleyici, Sonlu eleman metodu, ANSYS Workbench.

ACKNOWLEDGMENTS

CONTENTS page

LIST OF FIGURES   Page

LIST OF TABLES **Page**

CHAPTER 1

INTRODUCTION

Backhoe loader is a mobile machine which *digs*, *elevates*, *loads* and *swings* materials by the action of its mechanism consists of backhoe and loader parts as shown in figure 1.1.

Backhoe parts are *boom, arm, backhoe bucket* and loader parts are *loader arm and loader bucket*. The *most important* parts for backhoe and loader parts are *hydraulic cylinders*.

Backhoe loader is generally preferred in intercity applications due to its small size and multi functionality compared to other heavy duty machines. Due to its heavy working conditions its parts exposed to high load values and wear. The parts of the machine and machine itself must work safely under the worst conditions.

Backhoe loader parts like boom, arm, and loader arm limit the life expectancy of the backhoe loader. Therefore, backhoe loader parts must be strong enough to cope with caustic working conditions. It can be concluded that, strength analysis is an important step in the design of backhoe loader parts.
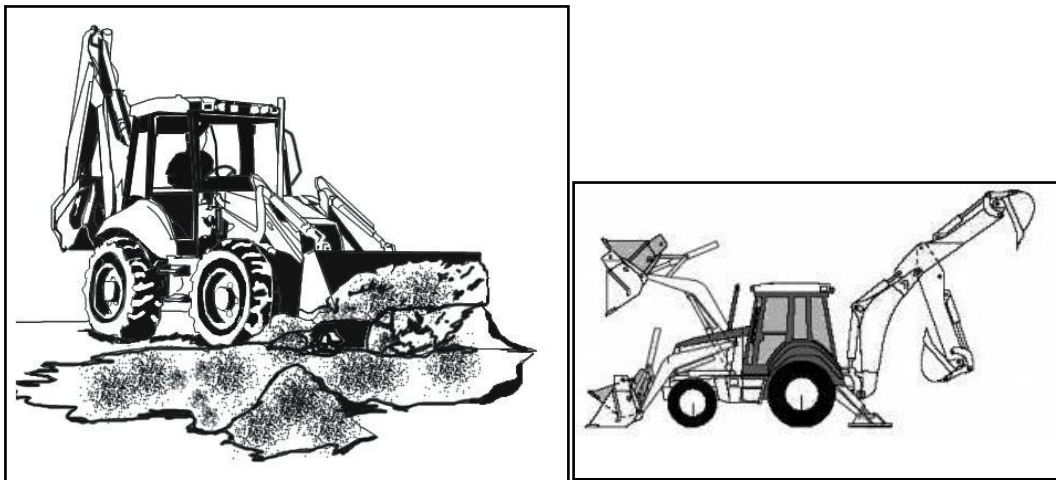
Figure 1.1 Backhoe-loader machine.

Finite element analysis (FEA) is the most powerful technique in strength calculations of the structures working under known load and boundary conditions. Especially in automotive sector, using finite element analysis methods and programs help us to do more reliable designs in very short time. These analyses show us the critical points of our design early and so we can improve our design before doing prototypes.

This study aims to improve backhoe- loaders back and front arms. To achieve this backhoe-loader back arm and front arm have been analyzed with maximum load and boundary conditions. Solid geometries of back and front arms which have been designed by CATIA CAD have used to do FEA.

The front arm has been analyzed with four different conditions which are namely, symmetrical and unsymmetrical loading while loader cylinder is active and symmetrical and unsymmetrical loading while bucket cylinder is active. The back arm has been analyzed with two different conditions which are namely, loading while arm cylinder is active and loading while bucket cylinder is active.

The analysis has been carried out using ANSYS Workbench finite element analysis program. After design of solid geometries, they are imported to ANSYS Workbench and then necessary parameters such as material properties, boundary conditions, connections and act. are entered to the program. After solutions are done maximum stress locations are determined and if necessary some improvements are done both for back and front arms. Finally safety factors for old geometries and improved geometries are compared.

After introduction given in this chapter, the thesis continue with a literature-review for FEA in chapter 2 .Second concepts of FEA and ANSYS Workbench is given in chapter 3. Then Static force analysis and FEA of back arm is given in chapter 4 and static force analysis and FEA of front arm is given in chapter 5. Finally conclusions are summarized in chapter 6.

CHAPTER 2

LITERATURE SURVEY

2.1. Introduction

In this chapter, a brief literature survey which is related to finite element analysis of working machine (excavator, backhoe loader, etc.) is presented.

2.2 Some Studies on Finite Element Analysis

Finite element analysis (FEA) has become common in recent years, and is now the basis of a multibillion dollar per year industry. Numerical solutions to even very complicated stress problems can now be obtained routinely using FEA, and the method is so important that even introductory treatments of Mechanics of Materials.

Özer [1] studied strength analysis of boom-stick groups (Backhoe-loader back arms) having different digging reach by using finite element analysis method. A correlation between shape parameters of boom-stick groups having different digging reach is found with respect to analysis results. By using this correlation, boom-stick groups having different digging reach designed with Solid works and finite element analyses were conducted by ANSYS Workbench.

Yener [2] designed a computer interface, which links the user to commercial Finite Element Analysis (FEA) program, MSC. Marc -Mentat to make automatic FE analysis of an excavator boom by using DELPHI as platform. This interface was capable of creating finite element model of an excavator boom by using a set of design parameters. Then the finite element analysis of the excavator boom was performed and optimum shapes for an excavator boom for different loading conditions with respect to maximum stress are searched. As a result of this study optimum boom shapes for the analyzed excavator was found.

Dağ et al. [3] used finite element analysis to develop three dimensional parametric finite element models for the boom of a 22 ton capacity HMK220LC-2 model excavator which is currently being manufactured by HIDROMEK Company. It is assumed that the excavator is subjected to constant amplitude variable loading and the effects of changes in the boom design on fatigue life is examined using the endurance limit and Goodman approaches.

Çetin [4] designed a demolition boom for hydraulic excavator with operation weight of 30 ton. With this construction a higher reach of capacity was gained. Firstly the mechanism design was performed to determine the basic link dimensions. In the second step the structural shape of the boom was estimated to perform static stress analysis. The EXCEL program was chosen due to the ease of repetitive calculations and applying the changes in structure parameters. The demolition boom was modeled by PRO-ENGINEER, and consequently the model was analyzed by using MSC. Marc- Mentat,a FEM program. According to the FEA results the model was revised.

Smolnicki et al. [5] applied the FEA for the rotation joint of the single-bucket excavator body consists of a torque slewing bearing subjected to a compound set of loads to obtain a solution, along with a description of how an appropriate model is to be built. They also discussed the sample results.

Bosnjak et al. [6] discussed the results of the investigation of occurrence of cracks in the structure of bucket wheel excavator (BWE) slewing platform, the repair procedure and the reconstruction of the slewing platform. In their study results of the FEA pointed out the pronounced stress concentration in the zones of crack occurrence. The values of calculated stresses in the said zones exceed the yield stress of the material. The design solution for the slewing platform reconstruction was chosen based on the comparative analysis of stress–strain states of alternative solutions. Experimental analysis of the stress state of the reconstructed slewing platform in regular working conditions confirmed the validity of the reconstruction design.

Karamolla [7] studied analysis of displacements and vibrations versus the applied loads of tower cranes were considered by means of FEM. Beam elements, which were consisted of tower cranes, were used for the formulation of the finite element method to obtain the results; and SAP2000 program was used as computer programming language. As a result, the supposed wind effects were low effective and the applied loads and vibrations were more effective on the tower crane structures were obtained.

Bosnjak et al. [8] applied FEA for the bucket wheel excavator (BWE) portal tie-rod support. At their study, the results of FEA pointed out the occurrence of pronounced stress concentration, whereby multiple stresses in the failure zone exceed the yield stress of the basic material. Also they did experimental investigation on fracture surfaces by scanning electron microscope (SEM) and light microscope (LM) which revealed the existence of porosities and inclusions in the weld metal. With their results they concluded that the failure of the support was the consequence of superposition of the negative effects caused by inadequate shaping and dimensioning of the support assembly for given load conditions, as well as influences of mentioned defects of the metal weld structure.

Rusinski et al. [9] performed the finite element analysis of a mine's loader boom. In their study numerical and experimental approach was considered. The finite element method was used for numerical simulation. The objectives were achieved by numerical simulation of cracked loader boom, material evaluations of specimens and comparison of results achieved from both approaches. The finite element analysis for the jib boom provided information about stress distribution for extreme load conditions. The study included macroscopic and fractographic inspection, microscopic evaluation as well as hardness tests of the material used for the jib boom. As a result, the causes of damage of a loader jib boom used at an underground copper mine were found.

Çolpan [10] performed the finite element analysis of linkage which is an important part of a kind of construction machine, namely of a wheel loader. Different linkage designs were compared with each other and as a result of this

comparison Volvo 110 E model wheel loader's TP linkage was preferred and designed because of its advantages against traditional Z-bar linkage design. The TP linkage was designed with the help of Solid works program. Distortion- energy, maximum shear stress and displacement analysis were performed for three different material chosen for the modeled linkage. Analyses were performed via ANSYS Workbench.

Karahan [11] designed two levels telescopic crane and analyzed by finite element method. Sheet thickness for main element stationary boom carrying load was determined by performing stress analysis in ANSYS workbench with finite element method. The critical locations determined in stress analysis were improved doing more strong and costs decreased by choosing fewer sheet thickness value of main construction. As for design of the telescopic boom, optimum choice was determined according to analysis results by considering dimension and thickness of standard profile cross section.

Karlinski et al. [12] used finite element method to analyze protective structures for construction and mining machine operators. They gave the principles of constructing calculation models for numerical simulations in virtual space by the finite element method. A detailed example of FEM tests on a protective structure is provided.

Derlukiewicz and Przybylekv [13] studied FEM strength analysis of telescopic jib mounted on mobile platform. They used the FEM analysis to see maximum stress points and to make construction design optimization quickly.

Bayrakceken et al. [14] studied analysis of power transmission system on vehicles and a universal joint yoke and a drive shaft. Fracture analysis of a universal joint yoke and a drive shaft of an automobile power transmission system were carried out. Spectroscopic analyses, metallographic analyses and hardness measurements were carried out for each part. For the determination of stress conditions at the failed section, stress analyses were carried out by the finite element method.

Miralbes and Castejon [15] presented a new methodology of calculation by means of the FEA applied to crane jibs. This analysis was carried out in terms of strength and stiffness, and for any type of crane jib: telescopic crane, lattice crane, closed beam crane, etc. There were simulated different load cases and boundary conditions that the structure should bear. This load cases obtained from normal and extreme operation of the crane. Furthermore, the welding of some parts were simulated and analyzed, and it was carried out a comparative analysis between the experimental results and the numerical results for some load cases. Once this correlation was obtained the methodology of calculation and the numerical results were validated.

Kalkan [16] analyzed the agricultural tractor protective cab under static load by using finite element analysis static testing methods and respective acceptance conditions regulated in TS 3412. Then ANSYS finite element model of the protective cab, for which measured force vs. displacement curve already known was constructed and displacement boundary conditions were applied. FEM results and the experimental results were compared.

2.3 Conclusion on Literature Review

The following conclusions were obtained from the literature reviews;
- In literature, finite element analyses are used in design improvement and optimization purposes for many machine parts.
- There are more studies about excavator and its components but although there are a lot of backhoe loader producers, there is less study on backhoe loader.

The main goal of this thesis is the analysis of Backhoe loader front and back arms. The specific objectives are:

- To find maximum stress points of back and front arms.
- To improve the critical points.
- To see factor of safety of the parts and improve them.

CHAPTER 3

FINITE ELEMENT ANALYSIS

3.1. Introduction

In this chapter, a brief introduction of finite element method (FEM) is presented and then some information about ANSYS Workbench analysis program is presented.

3.2 Finite Element Method

Finite element is one of the numerical method which used to obtain solutions for many engineering problem including structural stress, static and dynamic problems, heat problems, fluid, electromagnetic problems etc.

In fact working principle of FEM is easy. Problems are mathematical models of real situations. In finite firstly, mathematical model is built then all system is divided to small elements which is called discretization. It has been widely used in solving structural, mechanical, heat transfer and fluid dynamics problems as well as problems of other disciplines. Some important terminologies used in FEM are;

Element- An element is a portion of the problem domain, also known as a cell, and is typically some simple shape like a triangle, square, or hexagon in 2D; or tetrahedron or rectangular solid in 3D.

Node - A node is a point in the domain, and is often the vertex of several elements.

Mesh- A mesh is a list of elements, nodes, and other data that describes the computational domain.

Shape functions- Shape functions or interpolation functions are used in the finite element analysis to interpolate the nodal displacements of any element to any point within each element.

The advancement in computer technology enables us to solve even larger system of equations, to formulate and assemble the discrete approximation, and to display the results quickly and conveniently. This has also helped the finite element method become a powerful tool.

Basic steps of FEM are;

1-Create and discrete the solution domain in the finite elements; that is subdivide the domain into nodes and elements.

2-Assure a shape function to represent the physical behavior of an element; that is an approximate continuous function is assumed to represent the solution of an element.

3- Develop equations for an element.

4- Assemble the elements to present the entire problem, construct global stiffness matrix.

5-Apply boundary and initial conditions and loading.

6-Solve the equations and obtain important information, like stress etc.

3.3 ANSYS Workbench Finite Element Analysis Program

3.3.1 General Information

ANSYS is one of the general-purpose finite element software that is used for structural, fluid mechanics, thermal, electromagnetic, harmonic response analysis and buckling analysis. ANSYS Workbench is an important and fast growing interface of ANSYS that allows engineers analyzing 3D models in a short time.

3.3.2 Program Capability

The ANSYS Workbench platform provides an integrated geometry design and analysis system that links all elements of the design process. The main features are [17];

- Bidirectional, parametric links with all major CAD systems

- Integrated, analysis-focused geometry modeling, repair, and simplification via ANSYS Design Modeler

- Highly-automated, physics-aware meshing

- Automatic contact detection

- Unequalled depth of capabilities within individual physics disciplines

- Unparalleled breadth of simulation technologies

- Complete analysis systems that guide the user start-to-finish through an analysis

- Comprehensive multiphysics simulation with drag-and-drop ease of use

- Flexible components enable tools to be deployed to best suit engineering intent

- Innovative project schematic view allows engineering intent, data relationships, and the state of the project to be comprehended at a glance

- Complex project schematics can be saved for re-use

- Pervasive, project-level parameter management across all physics

- Automated what-if analyses with integrated design point capability

3.3.3 Connections, Contacts and Joints

While simulating real physical models with CAD systems, one needs some connections to connect bodies together. Similar to CAD systems, while modeling (model can design by using design modeler of Workbench or directly imported from CAD system) these systems by using ANSYS Workbench, one needs some connections include contact regions, joints and/or springs.

Contact conditions are formed where bodies meet. When an assembly is imported from a CAD system, contact between various parts is automatically detected. In addition one can also set up contact regions manually. Structural loads and heat flows can be transferred across the contact boundaries and "connect" the various bodies. Depending on the type of contact, the analysis can be linear or nonlinear.

Once contact regions are established, one can examine the initial contact conditions of the assembly before loading and adjust a variety of settings that globally affect all contact regions, as well as settings that control the characteristics of individual contact regions. After solving, one can again examine results such as contact pressure and gap values.

A joint is an idealized kinematic linkage that controls the relative movement between two bodies. Joint types are characterized by their rotational and translational degrees of freedom as being fixed or free.

3.3.3.1 Contact Phenomena

The contact is generated by pair in ANSYS [19]. For the point-surface contact, the `point` is contact and the `surface` is target. For surface-surface contact, both contact and target are surfaces and they have to be specified which surface is contact and which is target.

The differences in the contact settings determine how the contacting bodies can move relative to one another. This is the most common setting and has the most impact on what other settings are available. Most of these types only apply to contact regions made up of faces only.

3.3.3.2 Type of the Contacts [18]:

Contact types used in ANSYS Workbench are given as;

Bonded: In Workbench this is the default configuration for contact regions. If contact regions are bonded, then no sliding or separation between faces or edges is allowed as shown in figure 3.1. The region can be thought as *glued* or *welded*.
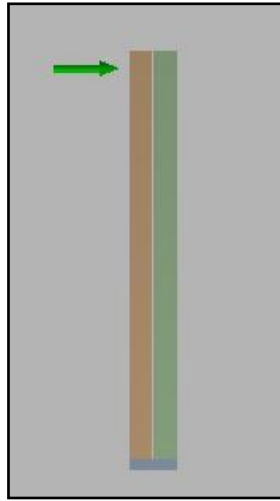
Figure 3.1 a) Bonded contact before force applied. **b)** Bonded contact after force applied.
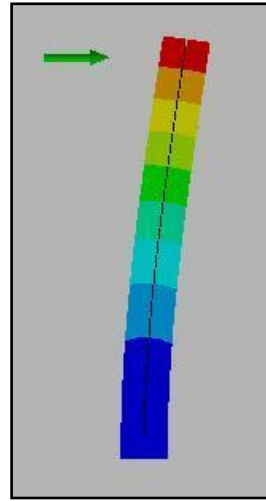
No Separation: This contact setting is similar to the bonded case. It only applies to regions of faces. Separation of faces in contact is not allowed, but small amounts of frictionless sliding can occur along contact faces (Figure 3.2).
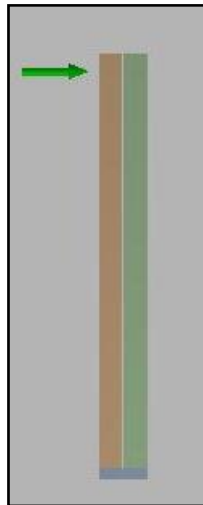
Figure 3.2 a) No separation contact before force applied. **b)** No separation contact after force applied.
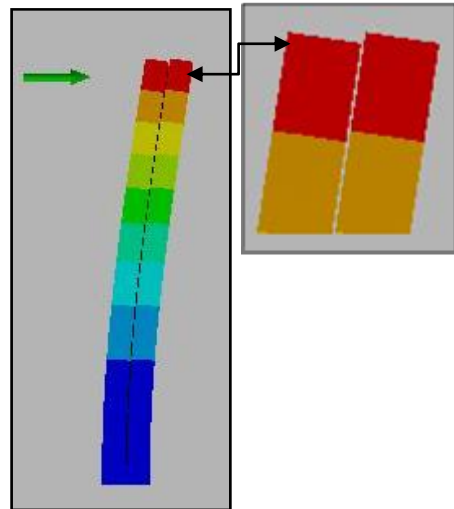
Frictionless: This setting models standard unilateral contact; that is, normal pressure equals zero if separation occurs. It only applies to regions of faces. Thus gaps can form in the model between bodies depending on the loading. This solution is nonlinear because the area of contact may change as the load is applied. A zero coefficient of friction is assumed, thus allowing free sliding (Figure 3.3)
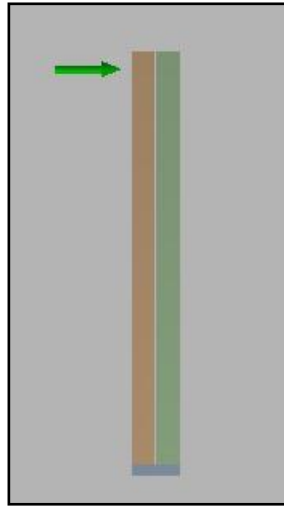
Figure 3.3 a) Frictionless contact before   **b)** Frictionless contact after
force applied.   force applied.
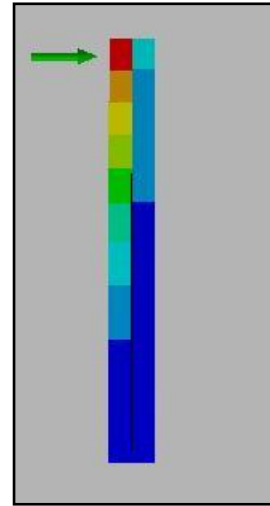
Rough: Similar to the frictionless setting, these setting models perfectly rough frictional contact where there is no sliding. It only applies to regions of faces. By default, no automatic closing of gaps is performed. This case corresponds to an infinite friction coefficient between the contacting bodies (Figure 3.4).
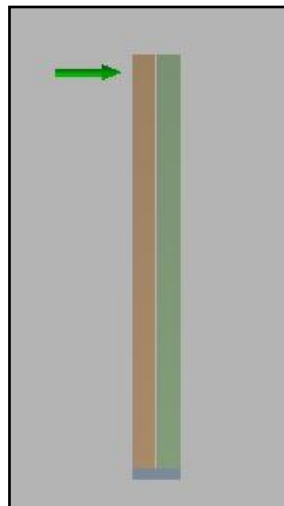
Figure 3.4 a) Rough contact before   **b)** Rough contact after
force applied.   force applied.
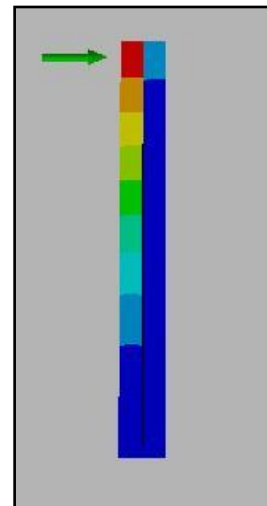
Frictional: In this setting, two contacting faces are exposed to shear stresses up to a certain magnitude across their interface before they start sliding relative to each other. It only applies to regions of faces. This state is known as "sticking." The model defines an equivalent shear stress at which sliding on the face begins as a

fraction of the contact pressure. Once the shear stress is exceeded, the two faces will slide relative to each other.

3.3.3.3 Contact Solution Algorithms [18, 19, 20]

For different interests and different kinds of problems, different algorithms can be chosen to solve the model. In ANSYS, there are several kinds of algorithm provided, namely;

- Augmented Lagrange
- Pure Penalty method
- Multipoint constraint (MPC)
- Normal Lagrange

- **Augmented Lagrange**: The augmented Lagrange method is an iterative series of penalty updates to find the Lagrange multipliers (i.e., contact tractions). Compared to the penalty method, the augmented Lagrange method usually leads to better conditioning and is less sensitive to the magnitude of the contact stiffness coefficient. However, in some analyses, the augmented Lagrange method may require additional iterations, especially if the deformed mesh becomes excessively distorted.
- **Pure Penalty**: This method requires both contact normal and tangential stiffness. The main drawback is that the amount penetration between the two surfaces depends on this stiffness. Higher stiffness values decrease the amount of penetration but these can lead to ill-conditioning of the global stiffness matrix and to convergence difficulties. Ideally, if a high enough stiffness is required that contact penetration is acceptably small, but a low enough stiffness that the problem will be well-behaved in terms of convergence or matrix ill-conditioning.
- **MPC**: Multipoint constraints equations are created internally during the ANSYS solve to tie the bodies together. This can be helpful if truly linear contact is desired or to handle the nonzero mode issue for free vibration that can occur if a penalty function is used. This setting is valid for both **Bonded** and for **No Separation** contact.

- **Normal Lagrange**: Normal Lagrange method does not require contact stiffness. Instead it requires chattering control parameters. Theoretically, normal Lagrange method enforces zero penetration when contact is closed and "zero slip" when sticking contact occurs. However normal Lagrange method adds additional degrees of freedom to the model and requires additional iterations to stabilize contact conditions. This will increase the computational cost. The algorithm has chattering problems due to contact status changes between open and closed or between sliding and sticking. The other main drawback of the normal Lagrange method is the over constraint occurring in the model. The model is over constrained when a contact constraint condition at a node conflicts with a prescribed boundary condition on that degree of freedom at the same node. Over constraints can lead to convergence difficulties and/or inaccurate results.

3.3.3.4 Types of Joints [18]:

General degree of freedom of any joint is given in Figure 3.5. There are nine different joint types in ANSYS Workbench based on rotations and translations. These are:
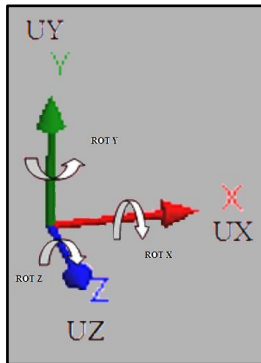
Figure 3.5 Coordinate frame

- Fixed Joint   : All degrees of freedom are constrained.

- Revolute Joint : Degrees of freedom of UX, UY, UZ, and ROTX, ROTY are constrained.

- Cylindrical Joint: Degrees of freedom of UX, UY, and ROTX, ROTY are constrained.

- Translational Joint: Degrees of freedom of UY, UZ, ROTX, ROTY, ROTZ are constrained.

- Slot Joint: Degrees of freedom of UY, UZ are constrained.

- Universal Joint: Degrees of freedom of UX, UY, and UZ, ROTY are constrained.

- Spherical Joint: Degrees of freedom of UX, UY, and UZ are constrained.

- Planar Joint : Degrees of freedom of UZ, ROTX, ROTY are constrained.

- General Joint: Fix All or Free X, Free Y, Free Z or Free All.

Connections given in these sections have been used in the FEA in suitable and necessary points.

CHAPTER 4

ANALYSIS OF BACK ARM

4.1 Introduction

Backhoe loader back parts namely stabilizer, boom and arm are shown in the Figure 4.1. In this thesis only arm is considered and analyzed for back part of the machine. Assumptions in the analysis are given in section 4.2. Static analysis and finite element analysis of the back arm of backhoe- loader are carried out in this chapter. Static force analysis of back arm is given in section 4.3 and then finite element analysis of back arm is given in the section 4.4.
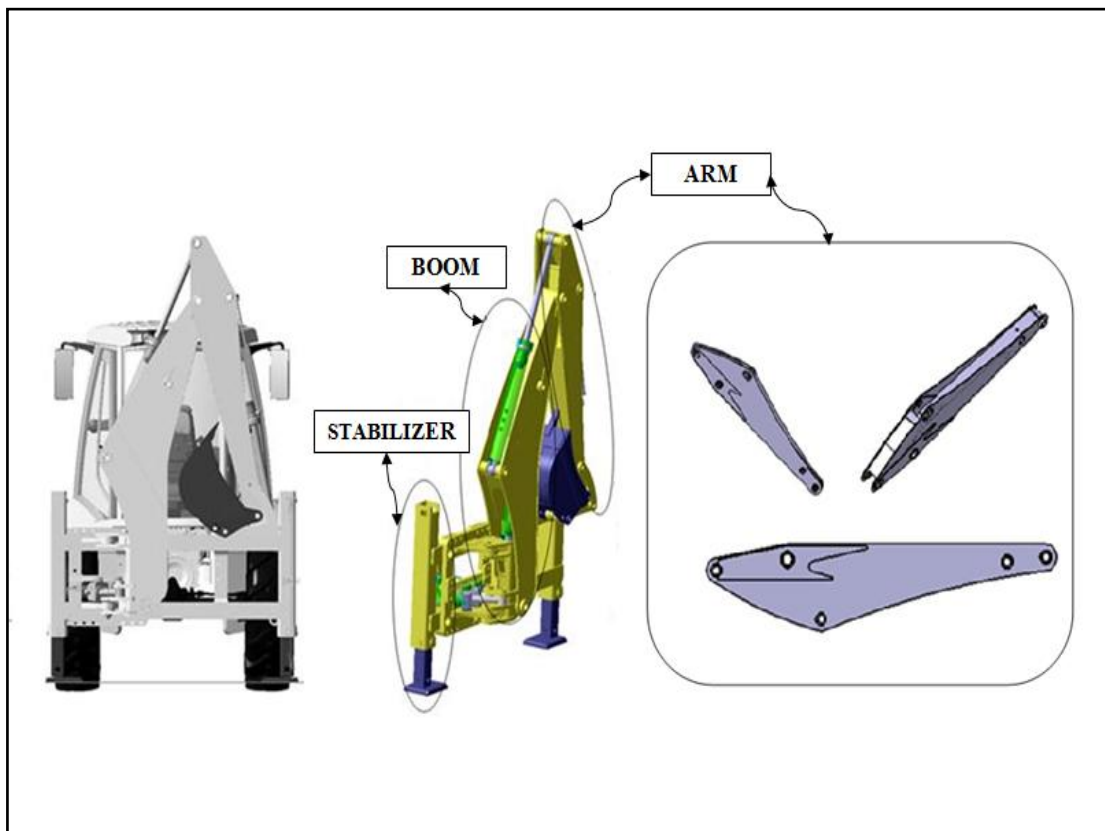
Figure 4.1 Back parts of Backhoe loader

4.2 Assumptions

The following assumptions have been done while doing analysis;

- It is assumed that material behavior is linear elastic and strains are small. Therefore, linear elastic analysis will be carried out.

- Pins and links are assumed as rigid.

- The loads are applied statically and symmetrically.

- It is assumed that material properties of structures after heat treatment (welding operation) are not changing.

4.3 Static Force Analysis

In order to calculate maximum breakout forces, force analysis is applied to mechanism. Two cases are examined in this study which are;
- While Arm cylinder is active,

- While Bucket cylinder is active,

4.3.1 Arm Cylinder is Active

As seen in the figure 4.2 there is cylinder force (called F_{arm}) which is related to the hydraulic pressure and the rod inner surface diameter. The hydraulic pressure depends on the hydraulic pump actuated by engine. So the cylinder forces are limited by the engine power, the pump capacity and the cylinder dimensions. The general cylinder force formula is:

$$F = P * A \qquad\qquad (4.1)$$

Where;
F: Cylinder force.
P: working pressure of the cylinder
A: Rod inner surface area where the oil pressure act
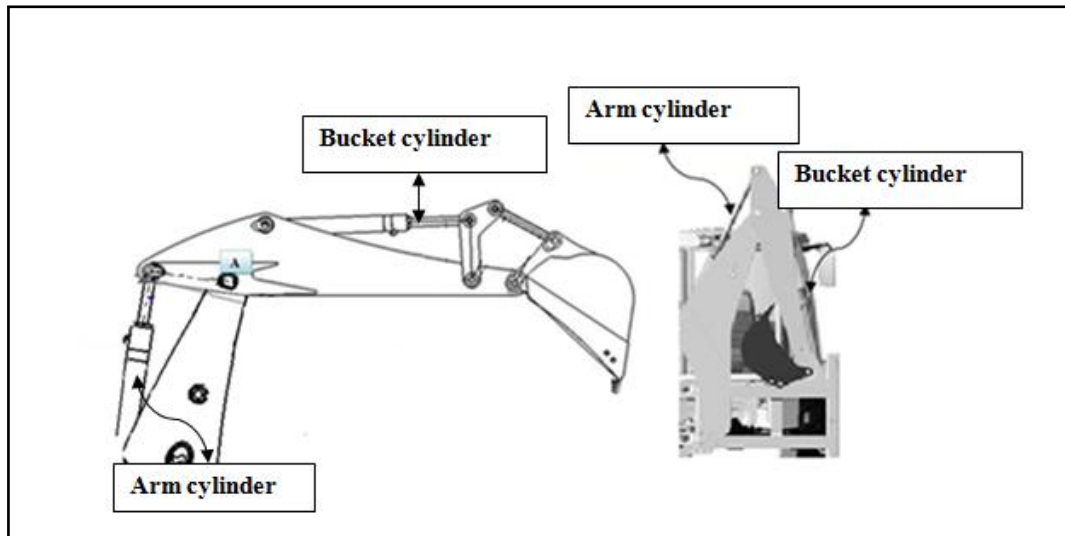
Figure 4.2 Backhoe-loader back arm cylinders

To determine the maximum applied breakout force, W, firstly maximum arm cylinder pressure is applied. Arm cylinder force is equals to;

$$F_{Arm} = P * A$$

$$A = \pi \frac{D^2}{4}$$

Where,

P is the maximum working pressure of the hydraulic arm cylinder and *D* is the diameter of the cylinder (piston side).

D = 110 mm

P = 230 bar

*F*_{*arm*} = **222620** N
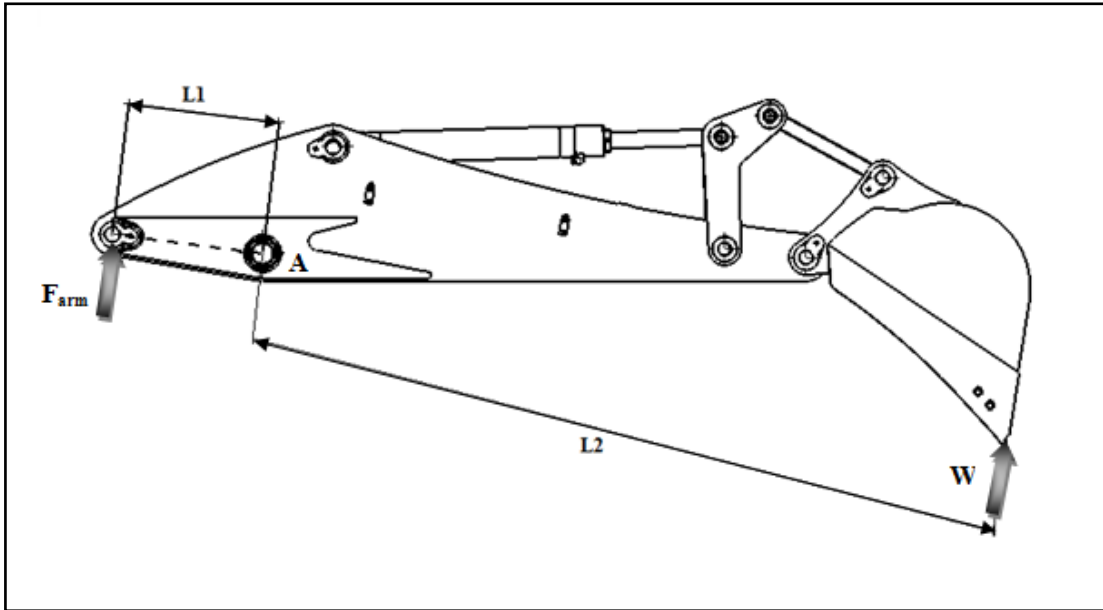
Figure 4.3 Free body diagram of back arm while arm cylinder is active

Free body diagram of back arm is given in the Figure 4.3. F_{Arm}, L_1 and L_2 are

F_{arm}: Backhoe arm cylinder force (N) =222620 N

W: Backhoe arm breakout force (N) = unknown

L_1: Perpendicular length from the point A to the action line of F (mm) = 515mm

L_2: Perpendicular length from the point A to the edge of the bucket (mm) = 2703mm

In order to find unknown values, all moments are taken at point A, then W is;

W = 42415 N

4.3.2 Bucket Cylinder is Active

While bucket cylinder is active; the bucket cylinder pressure is used to calculate maximum breakout forces and arm joint forces.

$F_{Bucket\ cylinder} = P * A$

Where;

P is the working pressure of the cylinder and *D* is the diameter.

D cylinder = 90 mm

P (hyd. pressure) = 230 bar

Then

$F_{Bucket\ cylinder} = 149020\ N$

To calculate bucket breakout force perpendicular distances (L_1, L_2, L_3, L_4, L_5, and L6) are shown in figure 4.8 and their values are;

L_1=515 mm

L_2=2703 mm

L_3=381 mm

L_4=472 mm

L_5=375 mm

L_6=890 mm
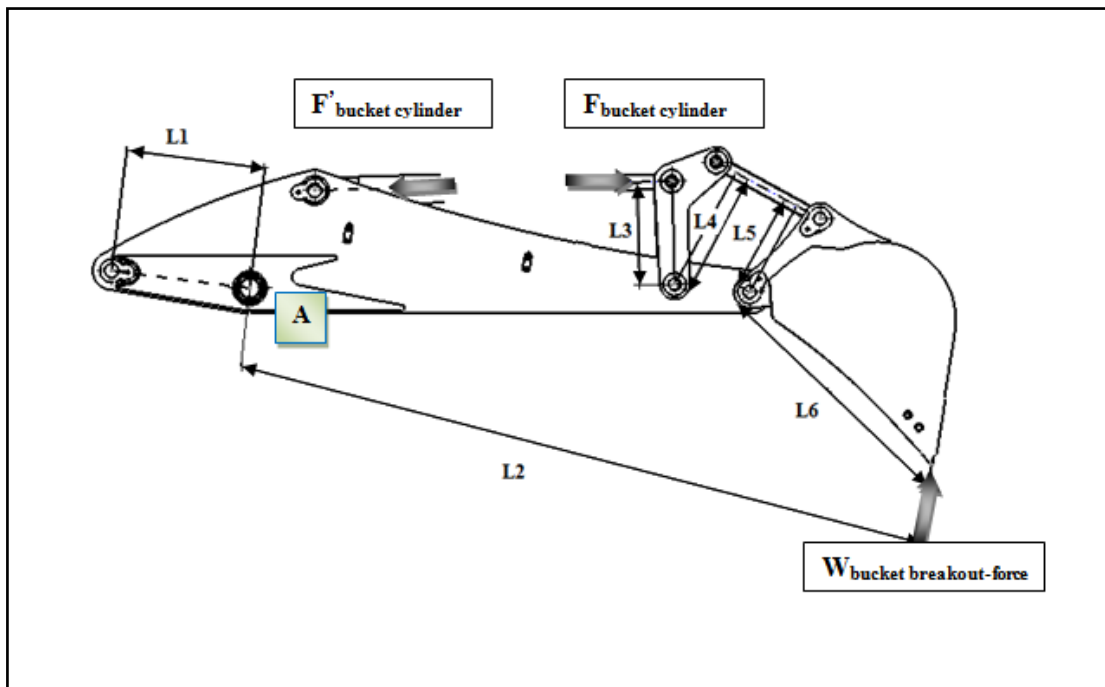
Figure 4.4 Free body diagram of back arm while bucket cylinder is active

$$W_{breakout} = F_{Bucket\ cylinder} * \frac{L_3}{L_4} * \frac{L_5}{L_6}$$

$$W_{breakout} = 149020 * \frac{381}{472} * \frac{375}{890} = 50683.7\ N$$

4.3.3 Arm Joint Forces

Maximum breakout force is calculated as 50683.7 N when bucket cylinder is used. Free body diagram of the back arm is given in Figure 4.5. F_4, F_5, F_6, F_7, and F_8 are joint forces and calculated with the use of statics as;

21

F4 = 149020 N

F5 = 139423 N

F6 = 11593.8 N

F7 = 33390 N

F8 = 33156 N

Arm force is calculated with the use of Figure 4.3 dimensions and its value is

F_{arm} = 266015,6 N
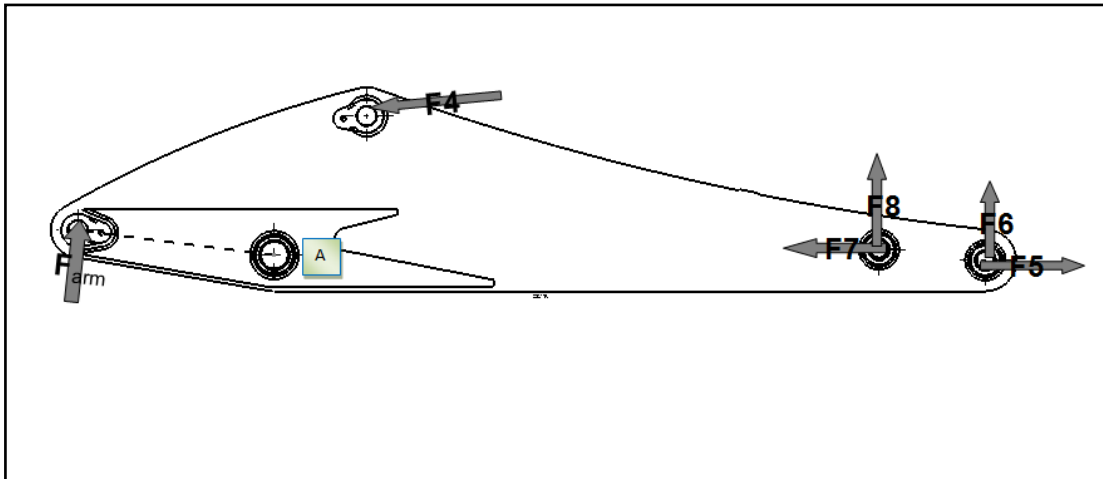
Figure 4.5 Joint forces while bucket cylinder active

4.4 Finite Element Analysis of Back Arm

Prepared solid model of the back arm is imported to the ANSYS Workbench program (figure 4.6). Finite element analysis will be carried out then if required necessary improvements will be done in the light of results. Static analysis will be carried out with the use of calculated maximum breakout force and joint reactions.
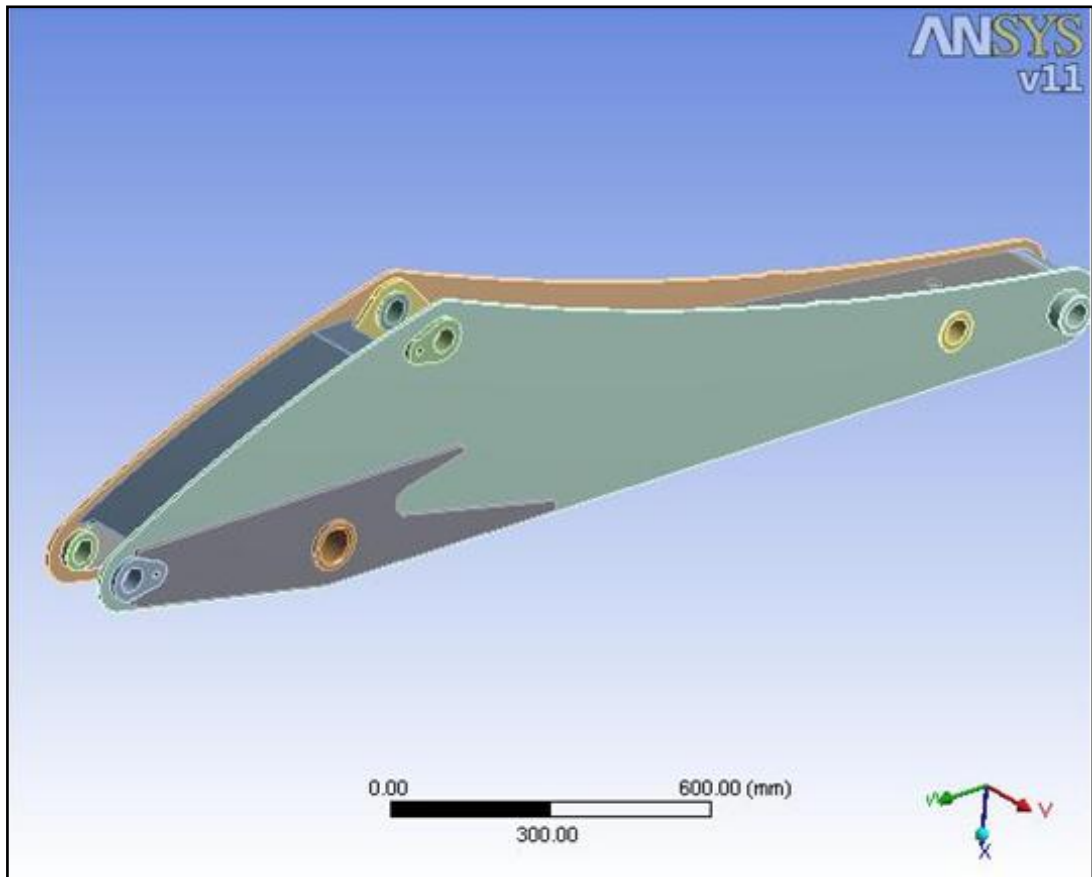
Figure 4.6 Solid model of Backhoe-loader back arm

Steps of ANSYS Workbench program are:

1) Create or import the geometry (The Solid geometry is imported which modeled in Catia CAD program),

2) Specify material properties of parts ,

3) Specify **Connections, Contacts and joints** (Detail information of these phenomena's are given in chapter 3)

4) Mesh the geometry, (ANSYS Workbench can generate mesh automatically and mesh properties can be changed or adjusted (element size, relevance, refinement etc.)

5) Apply boundary conditions and loads.

6) Solution,

7) Check the results

8) If the results are not satisfactory; improve the model with respect to the FEA results and analyze the new model.

4.4.1 Problem Definition

The Backhoe-loader back arm will be analyzed and if necessary, some improvements will be done. The back arm is modeled by CATIA CAD program and imported to ANSYS Workbench finite element program. In the following sections material properties, contact types, mesh properties, boundary conditions and loads will be defined.

4.4.2 Material Properties

The material of the back arm is St52-3 and bushes and pins materials are SAE 1040 steel and material properties are given in table 4.1 and 4.2.After the model is imported to ANSYS Workbench, material properties of each parts are given as shown in figure 4.7. ASSYS Workbench has some material database, it can be used directly or new material can be created. ST52-3 and SAE 1040 material properties are newly defined by entering their properties (young modulus, poison ratio, density act.).
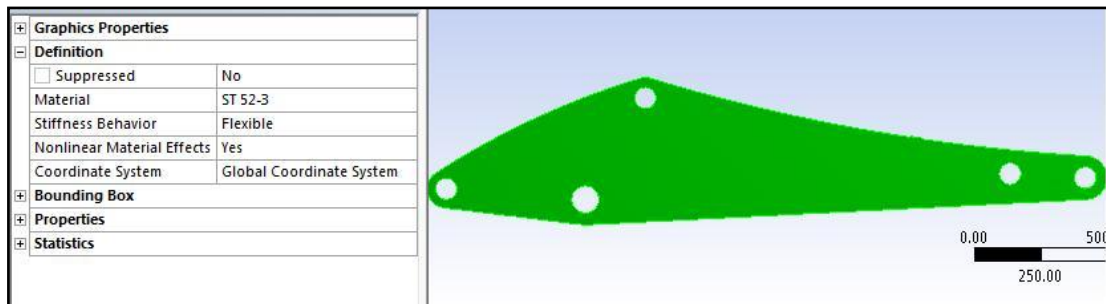
Figure 4.7 Material Properties of backhoe-loader back arm

Table 4.1 Properties of st52-3

Young's Modulus	210000 MPa
Poisson's Ratio	0.3
Density	7.85e-006 kg/mm³
Thermal Expansion	1.2e-005 1/°C
Tensile Yield Strength	355 MPa
Compressive Yield Strength	355 MPa
Tensile Ultimate Strength	520 MPa

Table 4.2 Properties of SAE 1040 steel

Young's Modulus	200000 MPa
Poisson's Ratio	0.29
Tensile Yield Strength	415 MPa
Tensile Ultimate Strength	590-620 MPa

4.4.3 Connections, Contacts and Joints

Bonded contact (properties given in the section 3.3.3.2) is selected for welded parts (figure 4.8). No extra joints and contact type are required to use.
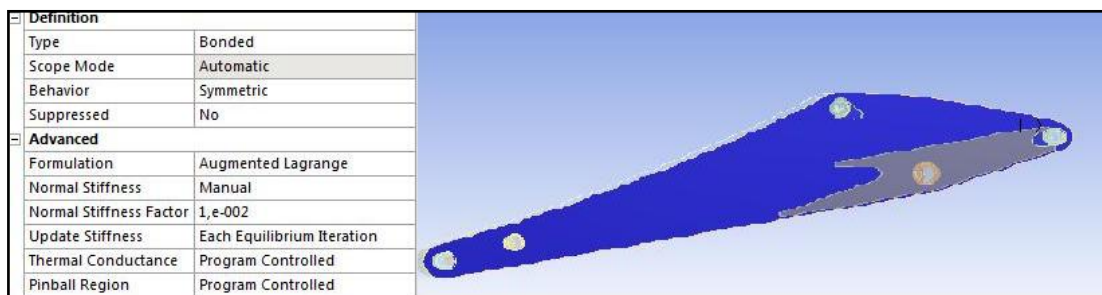
Figure 4.8 Contact type

4.4.4 Mesh Properties

Automatic mesh can be used that is produced by ANSYS Workbench. In this study mesh is created automatically, and then its mesh size is changed to obtain refined mesh. Meshed geometry is given in Figure 4.9.In this analysis, the developed model has 264048 nodes and 65708 elements. Element types used are Solid 186 and Solid 187;

Solid 186: is a higher order 3-D 20-node solid element.

Solid 187: is a higher order 3-D, 10-node solid element.
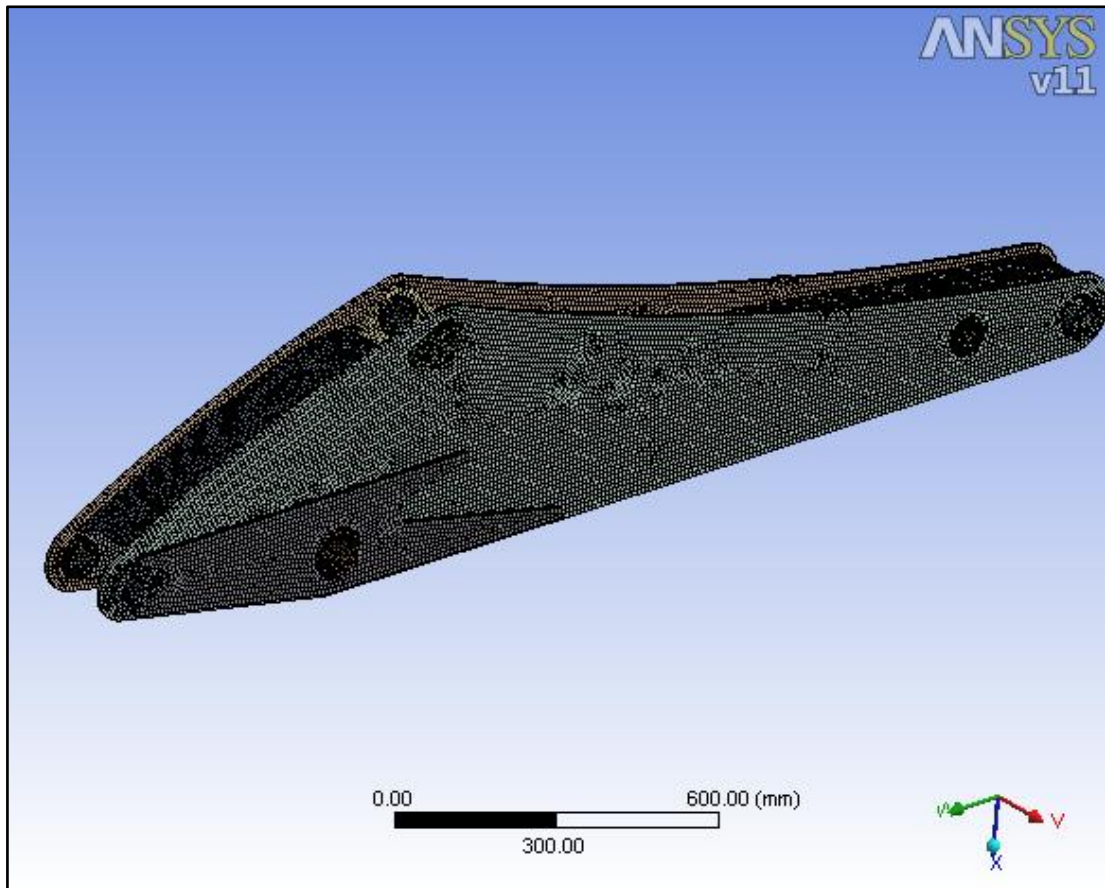
Figure 4.9 Mesh of back arm

4.4.5 Boundary Conditions and Loads

In order to calculate maximum stress points two different loading conditions were examined as bucket cylinder pressure and arm cylinder pressure. Maximum breakout force is calculated from bucket cylinder pressure. So, in finite element analysis this maximum force is used.

Points A, B are cylindrical supports and load is applied to points C, E, and D shown in figure 4.10. Forces at points C, E and D were calculated in section 4.3.2.
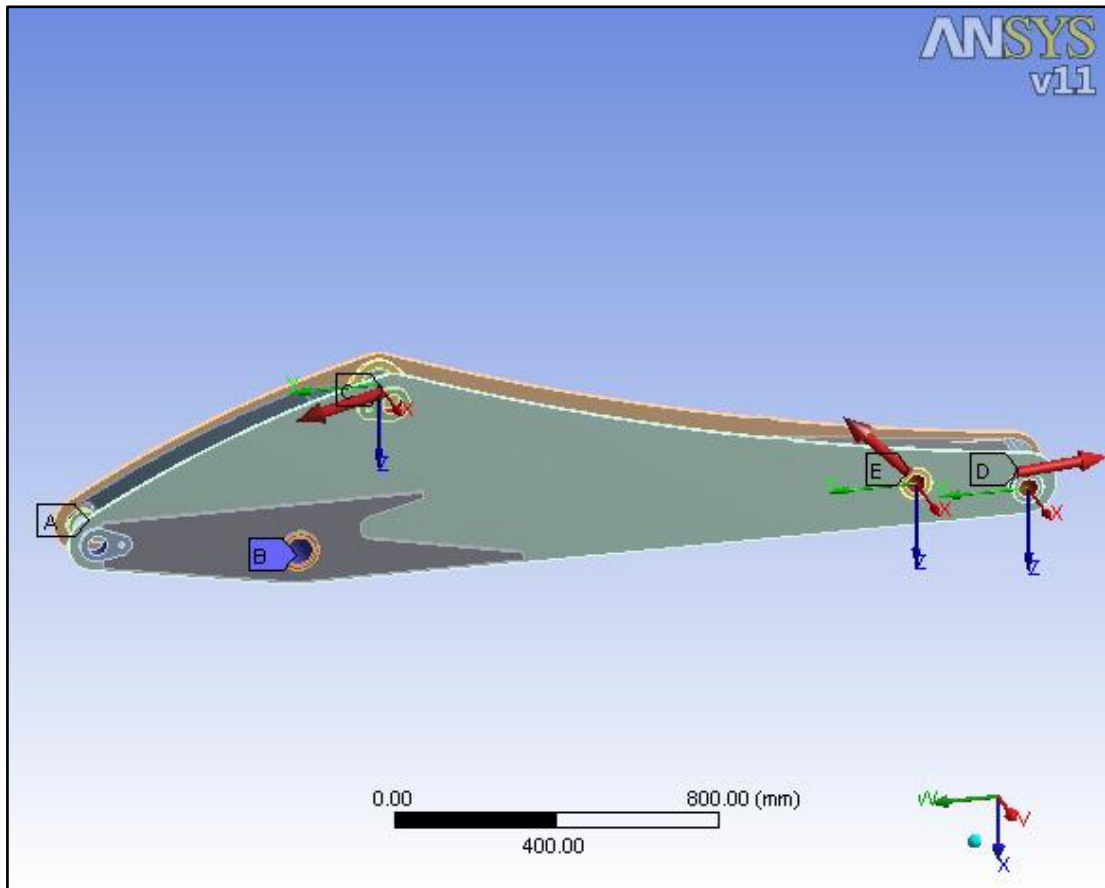
Figure 4.10 Boundary conditions of back arm

C = F4 = 149020 N

E is combination of F7 and F8

F7 = 33390 N

F8 = 33156 N

D is combination of F5 and F6

F5 = 139423 N

F6 = 11593. 8 N

4.4.6 Solution and Results

After the above mentioned steps (importing geometry, defining material properties, loading and applying boundary conditions), then solution is carried out. When the solution is done, it is possible to check all the parameters which we want to

investigate in the solution information, for example, stresses, strains, safety factor, reaction force, etc.

Reaction forces calculated in static analysis in section 4.3 are nearly equivalent to those calculated in ANSYS Workbench. So our analysis gives reasonable results.

Equivalent (von-misses) stress distribution of the back arm is shown in figures 4.11-4.13. Maximum stress in the arm is 222.83 MPa. So, these stresses should be reduced by making some improvements.
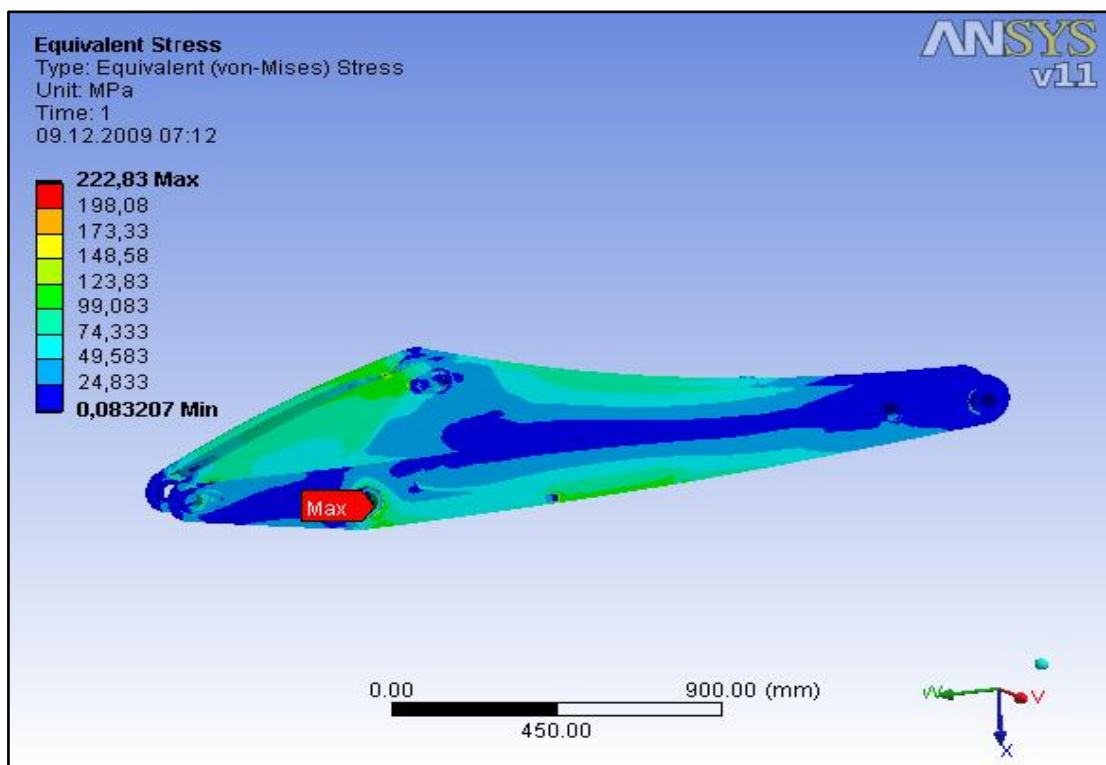
Figure 4.11 Equivalent stress distribution of original back arm
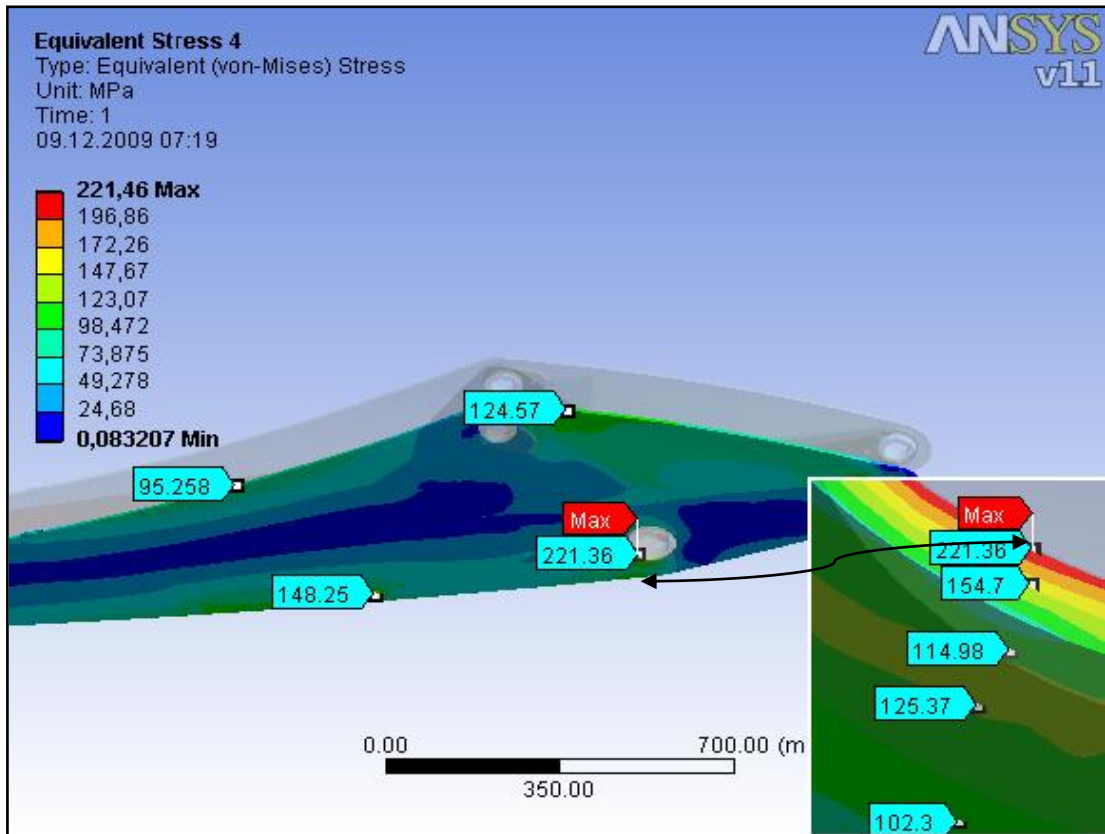
Figure 4.12 Equivalent stress distribution of original back arm left part
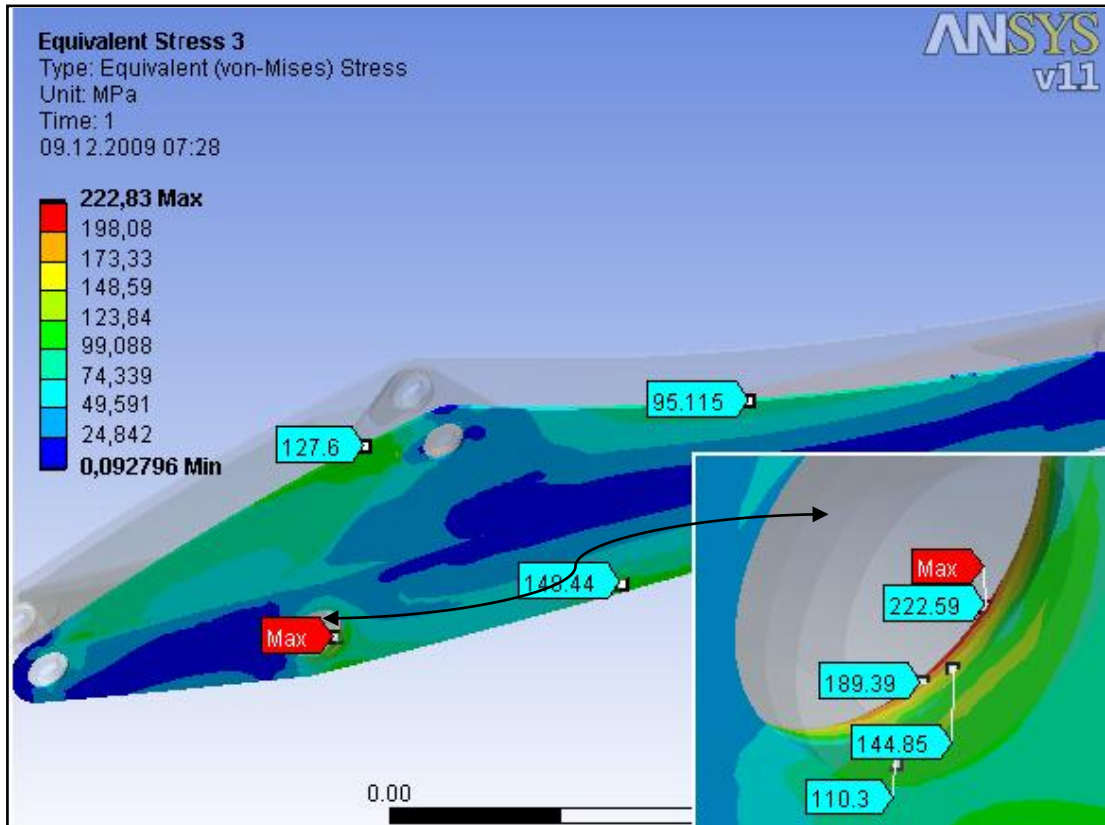
Figure 4.13 Equivalent stress distribution of original back arm right part

To reduce the maximum stress some improvements are done to maximum stressed point shown in figures 4.14 and 4.15. First reinforcement is carried out by putting circular plate back of outer plates. Second improvement is carried out by changing original reinforced plate that putted on face of outer plates.

First improvement is done shown in the figure 4.15. Analysis results of arm with this improvement are shown in figures 4.16-4.18. After first reinforcement maximum stress is reduced to 171 MPa on the back arm, 149 MPa in right and left outer plates. Then, second improvement is done shown in figure 4.19. After both improvements, calculated equivalent stress results are shown in figures 4.20-4.22. According to results maximum equivalent stress of whole structure is reduced to 171.13 MPa. Maximum equivalent stress of right and left outer plates is reduced to 140 MPa.
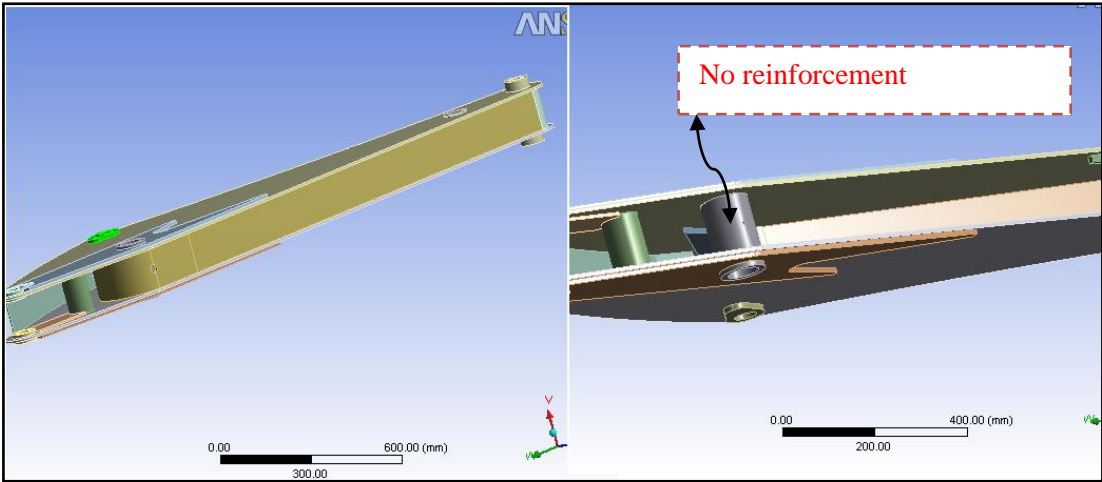
Figure 4.14 Original back arm without reinforcement
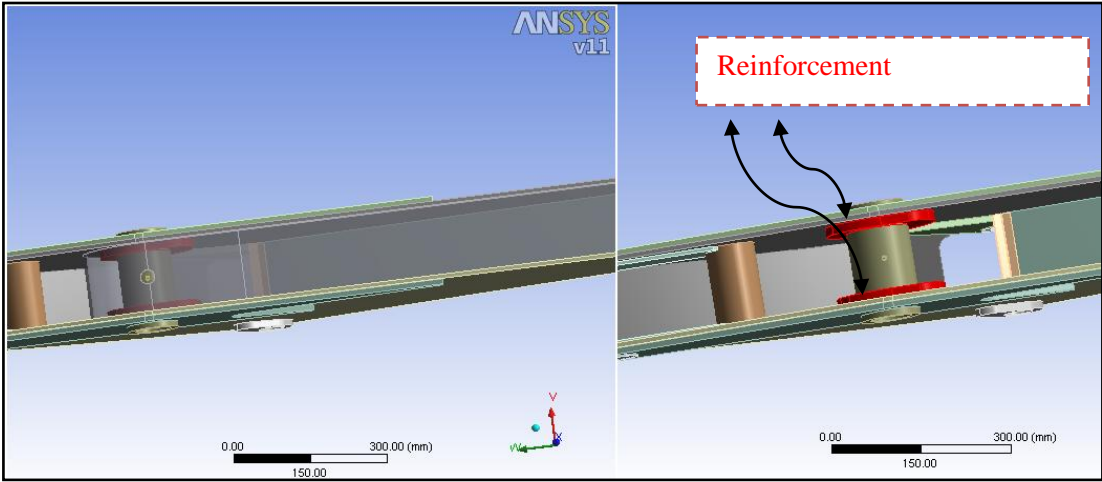
Figure 4.15 Original back arm with new reinforcement-1
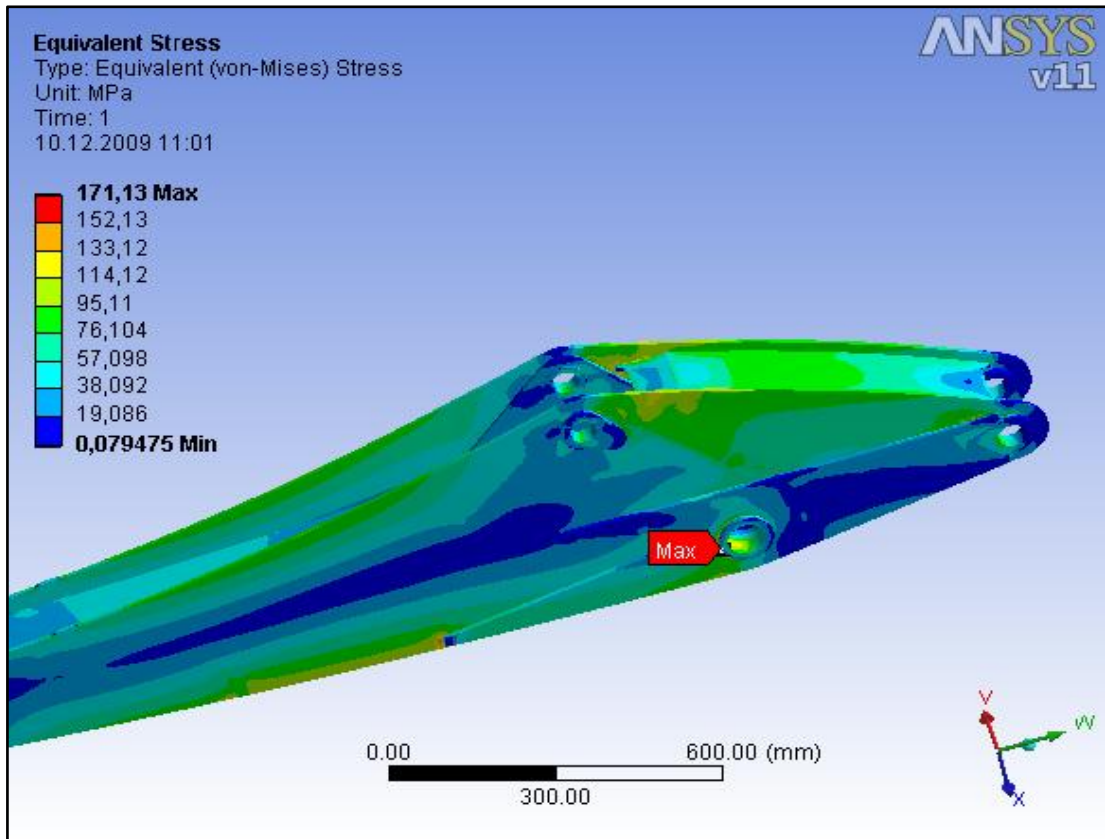
Figure 4.16 Equivalent stress distribution of back arm with new reinforcement-1
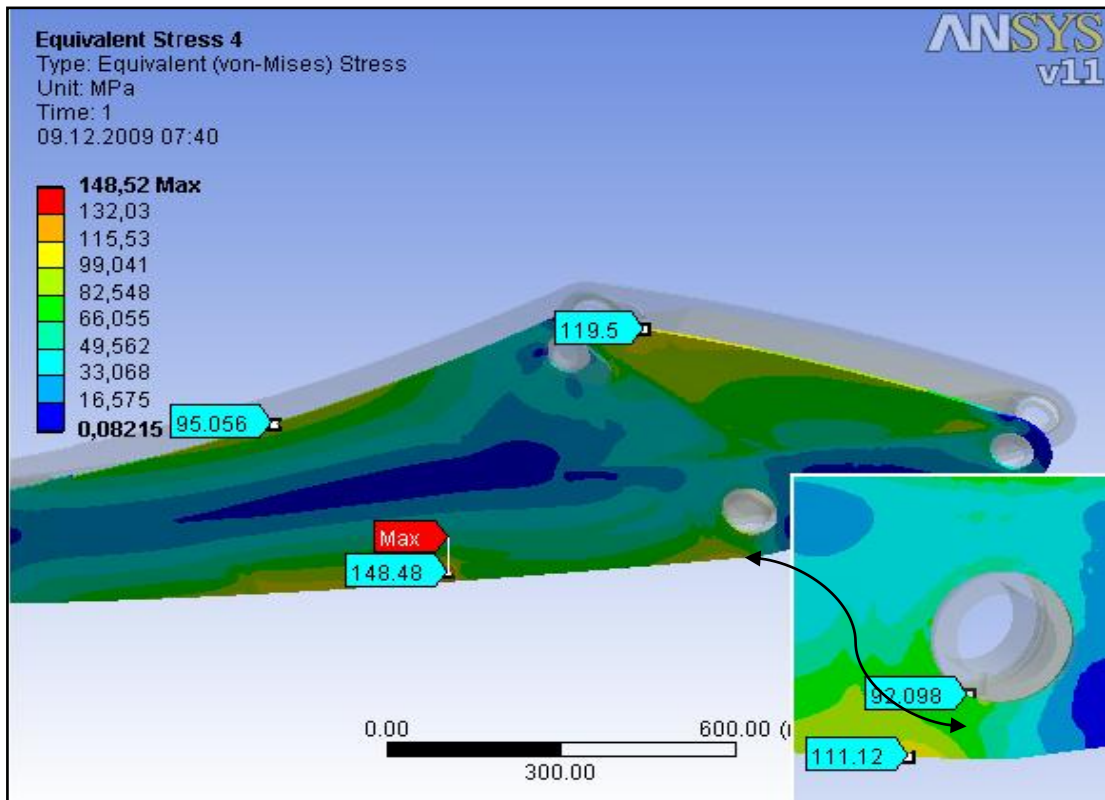
Figure 4.17 Equivalent stress distribution of back arm left part with new reinforcement-1

31
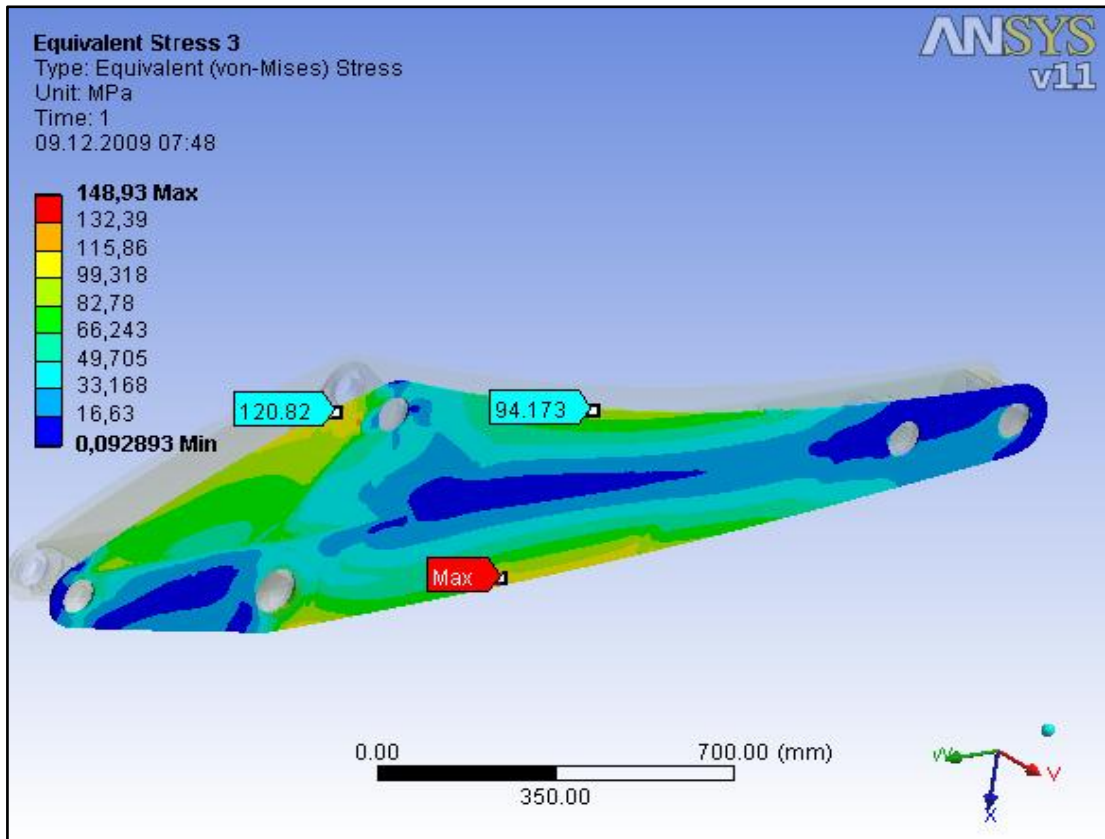
Figure 4.18 Equivalent stress distribution of back arm right part with new reinforcement-1
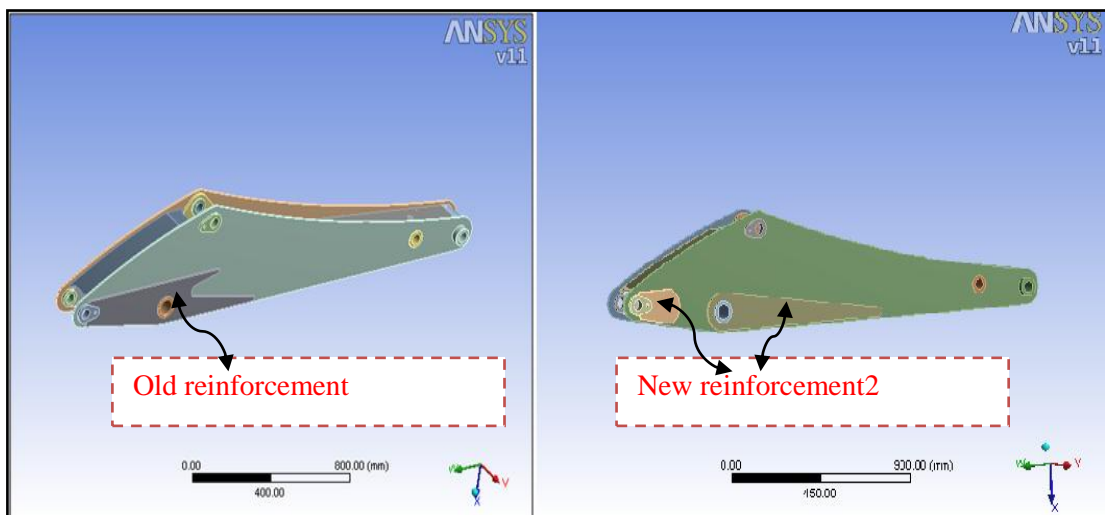
Figure 4.19 Back arm with new reinforcement-2
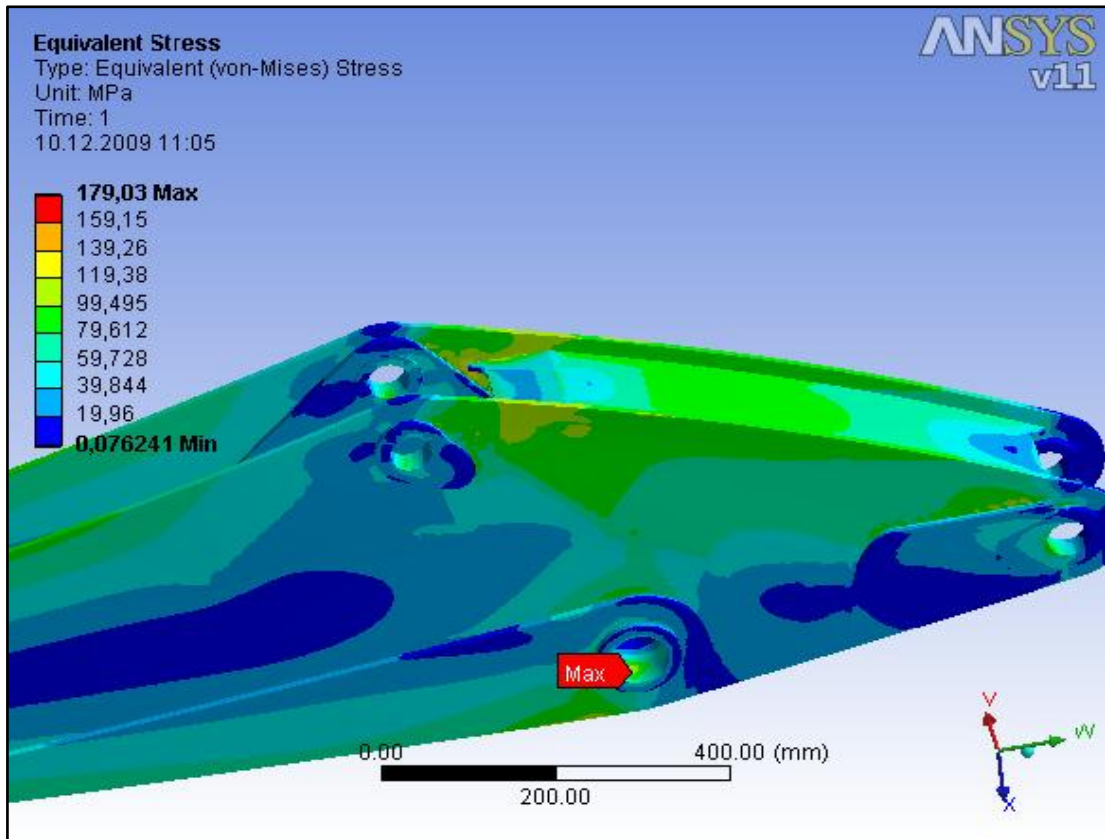
Figure 4.20 Equivalent stress distribution of back arm with new reinforcement-2
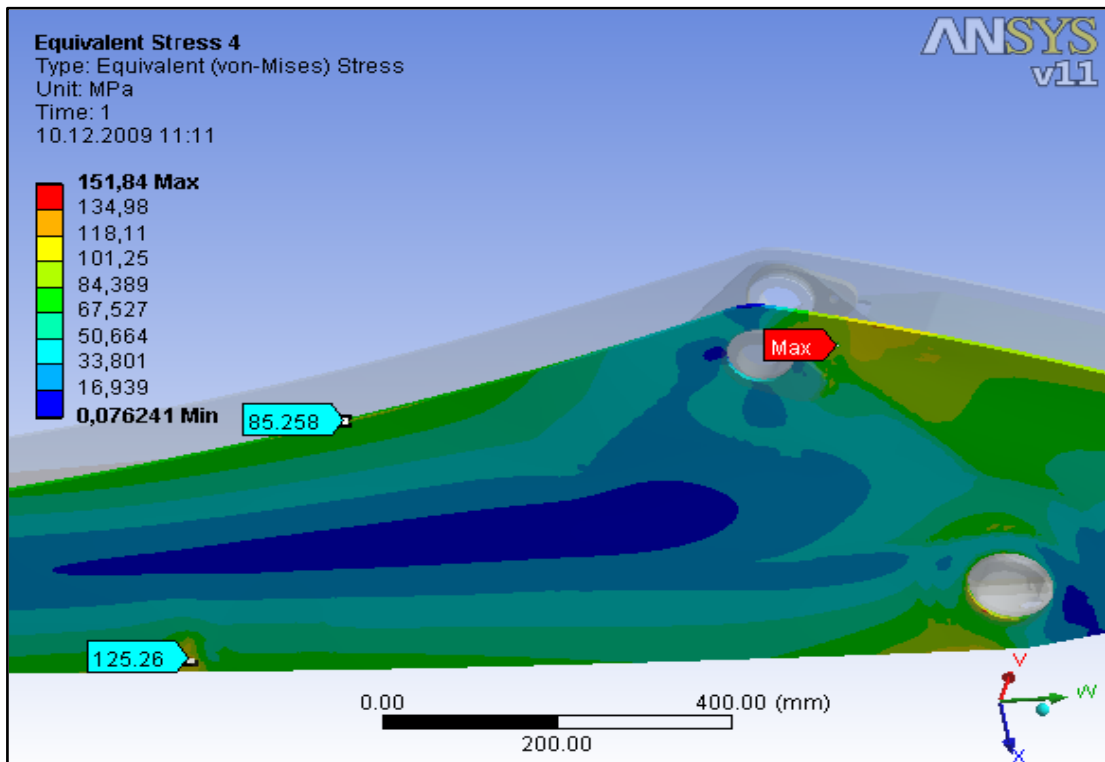
Figure 4.21 Equivalent stress distribution of back arm left part with new reinforcement-2
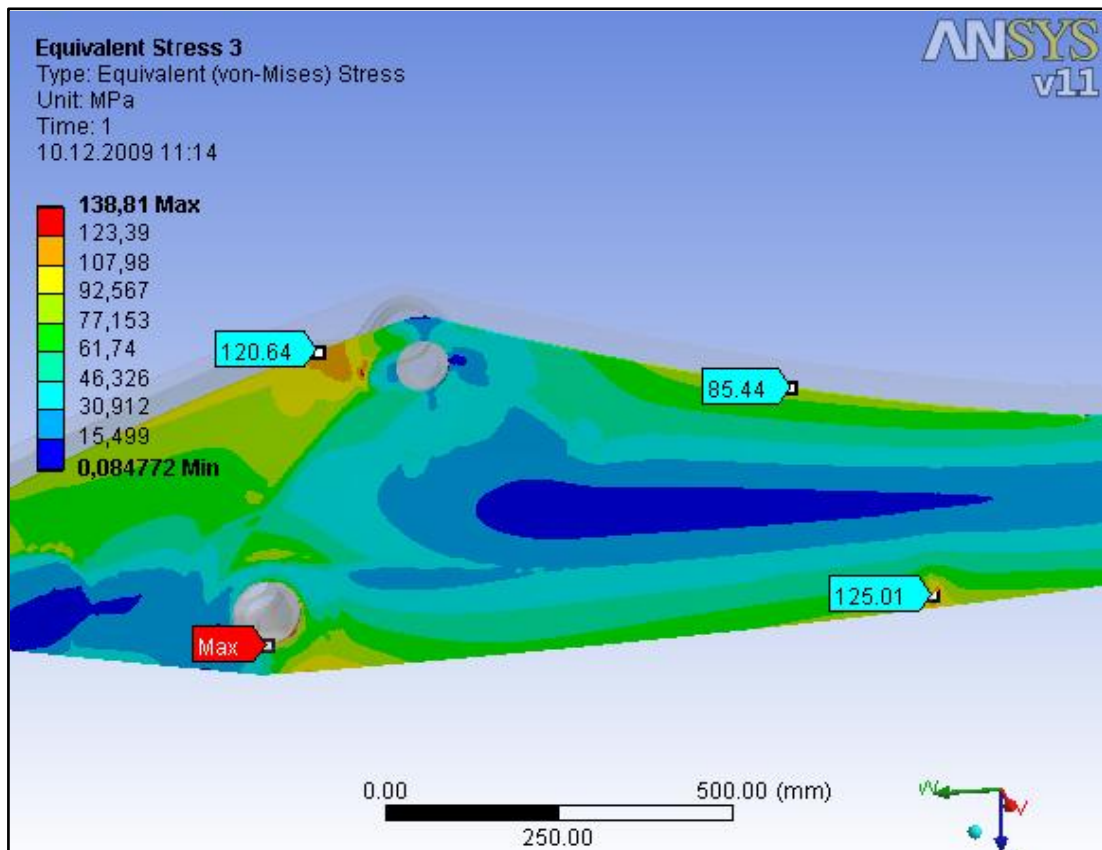
Figure 4.22 Equivalent stress distribution of back arm right part with new reinforcement-2

4.4.7 Safety Factor

Generally safety factor (SF) can be defined as the ratio of the ultimate strength of material to allowable stress. In the design processes, SF is firstly determined due to reliability of the design and then design is performed with respect to this SF. In this study, since already designed arms are used, firstly analyses have been carried out then SF has been compared.

ANSYS Workbench can show contour plot of the factor of safety. Figure 4.23 shows safety factors of back arm before improvement. Figure 4.23 shows safety factors of back arm after improvement. As seen from the figures minimum safety factor has increased to 1.98 from 1.59.
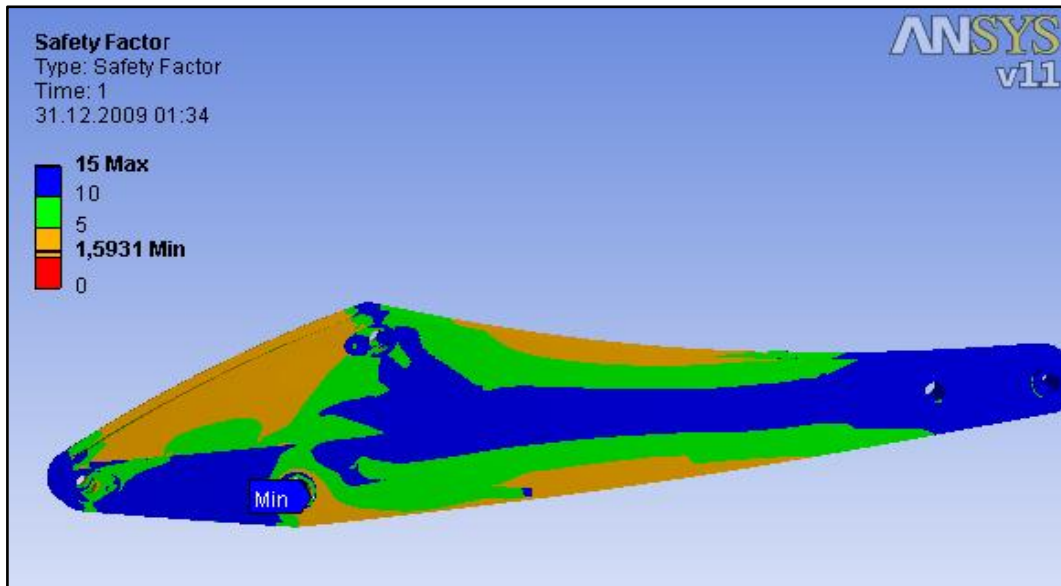
Figure 4.23 Safety factor of back arm before improvements
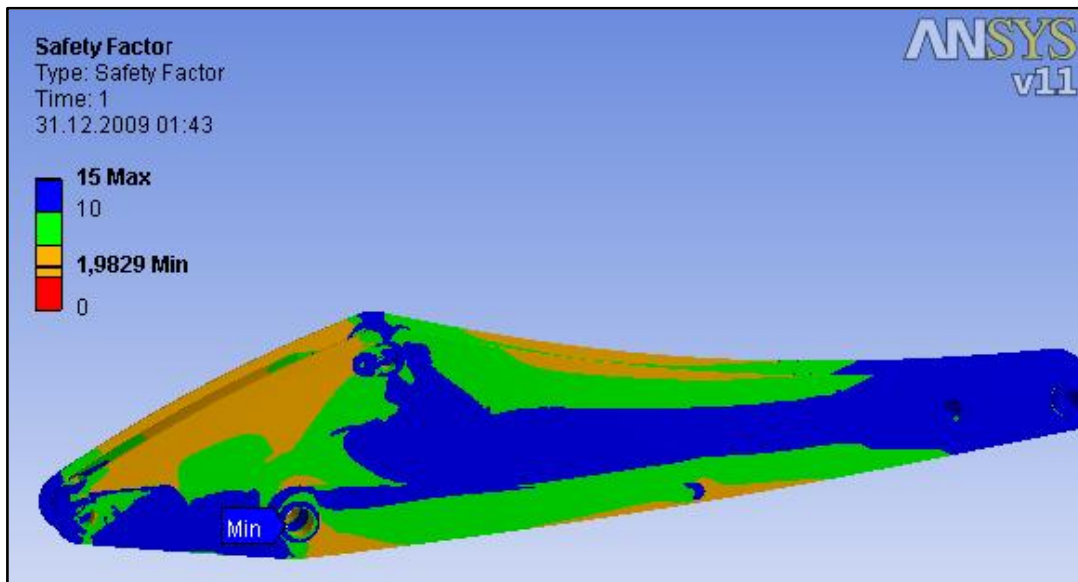
Figure 4.24 Safety factor of back arm after improvements

4.4.8 Conclusion on Back Arm

In this chapter, firstly static forces have been calculated by doing static force analysis. Then calculated forces used in the FEA. The static forces have been calculated at the two different conditions which are namely, loading while arm cylinder is active and loading while bucket cylinder is active. The back arm has been analyzed while bucket cylinder is active since maximum breakout force is calculated from bucket cylinder pressure.

Then FEA has been carried out in order to find maximum stress values and its location on back arm. Equivalent (von-misses) stress distribution of the back arm is shown in figures 4.11-4.13. Maximum stress in the arm is 222.83 MPa. So some improvements have been required to reduce the maximum stress. The improvements are shown in the figures 4.15 and 4.19. After improvements, maximum von misses stress is reduced to 171 MPa on the back arm and 140 MPa on the right and left outer plates. As seen in figures 4.23 and 4.24 safety factor after improvement is increased to 1.98 from 1.59.

CHAPTER 5

ANALYSIS OF FRONT ARM (LOADER)

5.1 Introduction

In this chapter, static analysis and finite element analysis of the front arm (loader) of backhoe- loader are produced. Loader arm which will be analyzed is shown in the figure 5.1. Assumptions in the analysis are given in section 5.2. Static force analysis of the front arm is given in section 5.3 and finite element analysis of the front arm is given in the section 5.4.
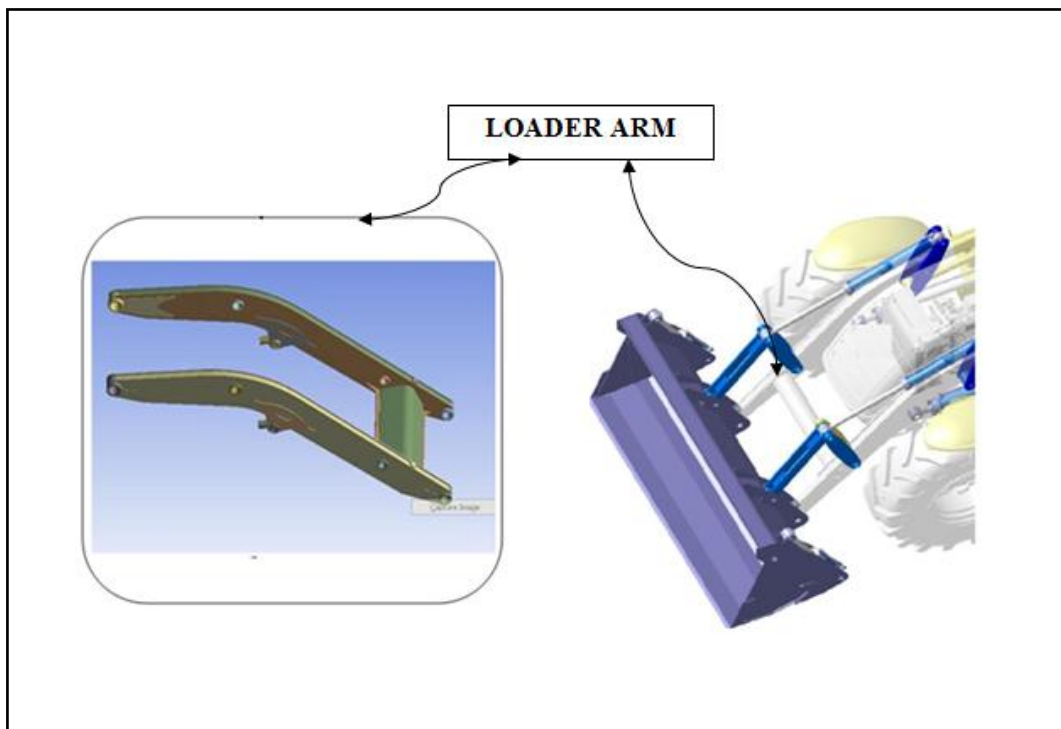
Figure 5.1 Loader arm of Backhoe-loader machine

5.2 Assumptions

The following assumptions have been done while doing analysis;

- It is assumed that material behavior is linear elastic and strains are small. Therefore, linear elastic analysis will be carried out.

- Pins and links are assumed as rigid.

- The loads are applied statically.

- Not only arm, bucket and connecting linkage will also be modeled.

- It is assumed that material properties of structures after heat treatment (welding operation) are not changing.

5.3 Static Force Analysis

In order to calculate maximum breakout forces, force analysis is applied to mechanism. Two cases are examined in this study which are;

- While loader cylinder is active,

- While bucket cylinder is active,

5.3.1 Loader Cylinder is Active

To calculate forces when loader cylinder active, firstly maximum loader arm cylinder force (figure 5.3) is calculated that is equals to;

$$F = P * A \qquad\qquad (5.1)$$

$$A = \pi \frac{D^2}{4}$$

Where;

P is the maximum working pressure of the cylinder and *D* is the diameter.

D cylinder = 90 mm

P (hyd. pressure) = 230 bar

F= 146319. 7 N
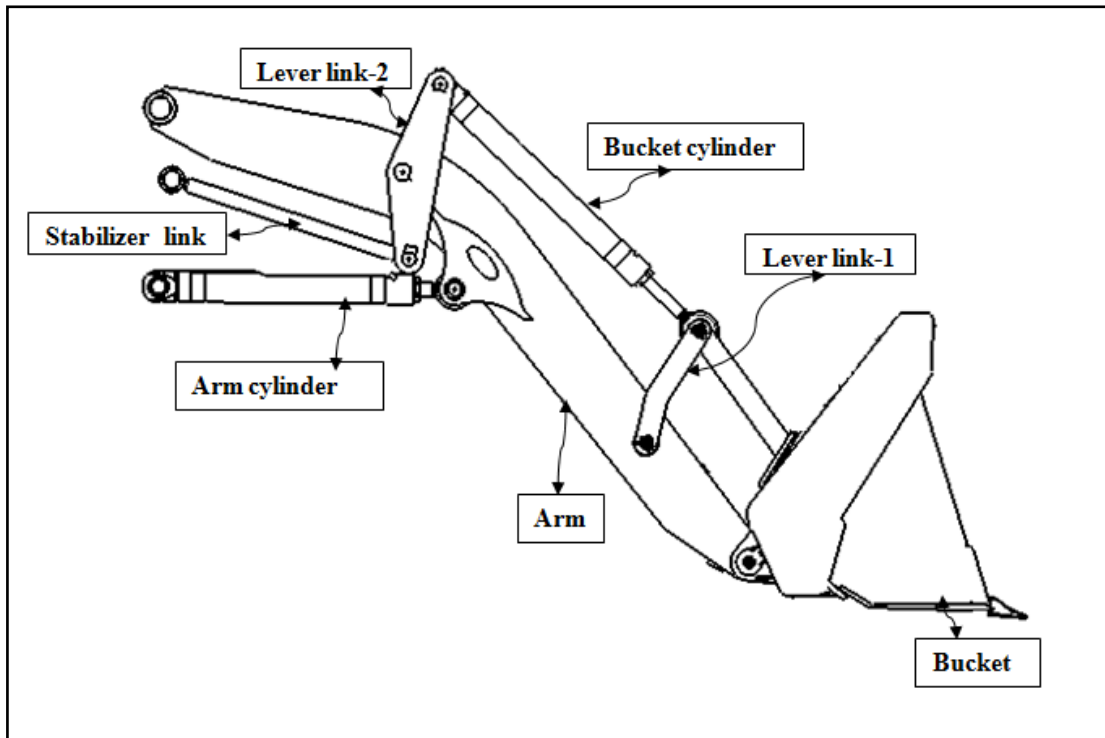
Figure5.2 Loader arm parts

Then, free body diagram of loader system is drawn (shown in the figure 5.3) and the known and unknown values are F, W, F_3, k, e, and f are equals to;

$\alpha = 42{,}37°$

$\beta = 53{,}01°$

$\gamma = 17{,}56°$
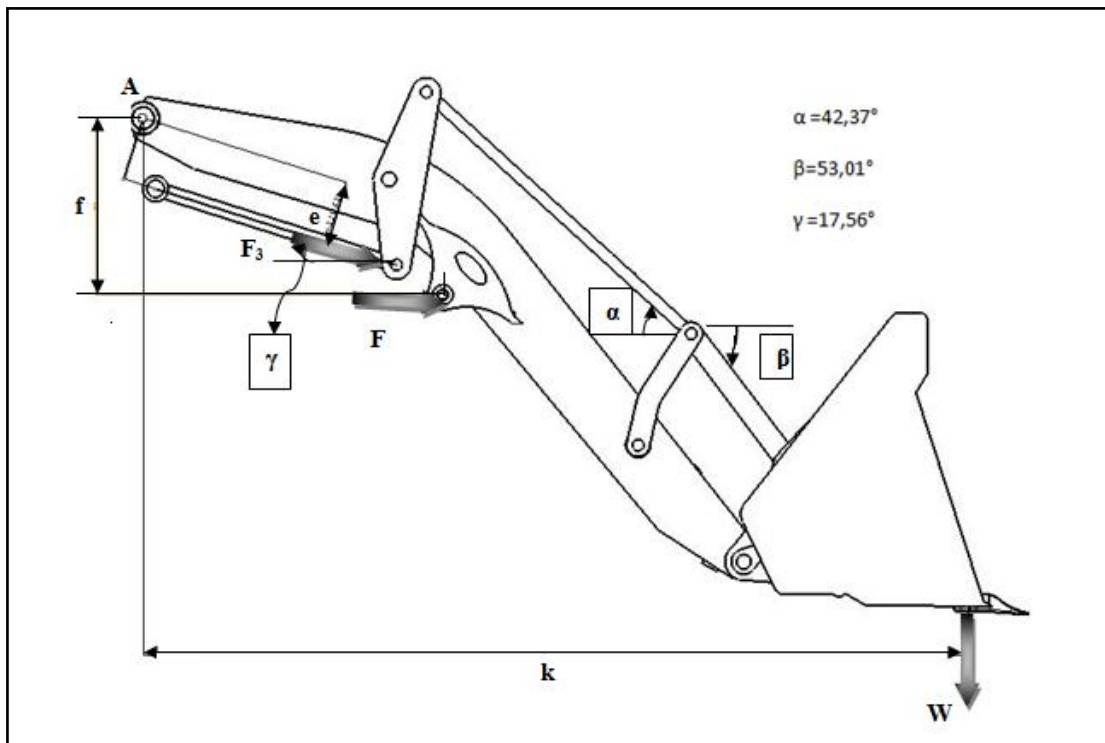
Figure5.3 Free body diagram of loader arm

F_{arm}: Loader cylinder force (N) = 146319.7 N

W: Loader arm breakout force (N) = unknown

F_3: Stabilizer link Force (N) = unknown

k: Perpendicular length from the point A to the edge of the bucket (mm) =2703 mm

e :Perpendicular length from the point A to the action line of F3 (mm) =381 mm

f: Perpendicular length from the point A to the action line of F (mm) = 615 mm

In order to find unknown values, moments are taken to the A and the result is:

$\sum M_A = 0$ then;

$$F * f - W * k + F_3 * e = 0$$

$$W = \frac{\lfloor F * f + F_3 * e \rfloor}{k} \tag{5.2}$$

F, f, e and k are known but F_3 is unknown so to find unknown values other free body diagrams will be drawn.
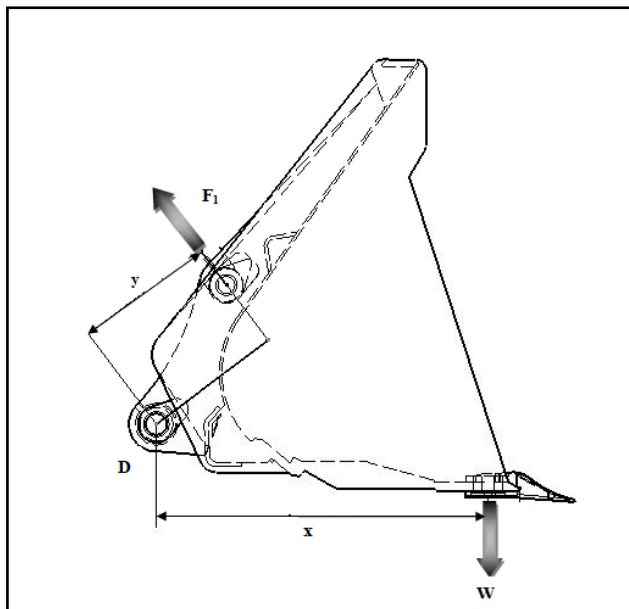
Figure5.4 Free body diagram of bucket

Moment about point D (figure 5.4) gives

$\sum M_D = 0$ then;

$F_1 * y - W * x = 0$ *then,*

$$F_1 * y = W * x$$

$$F_1 = \frac{W * x}{y} \tag{5.3}$$

Figure 5.5 Free body diagram of lever link-1

Moment about point E (figure 5.5) gives

$\sum M_E = 0$ then;

$F_1 * a - F_2 * b = 0 \; then,$

$F_1 * a = F_2 * b$

$$F_2 = \frac{F_1 * a}{b} \tag{5.4}$$

With the use of equation (5.3), F_2 is

$$F_2 = \frac{W * a * x}{b * y} \tag{5.5}$$
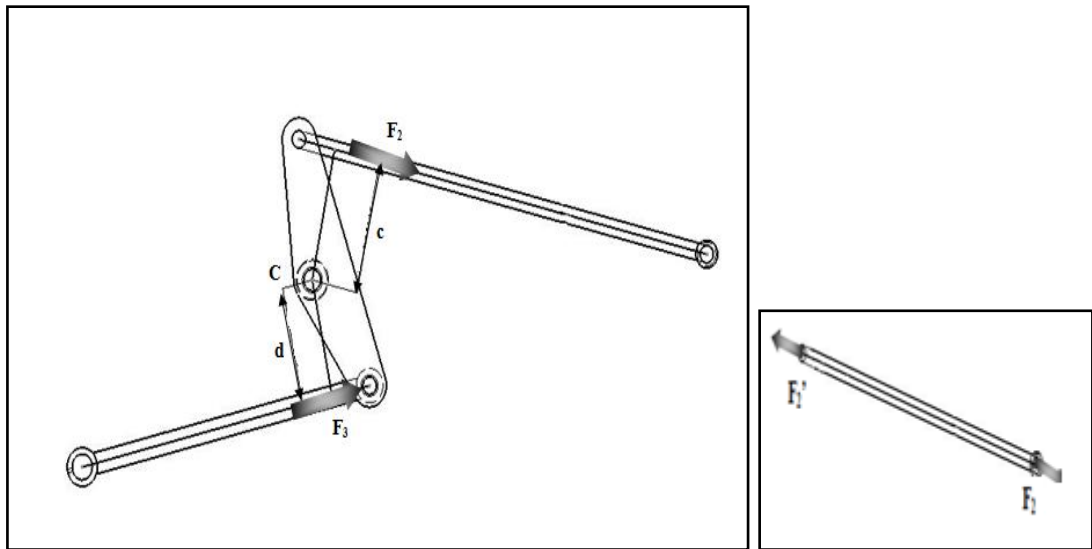
Two force member

Figure 5.6 Free body diagram of lever link-2

Moment about point C (figure 5.6) gives

$\sum M_C = 0$ then;

$F_3 * d - F_2 * c = 0$ then,

$F_3 * d = F_2 * c$

$$F_3 = \frac{F_2 * c}{d} \tag{5.6}$$

From eq. (5.5) $F_2 = \frac{W*a*x}{b*y}$ then,

$$F_3 = \frac{W * a * x * c}{b * y * d} \tag{5.7}$$

From eq. (5.2) and eq. (5.7) W is calculated as

$$W = \frac{\left\lfloor F * f + \dfrac{W * a * x * c * e}{b * y * d} \right\rfloor}{k}$$

If equation is simplified, W is reduced to,

$$W = \frac{\lfloor F * f + W * A \rfloor}{k}$$

Where

$$A = \frac{a * x * c}{b * y * d}$$

$$W = \frac{F * f}{[k - A]} \qquad (5.8)$$

To find breakout force W is multiplied with 2 since there are two arm cylinders.

$$W_{breakoutforce} = 2 * \frac{F * f}{[k - A]} \qquad (5.9)$$

$W_{breakoutforce}$: Loader arm breakout force (N)

F: Loader cylinder force (N) = 146319. 7 N

f : Perpendicular length from the point A to the action line of F (mm) = 615 mm

k : Perpendicular length from the point A to the edge of the bucket (mm) =2877 mm

$$A = \frac{a * x * c}{b * y * d}$$

a : Perpendicular length from the point E (figure 5.5) to the action line of F_1' (mm) = 381.58 mm

b : Perpendicular length from the point E (figure 5.5) to the action line of F_2 (mm) = 411.62 mm

c : Perpendicular length from the point C (figure 5.6) to the action line of F_2 (mm) = 311.49 mm

d : Perpendicular length from the point C (figure 5.6) to the action line of F_3 (mm) = 277.21 mm

x : Perpendicular length from the point D (figure 5.4) to the edge of the bucket (mm) =786 mm

y: Perpendicular length from the point D (figure 5.4) to the action line of F_1 (mm) =331.6 mm

Then when we put these values to the eq. 5.9;

$$W_{breakoutforce} = 2 * \frac{F * f}{[k - A]} = 77254.43 \, N$$

5.3.2 Bucket Cylinder is Active

To calculate forces when loader cylinder is active, firstly maximum loader bucket cylinder force (figure 5.7) are calculated that is equals to;

$$F = P * A \qquad\qquad (5.11)$$

$$A = \pi \frac{D^2}{4}$$

Where;

P is the working pressure of the cylinder and *D* is the diameter.

D cylinder = 80 mm

D rod =40 mm

P (hyd. pressure) = 230 bar

Then force in bucket cylinder becomes
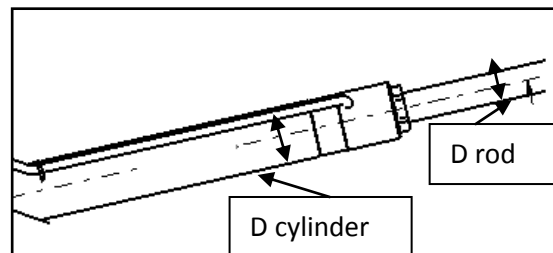
F $_{bucket\ cylinder}$ = F$_2$ = 86664 N
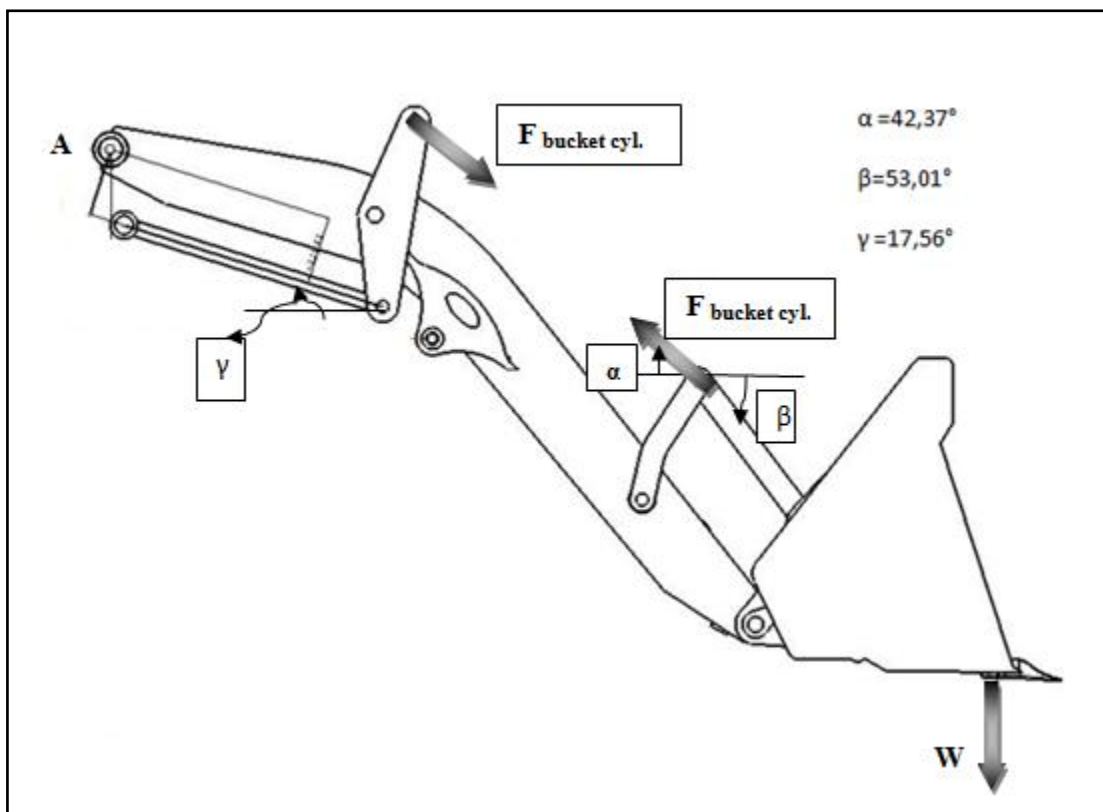
Figure 5.7 Free body diagram of loader when bucket cylinder active

In order to find maximum bucket breakout force free body diagram which are shown in the figures 5.8 and 5.9 are prepared.
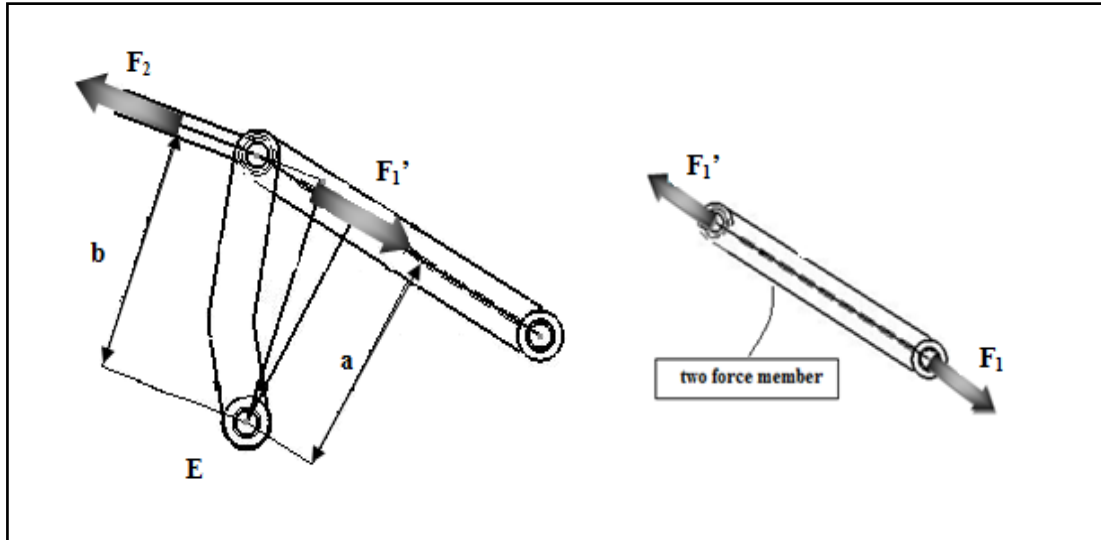
Figure 5.8 Free body diagram of lever link-1

Moment about point E (figure 5.8) gives

$\sum M_E = 0$ then;

$F_1 * a - F_2 * b = 0$ *then,*

$F_1 * a = F_2 * b$

$$F_1 = \frac{F_2 * b}{a} \tag{5.12}$$

$F_2 = 86707.9$ N

a: Perpendicular length from the point E (figure 5.8) to the action line of F_1' (mm) = 381.58 mm

b: Perpendicular length from the point E (figure 5.8) to the action line of F_2 (mm) = 411.62 mm

$$F_1 = \frac{F_2 * b}{a} = 93486.6 \, N$$
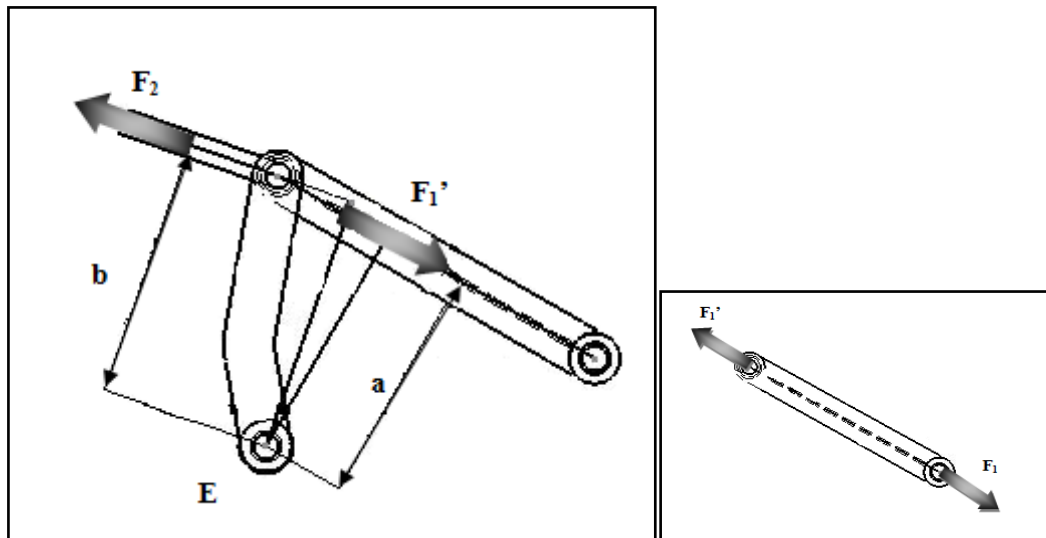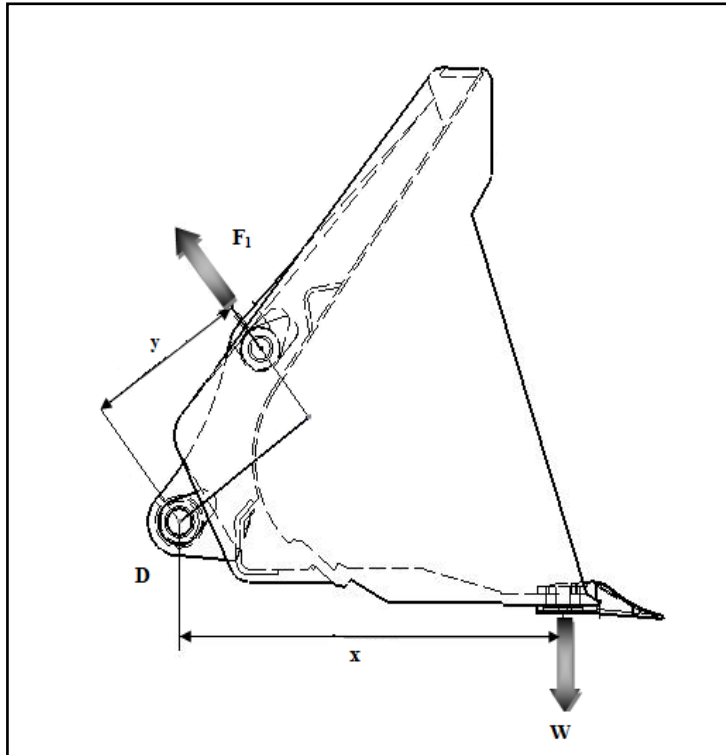
Figure 5.9 Free body diagram of bucket

Moment about point D (figure 5.9) gives

$\sum M_D = 0$ then;

$F_1 * y - W * x = 0$ *then*,

$F_1 * y = W * x$

$$W = \frac{F_1 * y}{x} \qquad\qquad (5.13)$$

$F_1 = 93486.6 \ N$

Where

x : Perpendicular length from the point D (figure 5.9) to the edge of the bucket (mm) =786 mm

y: Perpendicular length from the point D (figure 5.9) to the action line of F_1 (mm) =331.6 mm

$$W = \frac{F1 * y}{x} = 39440.42 \ N$$

$$W_{breakoutforce} = 2 * \frac{F1 * y}{x} = 78880.84 \ N$$

46

5.4 Finite Element Analysis of Front (Loader) Arm

Finite element analysis of front (loader) arm of backhoe-loader has been carried out and necessary improvements have been done in the light of results. Firstly, static analysis has been carried out and then these forces are used in FEA. After that safety factor of part is determined. While doing analysis, ANSYS Workbench (detail information of program was given in chapter 3) package program has been used.
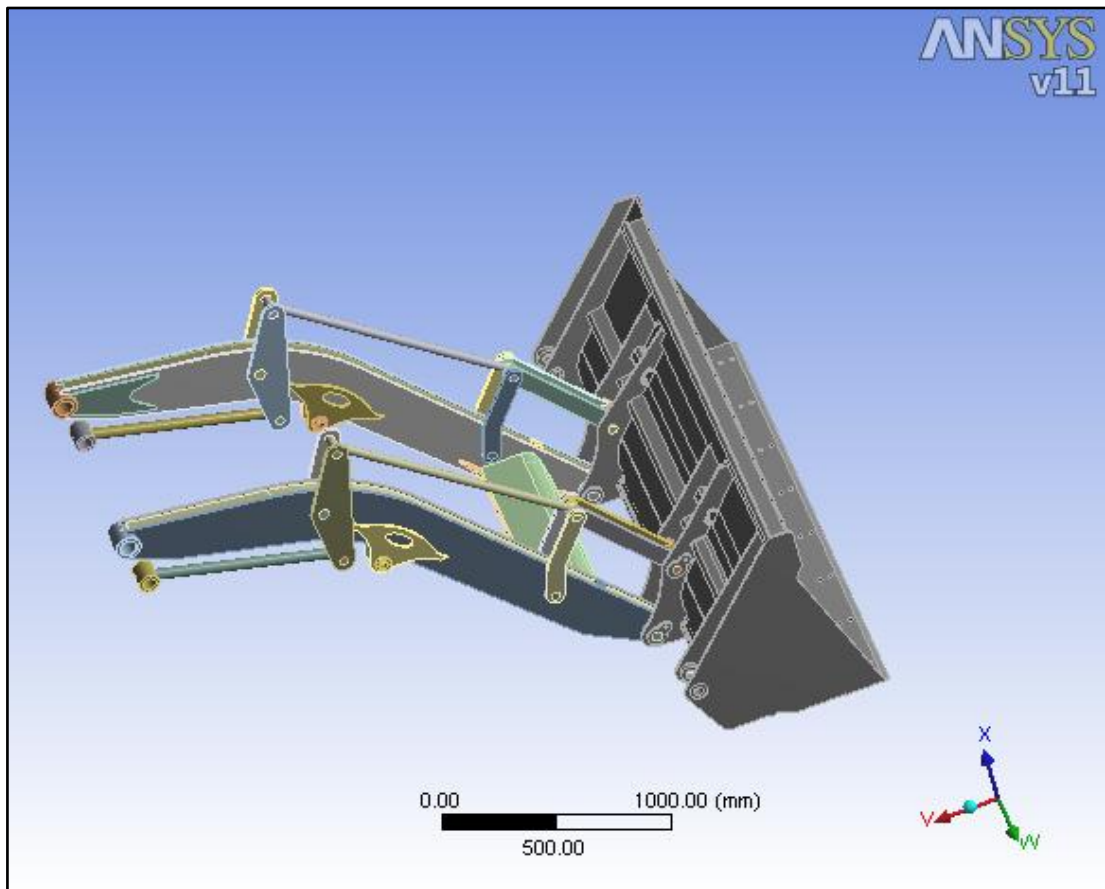
Figure 5.10 Backhoe-loader loader arm solid model.

5.4.1 Problem Definition

The Backhoe-loader front arm shown in figure 5.10 will be analyzed and also necessary improvements will be done for this part. The model is designed by CATIA CAD program and imported to ANSYS workbench analysis program. In the following sections material properties, contacts types, mesh properties, boundary conditions and loads will be defined.

5.4.2 Material Properties

The material which used to design front arm is St52-3 and for bushes and pins SAE 1040 steel is used and properties of this materials was given at table 4.1 and 4.2. After the model is imported to ANSYS Workbench material properties of each parts are given by selecting each part. Defined material properties can be used or new material can be created. In this study we created our own material ST52-3 and SAE 1040 by entering their properties (young modulus, poison ratio, density act.) as seen in the figure 5.11.
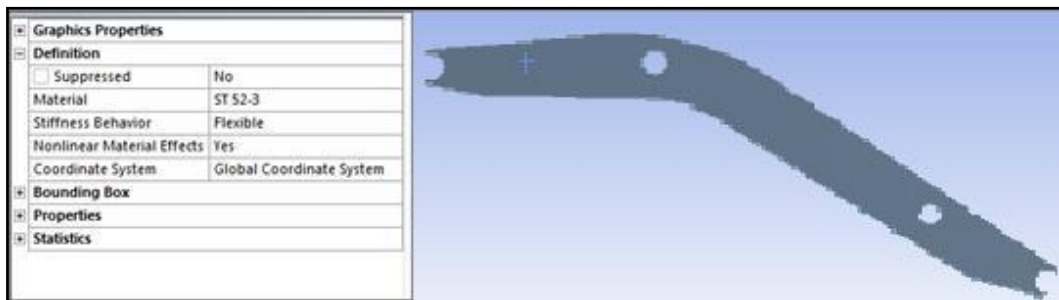
Figure 5.11 Material properties of backhoe-loader loader arm

5.4.3 Connections, Contacts and Joints

In the fem model of the front arm, different contact types and joints used together since whole system of the loader with arm, lever links and bucket are modeled. Information about contact types and joints was given in chapter 3 in the section 3.3.3.

Necessary contact types and necessary joint types are used in front arm assembly. For example revaluate joint is used between lever links and pins as showing in the figure 5.12. On the other hand bonded contact is used between body-1 and body-2 as showing in the figure 5.13.
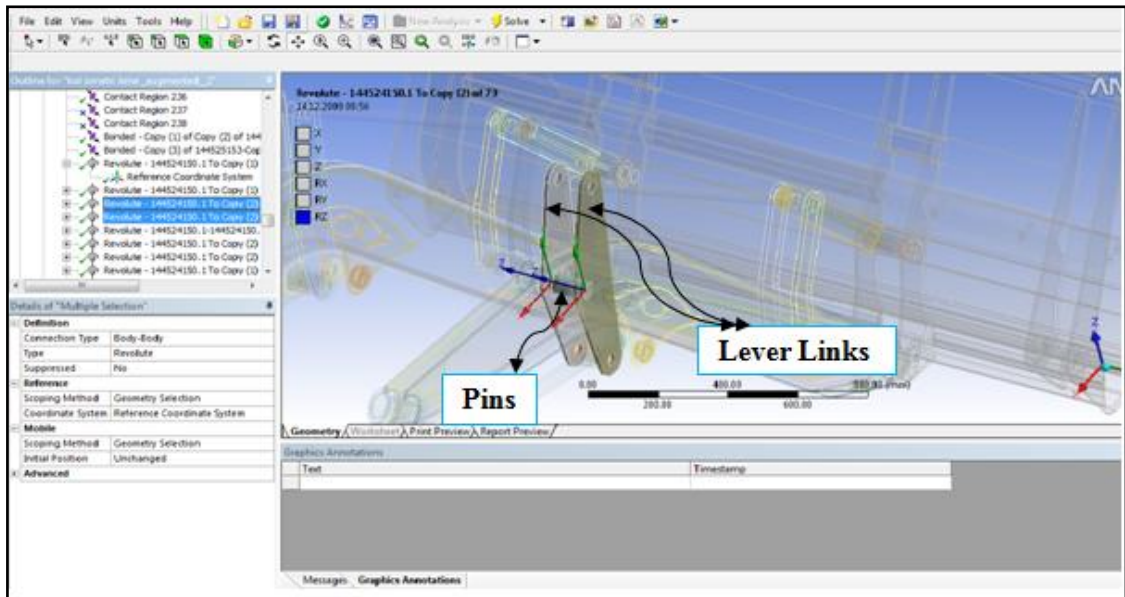
Figure 5.12 Revaluate joint between lever link and pin of loader arm.
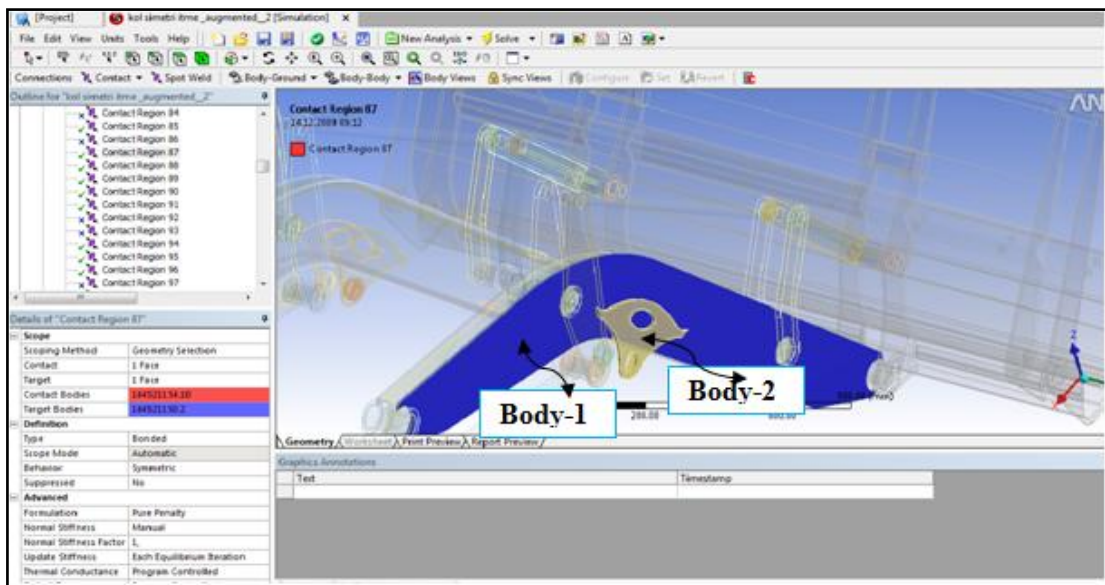
Figure 5.13 Bonded contacts between body-1 and body-2 of loader arm.

5.4.4 Mesh Properties

ANSYS workbench can generate mesh automatically and one can change or adjust mesh properties. In this study, firstly mesh done automatically, then more refined mesh is obtained by entering mesh size and other properties. Meshed view of front arm is shown in the figure 5.14. Meshed model has 223697 nodes and 73716 elements. Element types used are Solid 186 and Solid 187;

Solid 186: is a higher order 3-D 20-node solid element.

Solid 187: is a higher order 3-D, 10-node solid element.
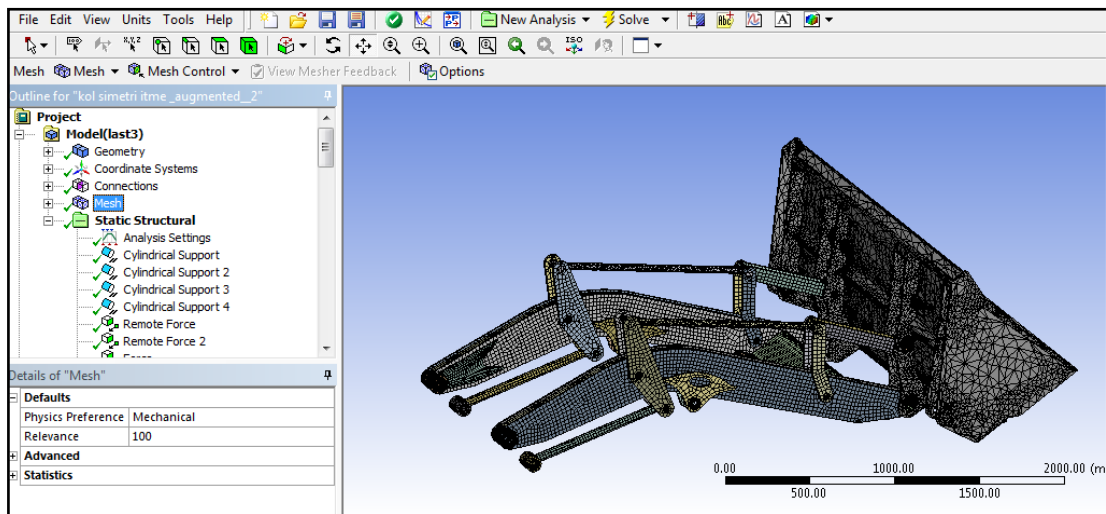
Figure 5.14 Mesh of the loader arm

5.4.5 Boundary Conditions and Loads

In order to determine maximum stress points, two condition of system are examined;

- While loader cylinder is active, (The forces used which are calculated in section 5.3.1**).**

  ➢ Symmetrical loading
  ➢ Unsymmetrical loading

- While bucket cylinder is active, (The forces used which are calculated in section 5.3.2)

  ➢ Symmetrical loading
  ➢ Unsymmetrical loading

The boundary conditions for each loading types are;

Symmetrical loading while loader cylinder is active;

For loader symmetrical loading the force F (maximum loader cylinder force) calculated in section 5.3.1 is applied from the points E, F shown in the figures 5.15 and 5.16. Points A, B, C, D are cylindrical supports.

Also the bucket is fixed with the zero remote displacement at point K shown in the figure 5.15. These boundary conditions refer to the situation of that the loader try to the load which could not afford.

F= 146319.7 N
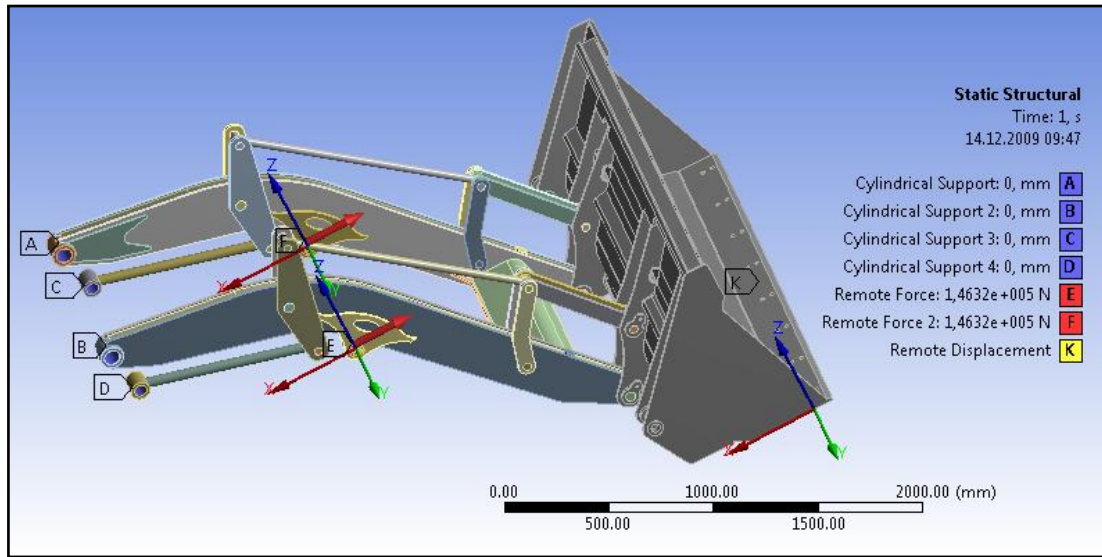
Figure 5.15 Isometric views of boundary conditions of loader symmetrical loading
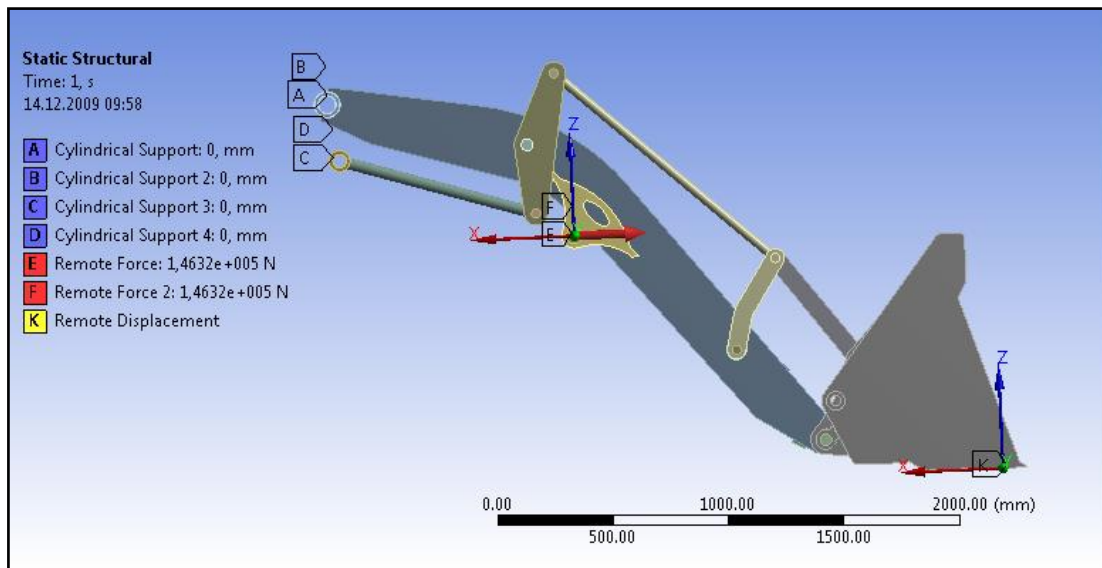
Figure 5.16 Front views of boundary conditions of loader symmetrical loading

Unsymmetrical loading while loader cylinder is active;

For loader unsymmetrical loading breakout force W (maximum loader breakout force) calculated in section 5.3.1 is applied from the points H, I shown in the figures 5.17 and 5.18. Points A, B, C, D, K and J are cylindrical supports shown in the figure

5.17. These boundary conditions refer to the situation of that the loader is fixed from the one of bucket edge.

$W_{breakout\ force} = 77254\ N$
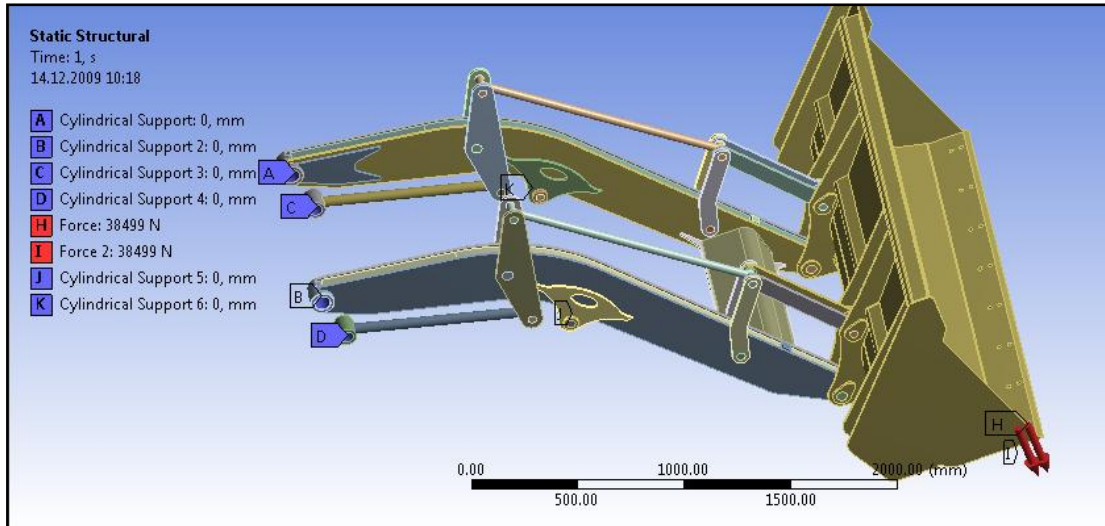
Figure 5.17 Isometric views of boundary conditions of loader unsymmetrical loading
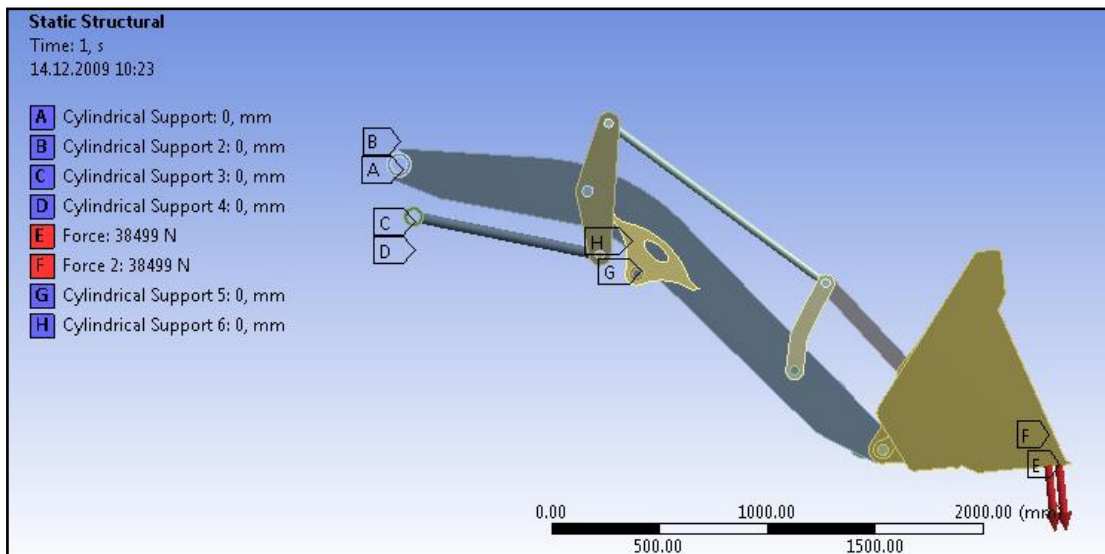
Figure 5.18 Front views of boundary conditions of loader symmetrical loading

Symmetrical loading while bucket cylinder is active;

For loader symmetrical loading while bucket cylinder is active the force F (maximum bucket cylinder force) calculated in section 5.3.2 is applied from the points K, L, M, J shown in the figures 5.19 and 5.20. Cylindrical supports are applied A, B, C, D, H and I points. Also the bucket is fixed with the zero remote

displacement at the point of G. This boundary condition refer to the situation of that the loader is working to the load with bucket cylinder which could not be load.

$F_{bucket\ cylinder} = F_2 = 86664$ N
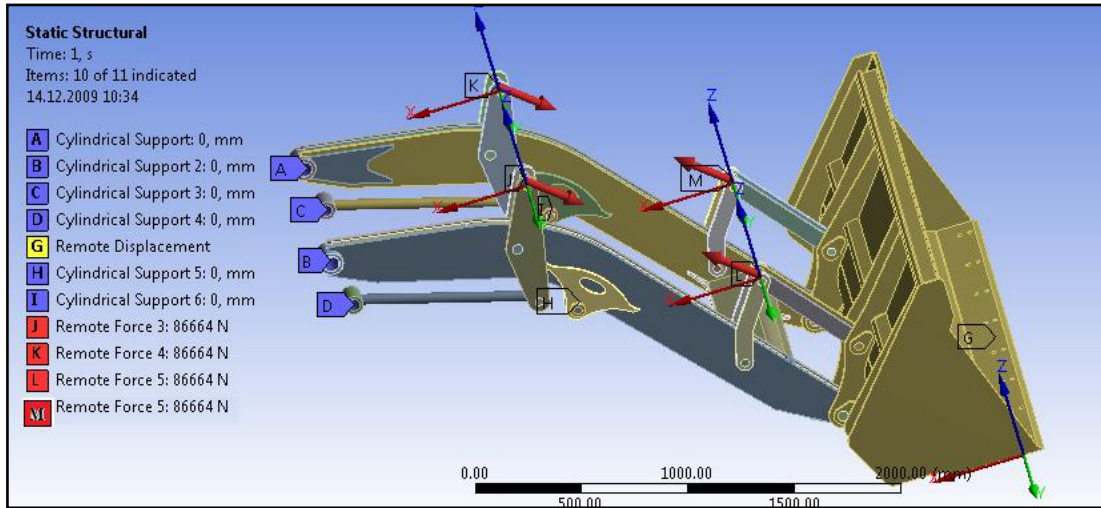
Figure 5.19 Isometric views of boundary conditions of loader symmetrical loading when bucket cylinder is active
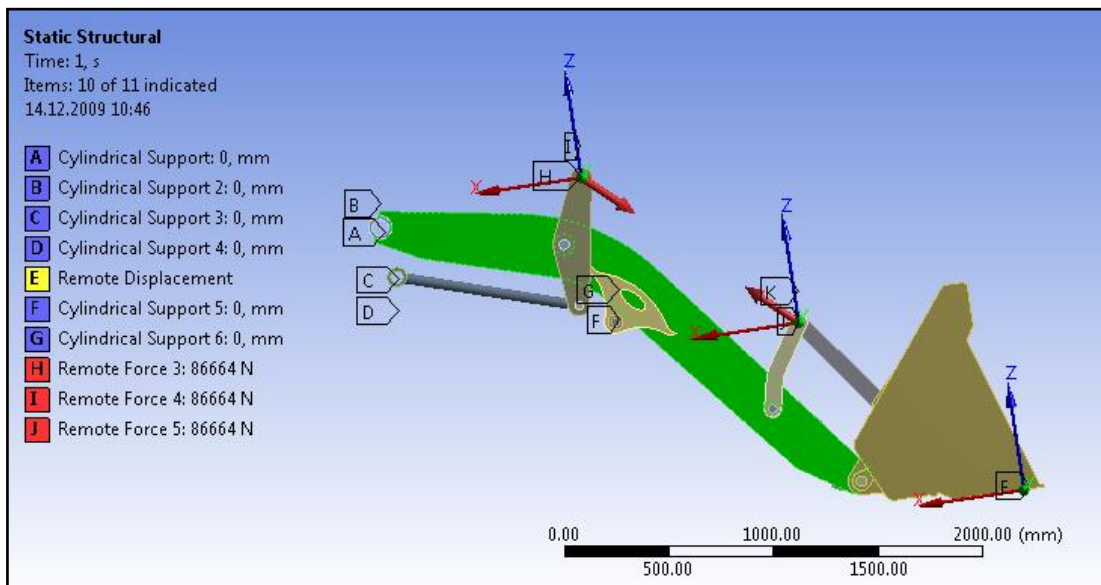
Figure 5.20 Front views of boundary conditions of loader symmetrical loading when bucket cylinder is active

Unsymmetrical loading while bucket cylinder is active;

The condition is same as the unsymmetrical loading while loader cylinder is active. $W_{breakout\ force}$ (maximum bucket breakout force) calculated in section 5.3.2 from the equation 5.13.

$$W_{breakoutforce} = 78880.84\ N$$

5.4. 6 Solution and Results

In this section finite element analysis of Front arm is presented. After importing geometry, defining material properties, loading and applying boundary conditions, solution is carried out. When the solution is done, it is possible to check all the parameters like stresses, strains, safety factor, reaction force, etc.

Analyses have been varied out for two different loadings as symmetric and unsymmetrical situations.

Reaction forces calculated in static analysis in section 5.3 are nearly equal to the calculated forces in ANSYS Workbench. So, our analysis gives reasonable results. For example maximum breakout force, W, has been calculated 77254.43 N in the section 5.3.2 and as seen from the figure 5.21 this value has been obtained as 77167 N by using ANSYS Workbench at the conditions of symmetrical loading while loader cylinder is active. Also F_1 (figure 5.4) equals to $F_1 = 183118.2\ N$ and this value is obtained as 183041 N (total values of F_1 left and right) by using ANSYS workbench shown in the figure 5.22.
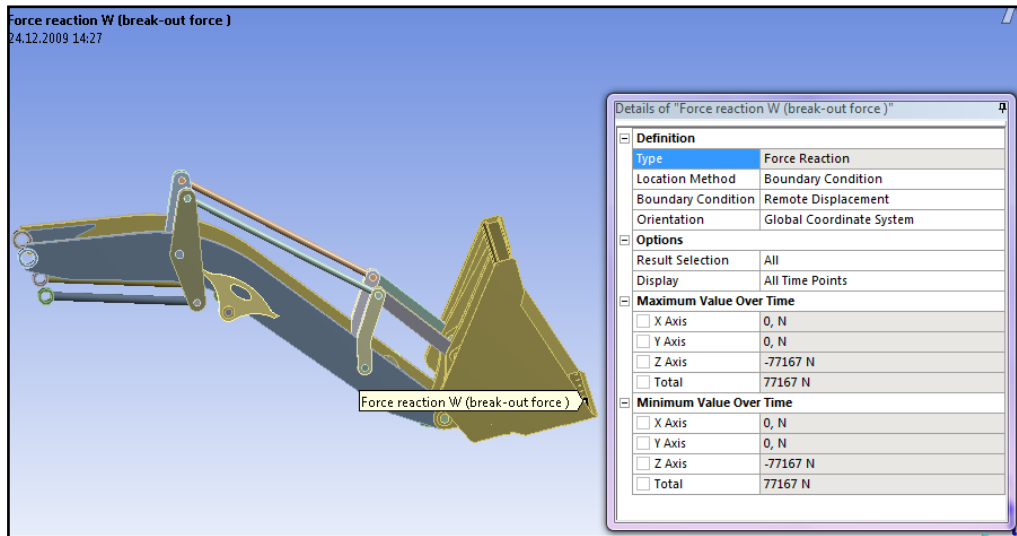
Figure 5.21 Reaction force W (Maximum breakout-force) at the conditions of symmetrical loading and loader cylinder active.
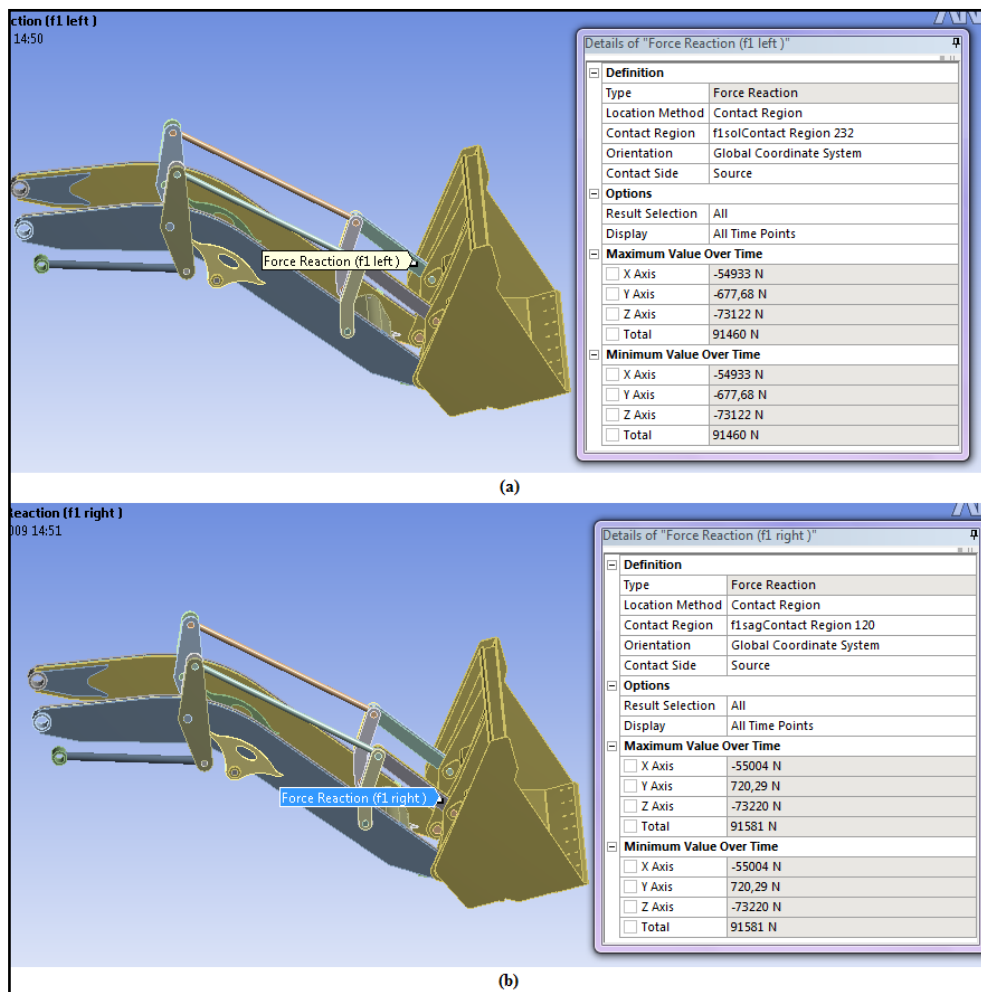
Figure 5.22 Reaction force F_1 at the conditions of symmetrical loading and loader cylinder active. (a) Force reaction F_1 left side (b) Force reaction F_1 right side

5.4.6.1 Analysis Results of Front Arm for Each Loading Types

Analysis results have been given for four different loading conditions and these are;

Analysis result of Symmetrical loading while loader cylinder is active;

First analysis is done considering symmetrical loading while loader cylinder is active and the equivalent (von-misses) stress distribution of loader is shown in figures 5.23-5.26. Especially maximum stressed zones are zoomed in figures.
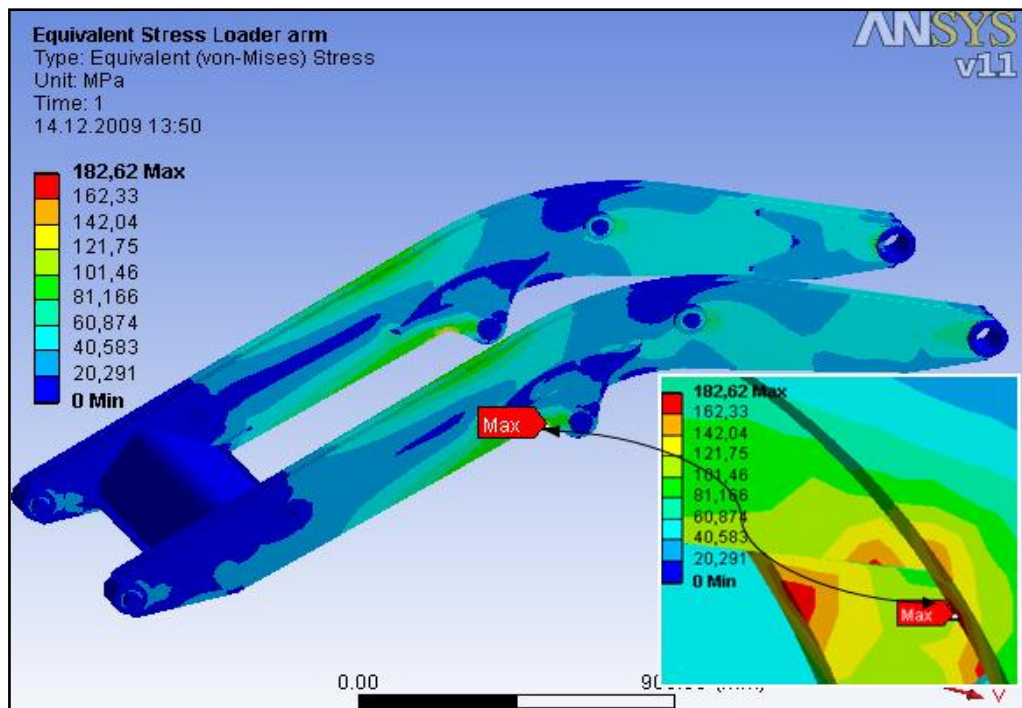
Figure 5.23 Equivalent stress distribution of loader arm

Figure 5.24 shows the equivalent (von-misses) stress distribution of the right and left side of the loader arm. Stress distributions and values of stresses are symmetrical for left and right side.
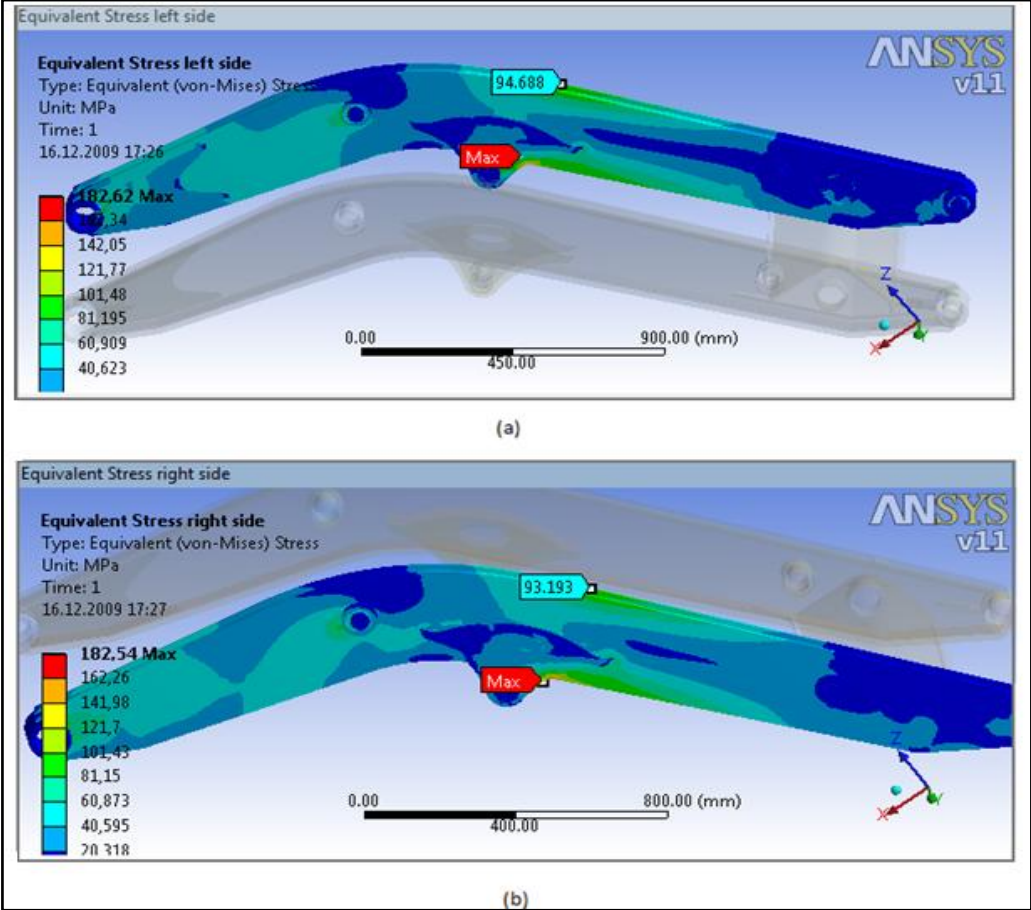
Figure 5.24 Equivalent stress distribution of symmetrical loading while loader cylinder is active. (a) Loader arm left side, (b) Loader arm right side
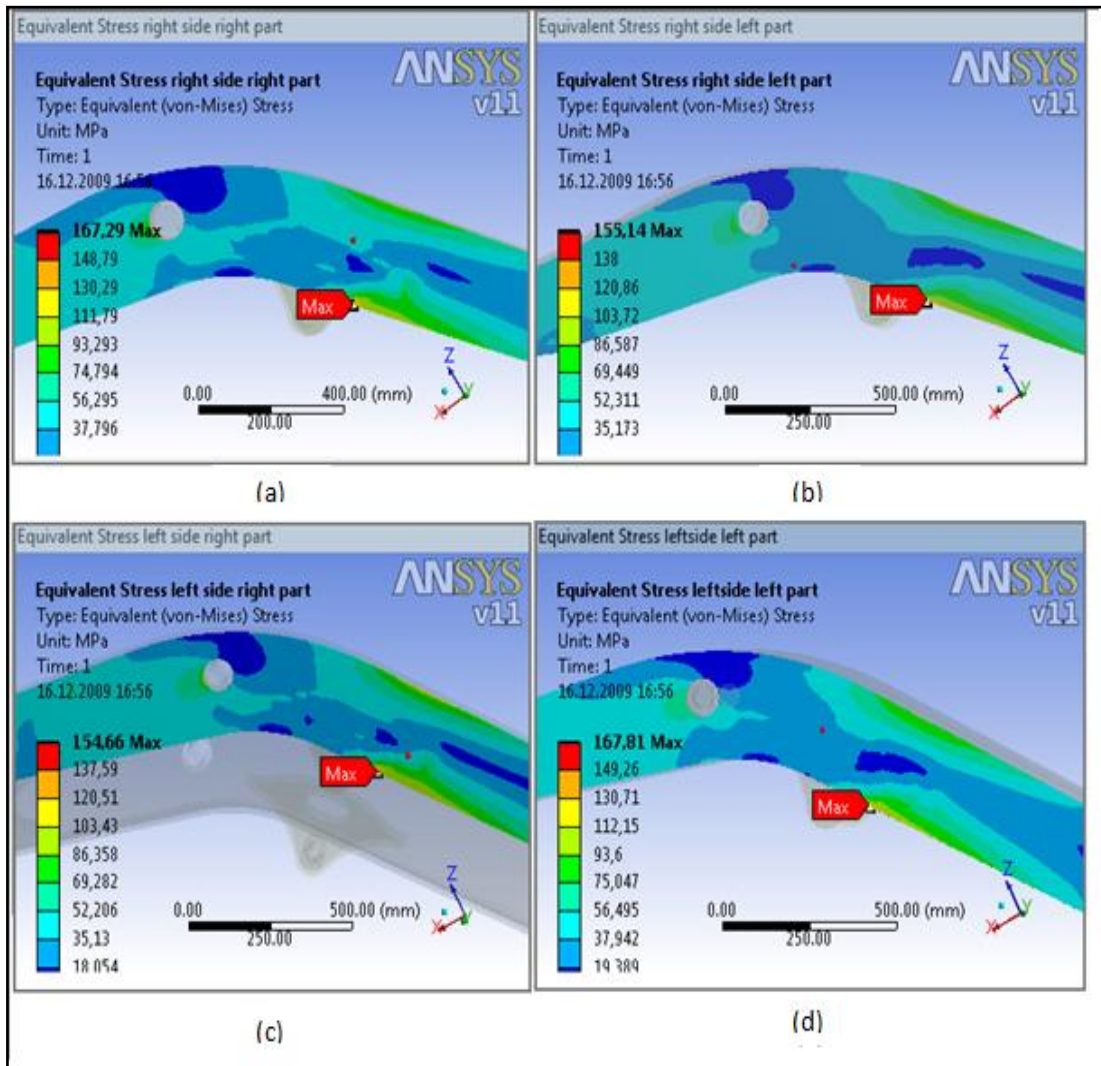
Figure 5.25 Equivalent stress distribution of symmetrical loading while loader cylinder is active. (a) Loader arm right side right part, (b) Loader arm right side left part, (c) Loader arm left side right part, (d) Loader arm left side left part.

Figure 5.25 shows the equivalent (von-misses) stress distribution of the right and left parts of the loader arm.

Figure 5.26 Equivalent stress distribution of symmetrical loading while loader cylinder is active. (a) Loader arm right side right support, (b) Loader arm right side left support, (c) Loader arm left side right support, (d) Loader arm left side left support.

Figure 5.26 shows the equivalent (von-misses) stress distribution of the supports.

Analysis result of Unsymmetrical loading while loader cylinder is active;

Second analysis is done considering unsymmetrical loading while loader cylinder is active and the equivalent (von-misses) stress distribution of loader is shown in figures 5.27-5.30.

Figure 5.28 shows the equivalent (von-misses) stress distribution of the right side and left side of the loader arm. For unsymmetrical loading, maximum stress occurs at the right side of the loader arm and its value is 314 MPa as seen in the figure.

Figure 5.27 Equivalent stress distribution of loader arm

Figure 5.28 Equivalent stress distribution of **unsymmetrical** loading while loader cylinder is active. (a) Loader arm left side, (b) Loader arm side right side

Figure 5.29 Equivalent stress distribution of **unsymmetrical** loading while loader cylinder is active. (a) Loader arm right side right part, (b) Loader arm right side left part, (c) Loader arm left side right part, (d) Loader arm left side left part.

Figure 5.29 shows the equivalent (von-misses) stress distribution of the right and left parts of the loader arm. Maximum stress distribution is at the right and left part of the right side.

Figure 5.30 shows the equivalent (von-misses) stress distribution of the supports for unsymmetrical loading. Maximum stress occurs at the right side supports and its value is 314.69 MPa.

Figure 5.30 Equivalent stress distribution of **unsymmetrical** loading while loader cylinder is active. (a) Loader arm right side right support, (b) Loader arm right side left support, (c) Loader arm left side right support, (d) Loader arm left side left support.

Analysis result of Symmetrical loading while bucket cylinder is active;

Third analysis is done considering symmetrical loading while bucket cylinder is active and the Equivalent (von-misses) stress distribution of loader is shown in figures 5.31-5.34. Figure 5.31 shows the equivalent (von-misses) stress distribution of whole structure of front arm. Figure 5.32 shows the equivalent (von-misses) stress distribution of the right and left side of the front arm.
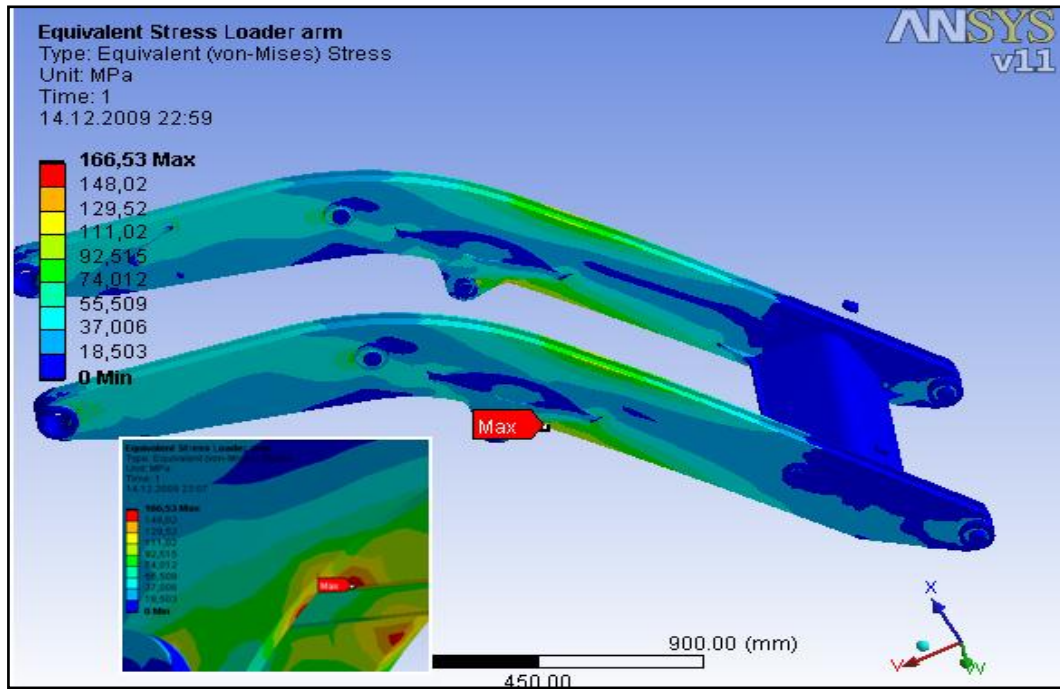
Figure 5.31 Equivalent stress distribution of loader arm while bucket cylinder is active
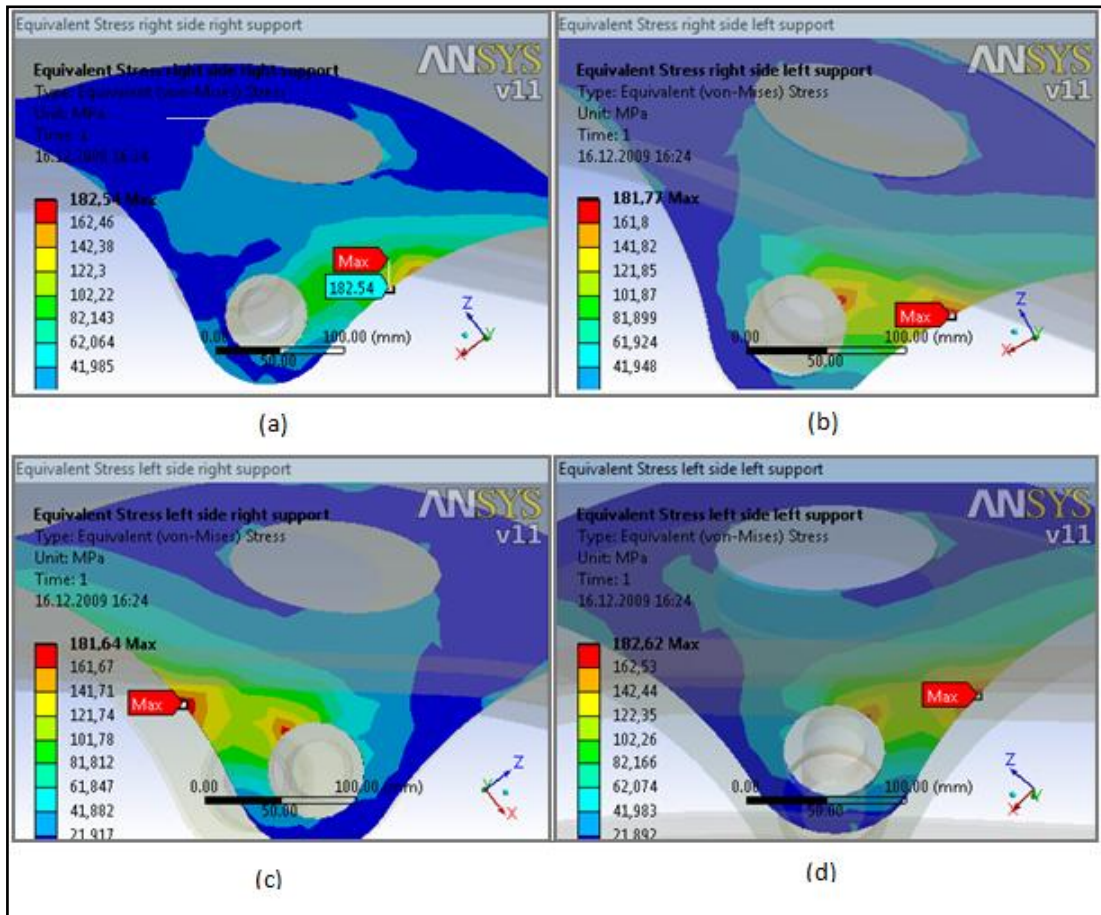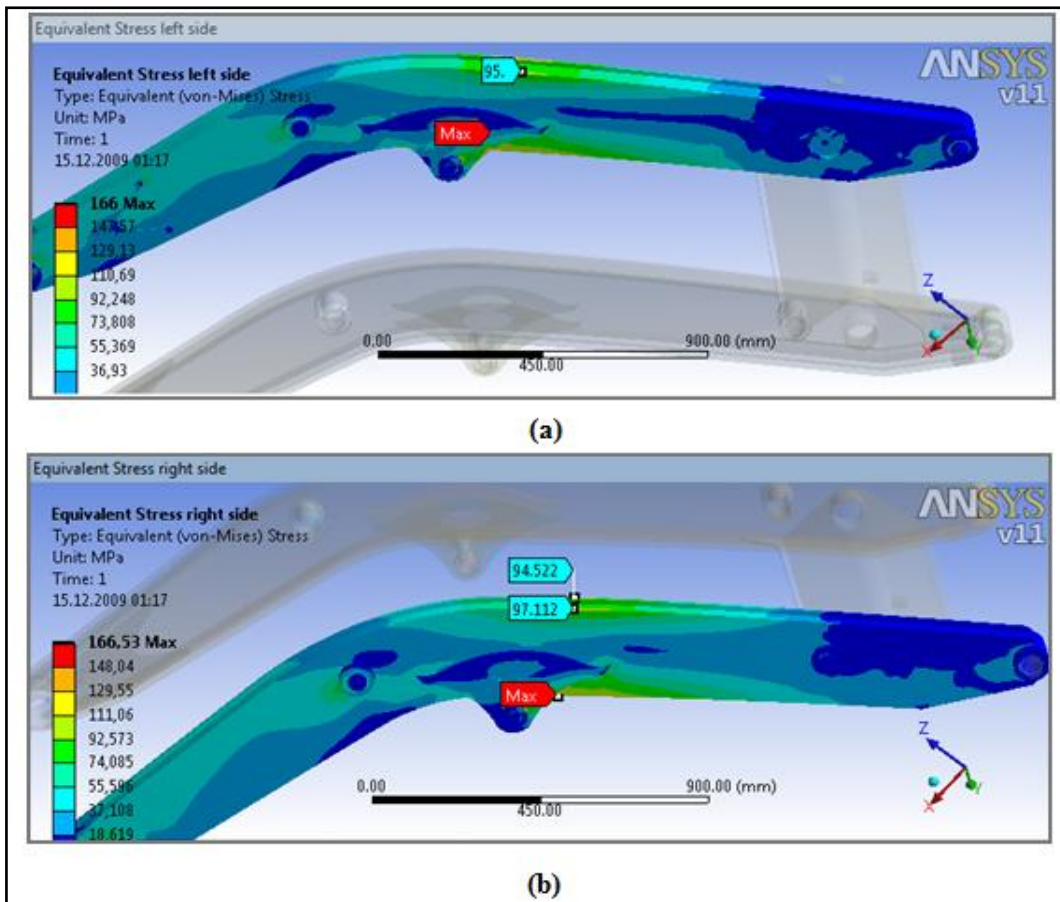

Figure 5.32 Equivalent stress distribution of **symmetrical** loading while **bucket cylinder** is active. (a) Loader arm left side, (b) Loader arm side right side
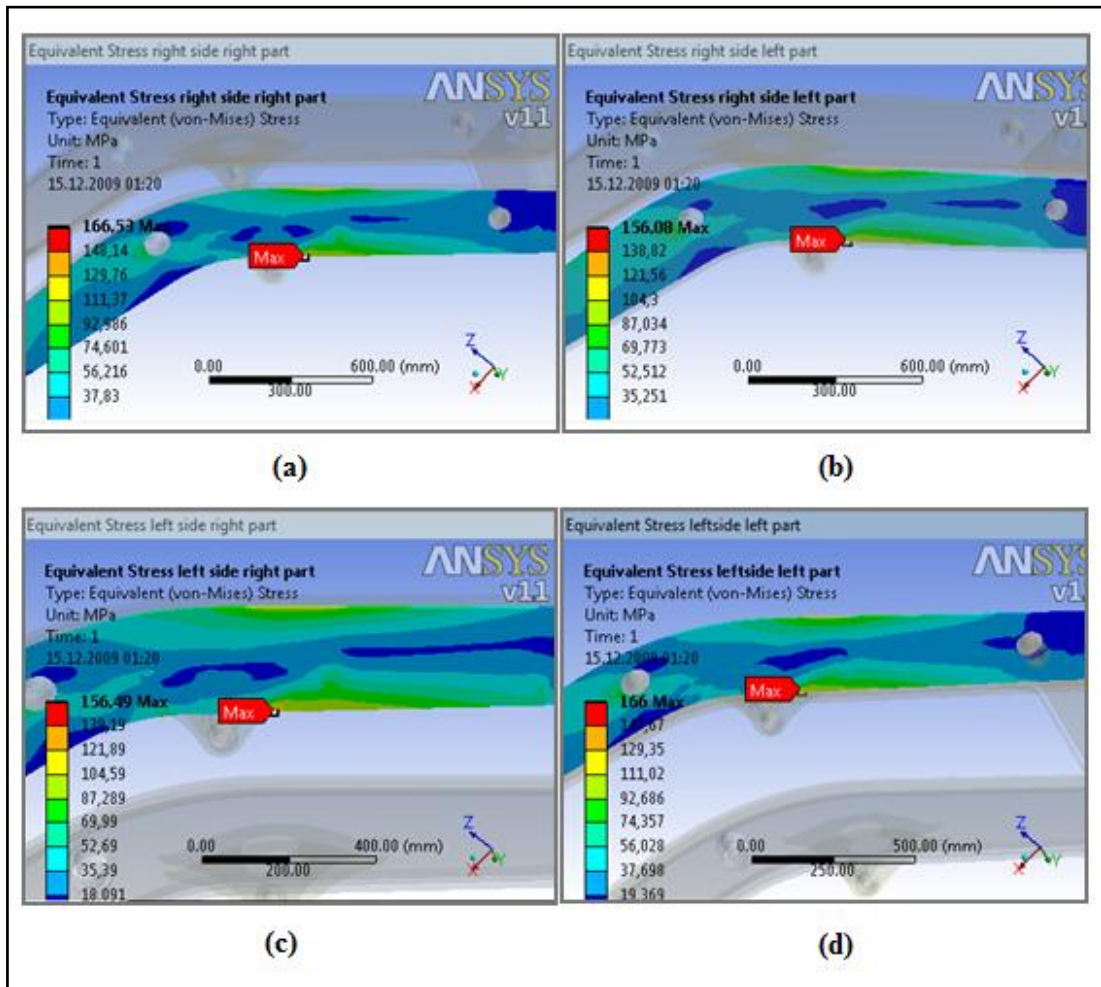
Figure 5.33 Equivalent stress distribution of **symmetrical** loading while **bucket cylinder** is active. (a) Loader arm right side right part, (b) Loader arm right side left part, (c) Loader arm left side right part, (d) Loader arm left side left part.

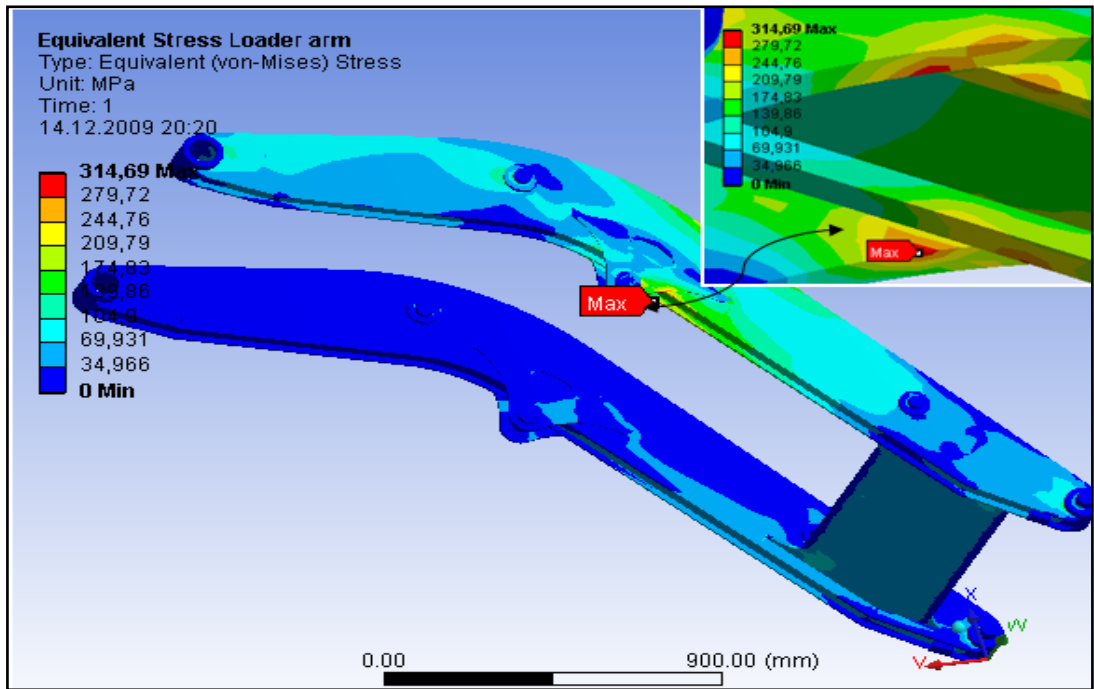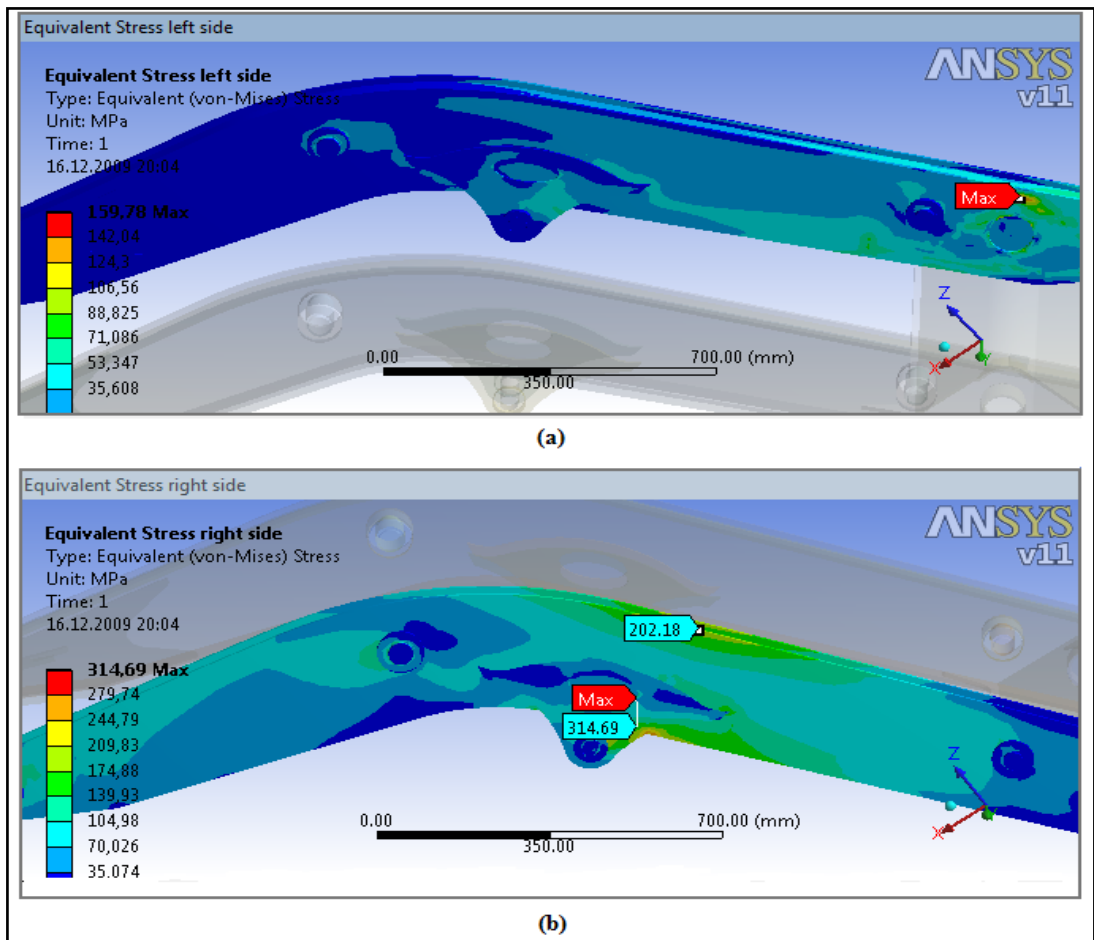Figure 5.33 shows the equivalent (von-misses) stress distribution of the right and left parts of the loader arm while bucket cylinder is active. As seen in the figure 5.33, stress distribution is symmetrical.

Figure 5.34 shows the equivalent (von-misses) stress distribution of the supports for symmetrical loading while bucket cylinder is active. Stress distribution is symmetrical and maximum value is 163.9 MPa.
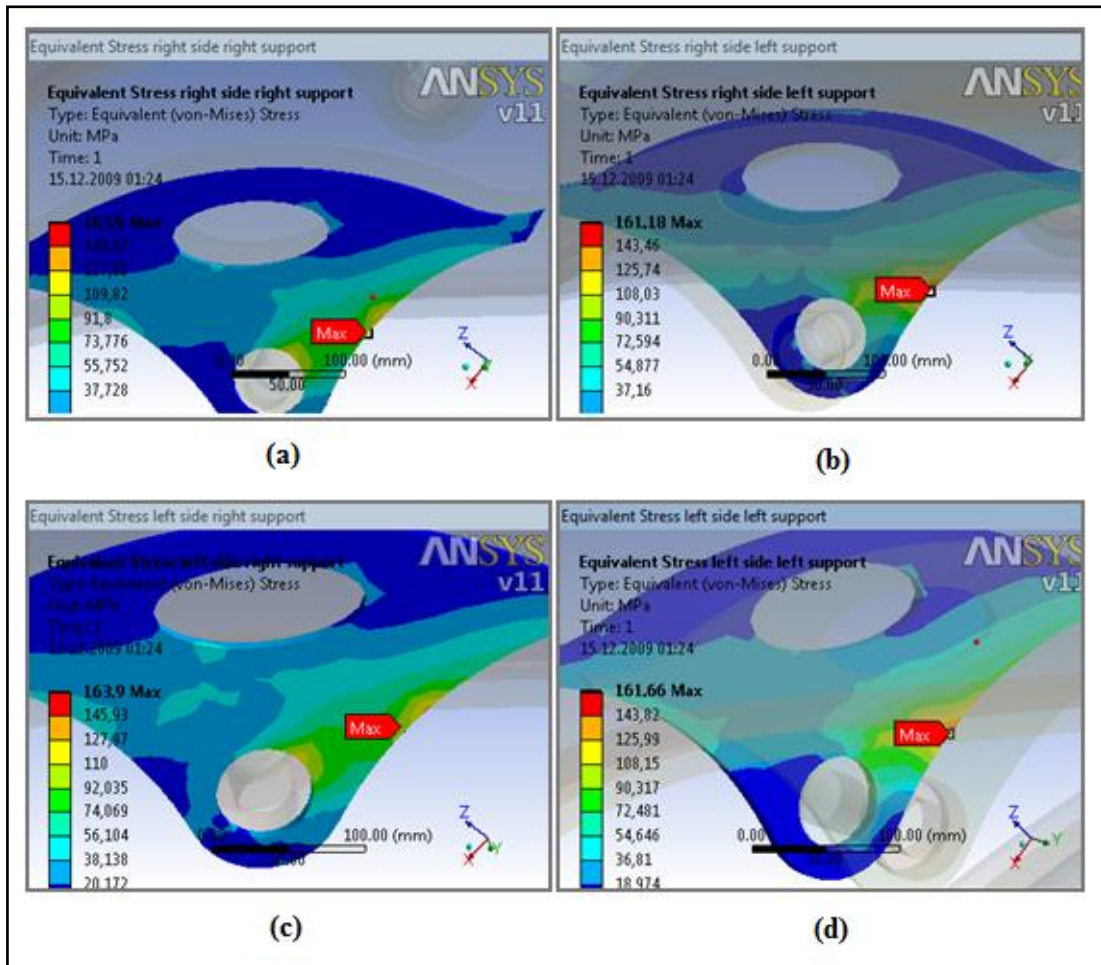
Figure 5.34 Equivalent stress distribution of **symmetrical** loading while **bucket cylinder** is active. (a) Loader arm right side right support, (b) Loader arm right side left support, (c) Loader arm left side right support, (d) Loader arm left side left support.

<u>**Analysis result of Unsymmetrical loading while Bucket cylinder is active;**</u>

Then analysis is done considering unsymmetrical loading while Bucket cylinder is active and the equivalent (von-misses) stress distribution of loader is shown in figures 5.35-5.38. Figure 5.35 shows the equivalent (von-misses) stress distribution of whole structure of loader arm. The maximum value is 322.39 MPa.
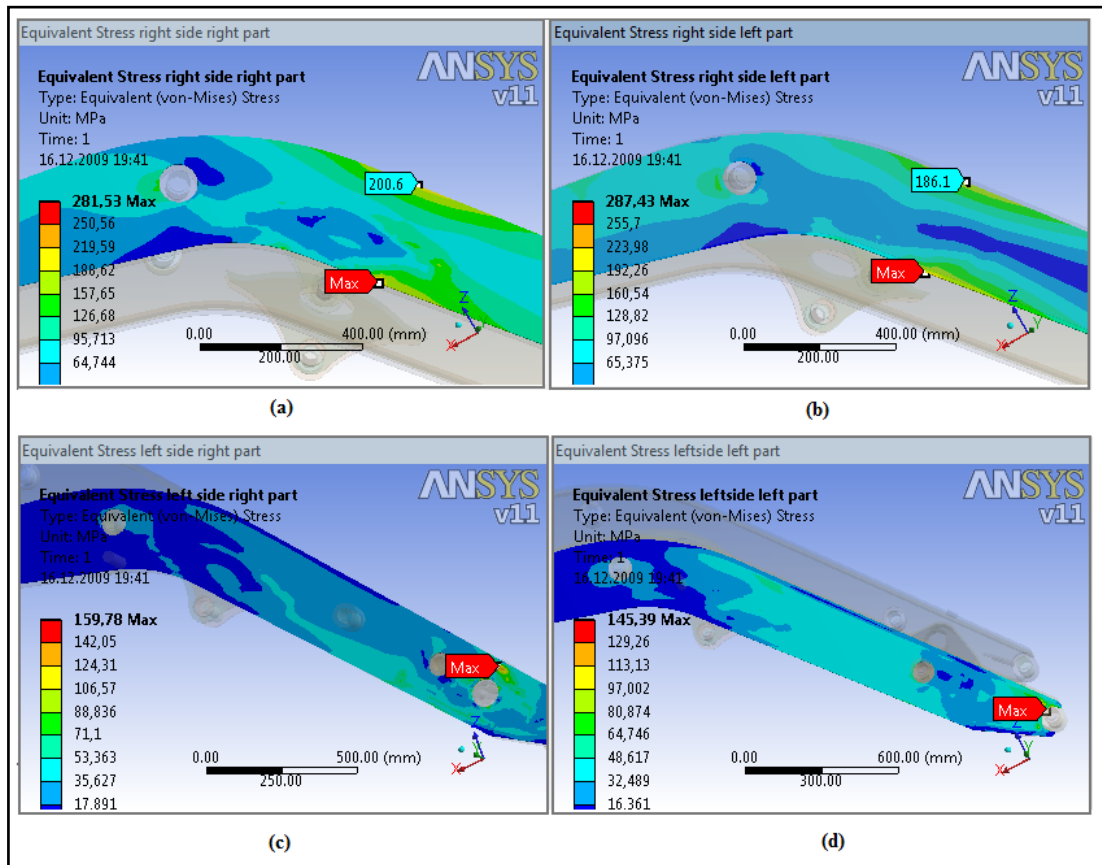
Figure 5.36 shows the equivalent (von-misses) stress distribution of the right and left side of the loader arm. For unsymmetrical loading maximum stress occurs at the right side of the loader arm.
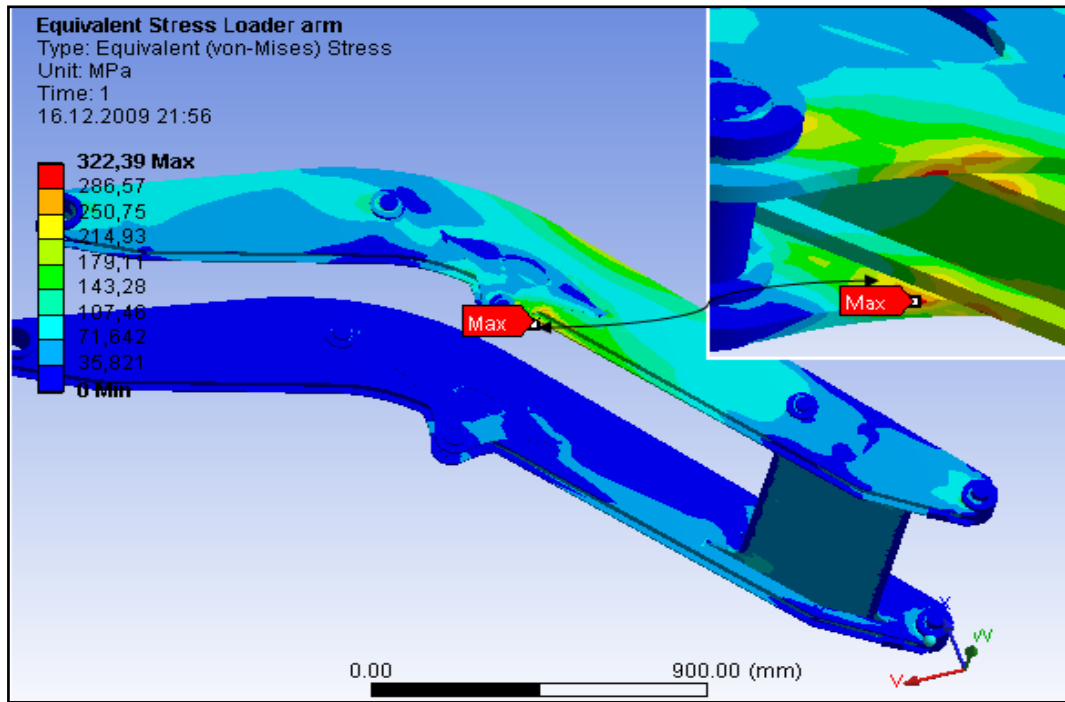
Figure 5.35 Equivalent stress distribution of loader arm while **bucket cylinder** is active
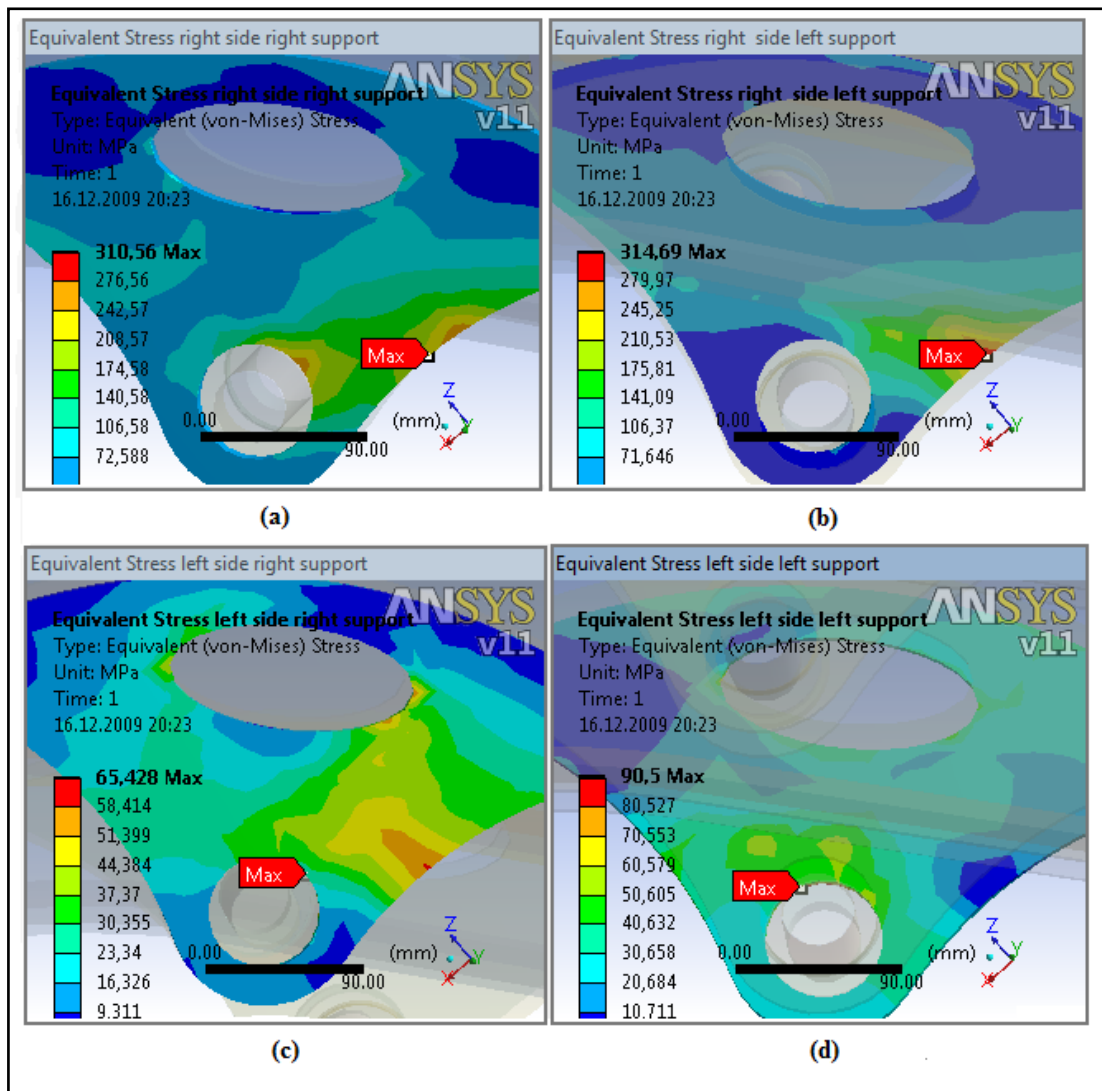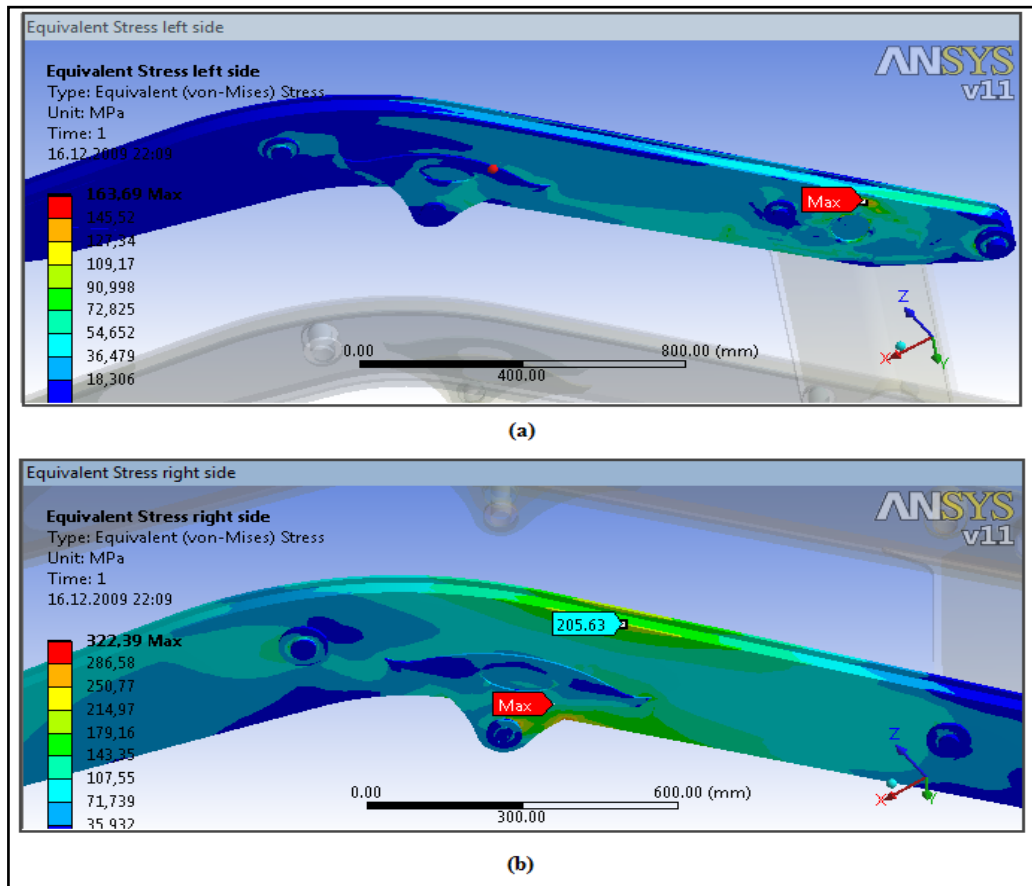

Figure 5.36 Equivalent stress distribution of **unsymmetrical** loading while **bucket cylinder** is active. (a) Loader arm left side, (b) Loader arm side right side
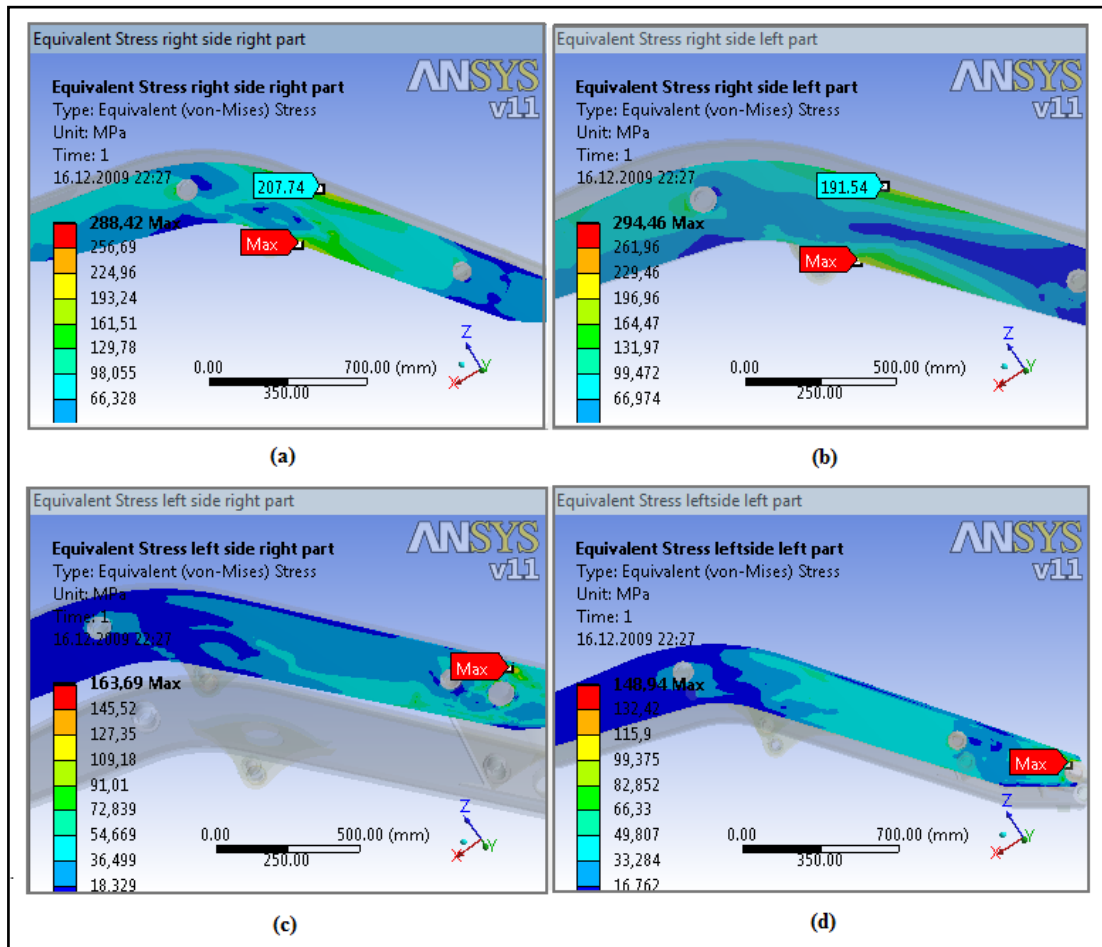
Figure 5.37 Equivalent stress distribution of **unsymmetrical** loading while **bucket cylinder** is active. (a) Loader arm right side right part, (b) Loader arm right side left part, (c) Loader arm left side right part, (d) Loader arm left side left part.

Figure 5.37 shows the equivalent (von-misses) stress distribution of the right and left parts of the loader arm. Maximum stress distribution occurs at the right and left part of the right side.

Figure 5.38 shows the equivalent (von-misses) stress distribution of the supports for unsymmetrical loading. Maximum stress distribution occurs at the right side supports and its value is 322.39 MPa.
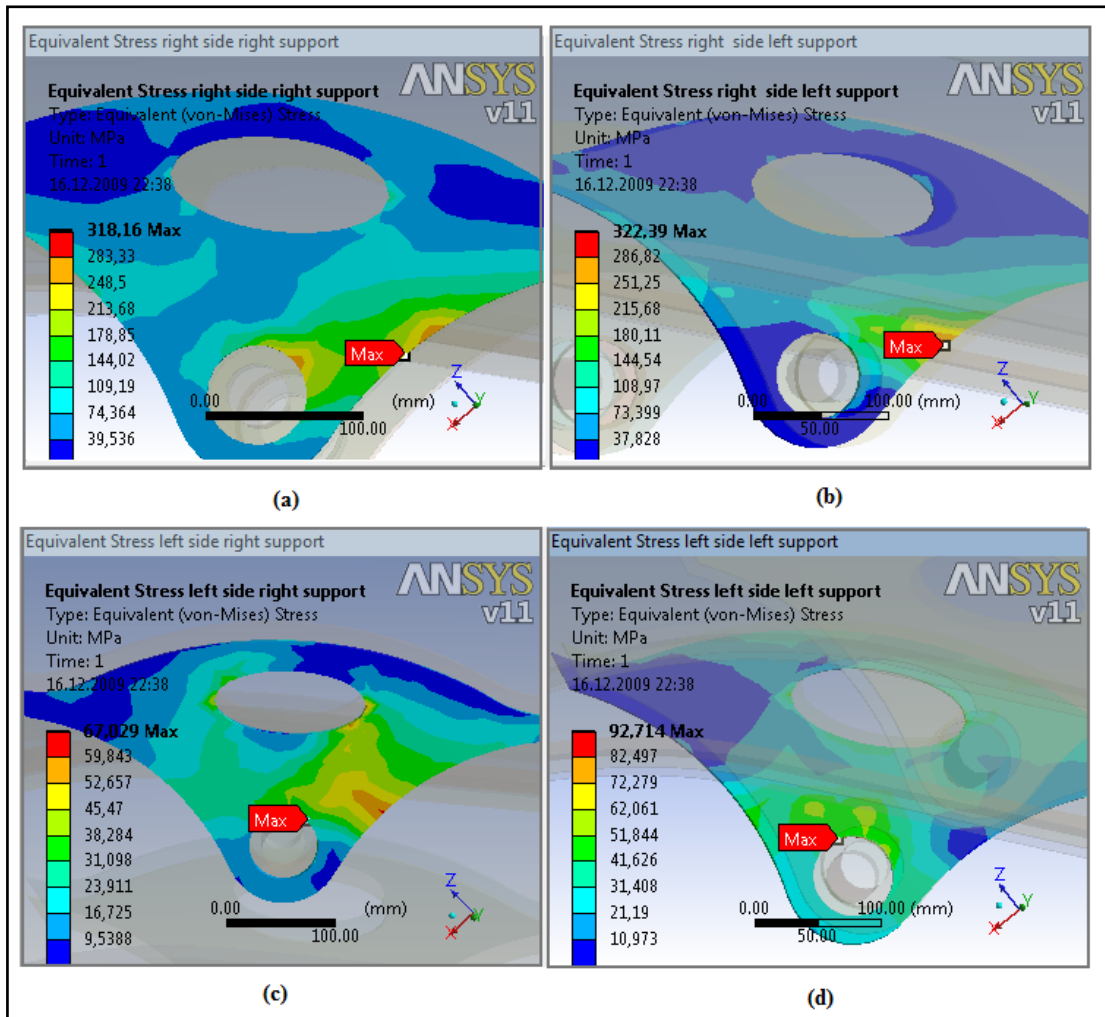
Figure 5.38 Equivalent stress distribution of **unsymmetrical** loading while **bucket cylinder** is active. (a) Loader arm right side right support, (b) Loader arm right side left support, (c) Loader arm left side right support, (d) Loader arm left side left support.

Stress results of front arm are given in figures 5.23-5.38. According to results maximum stress values and bodies are summarized in table 5.1 for both forces and boundary conditions.
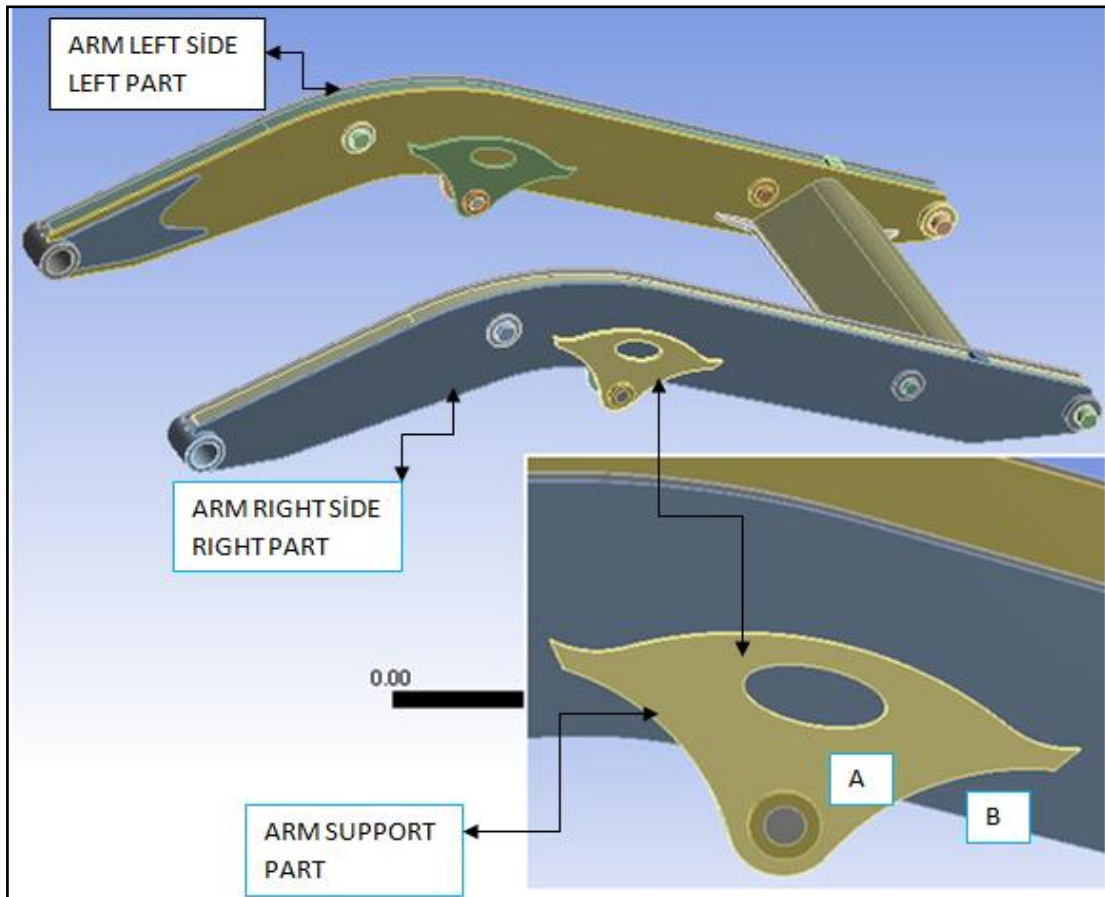
Figure 5.39 Loader arm

Table 5.1 Maximum stress points of original front arm for each loading types

	Maximum equivalent stress (MPa)	Bodies maximum stress occurs
Symmetrical loading while loader cylinder is active	182.62	Arm support part shown figures 5.23 and 5.26 (d)
Unsymmetrical loading while loader cylinder is active	314.69	Arm support part shown figures 5.27 and 5.30 (b)
Symmetrical loading while bucket cylinder is active	166.53	Arm right side right part shown figures 5.31 and 5.33 (a)
Unsymmetrical loading while bucket cylinder is active	322.39	Arm support part shown figures 5.35 and 5.38 (b)

To reduce the calculated stress values some improvements are done shown in the figure 5.40 and 5.41. Analysis result of each loading types with these improvement are given in the following sections. To reduce the maximum stress some improvements are done to maximum stressed points shown in table 5.1. First improvement is carried out by increasing thickness of the arm left side left part and arm right side left part 8 to 10 mm shown in the figure 5.40 and second improvement is carried out by changing original arm support with improved one shown in the figure 5.41. The maximum stress results with these improvements are given in section 5.4.6.2.
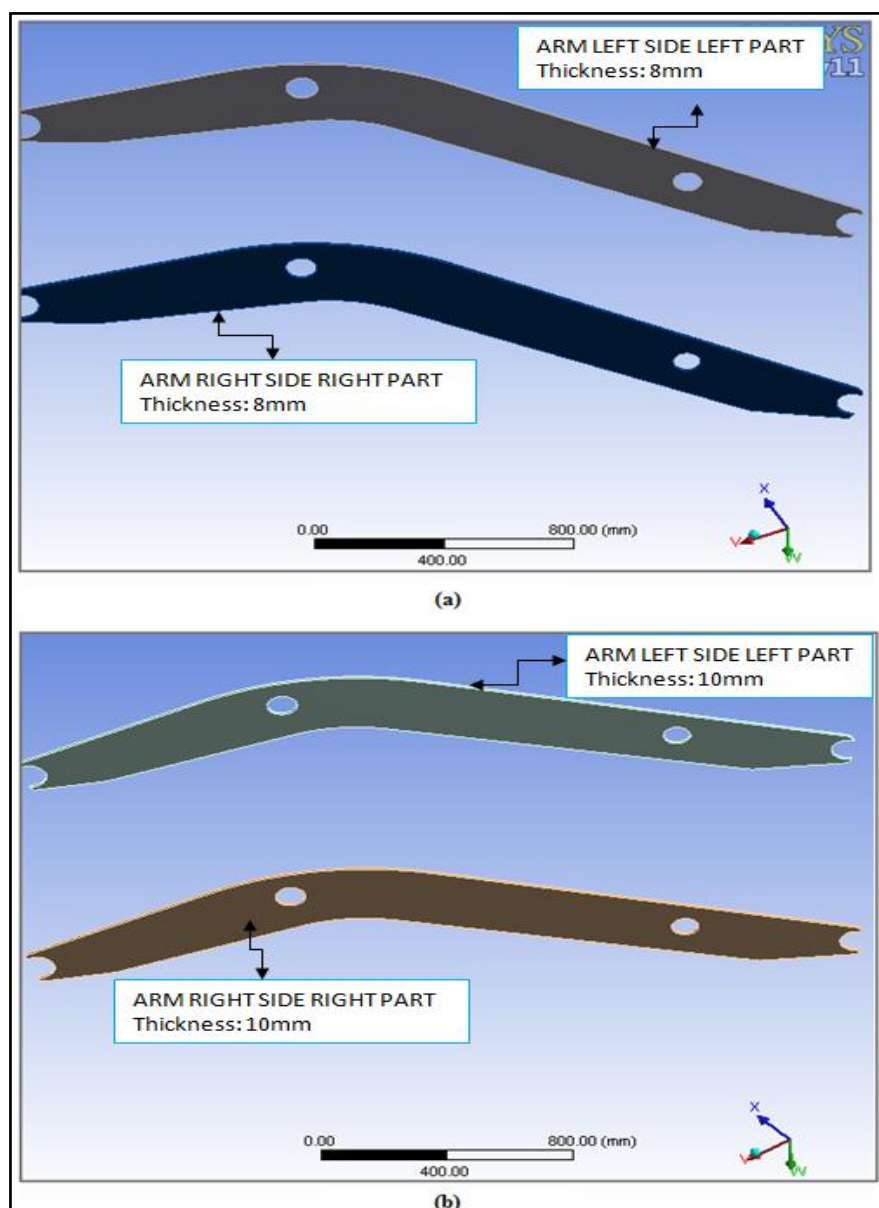
Figure 5.40 Arm right and left side parts. (a) Original arm right and left side parts. (b) Modified (improved) right and left side parts.
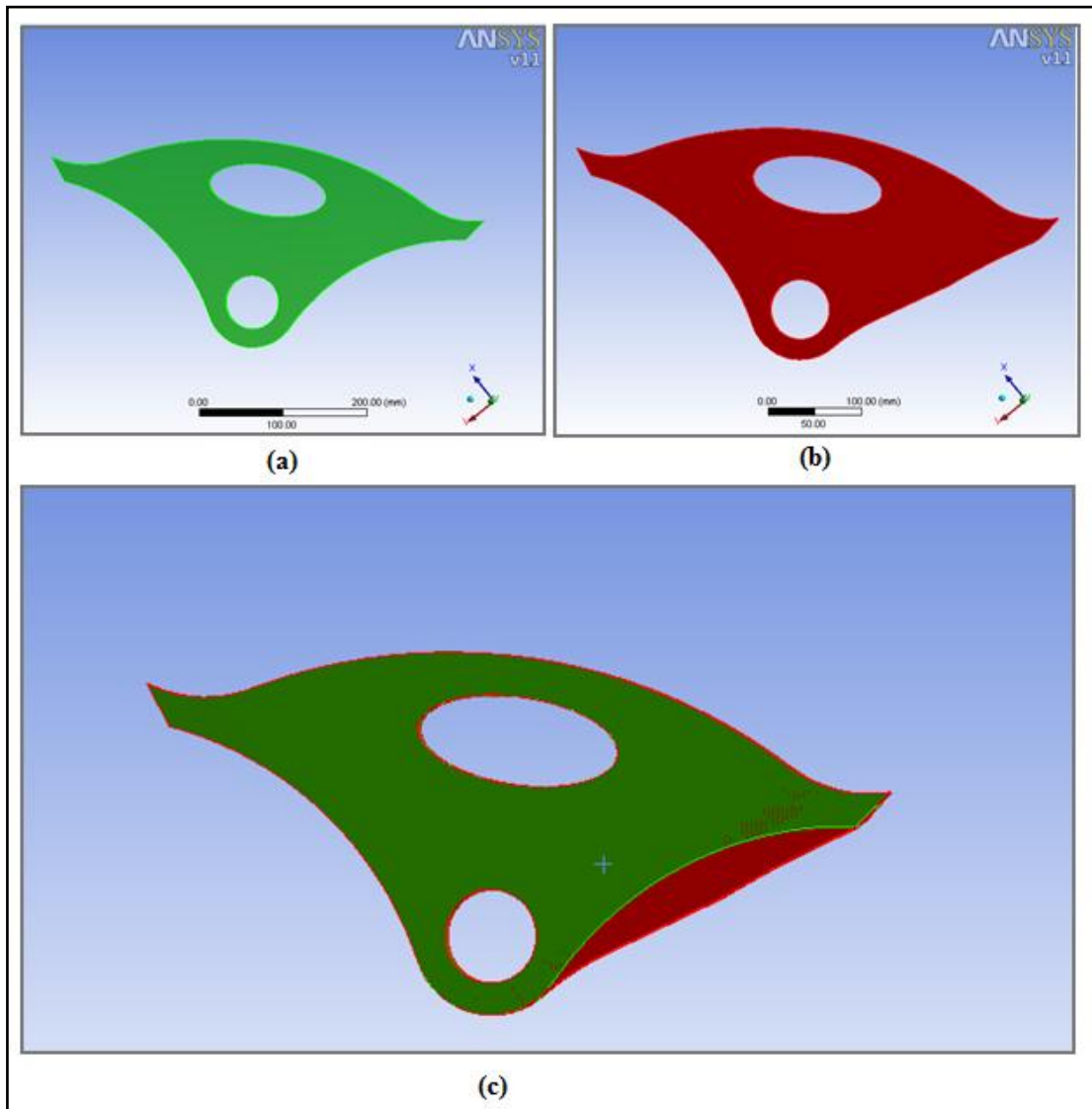
Figure 5.41 Arm support parts. (a) Original arm support (b) Modified (improved) arm support part (c) Original and modified arm support part together

5.4.6.2 Analysis Results of Front Arm for Each Loading Types with Improvements

Analysis results have been given for four different loading conditions and these are;

Analysis result of symmetrical loading while loader cylinder is active and with improvements;

With these improvement first analysis is done considering symmetrical loading while loader cylinder is active and the Equivalent (von-misses) stress distribution of loader is shown in figures 5.42 -5.45. These figures show maximum stress points of the loader arm with the applied boundary conditions. Maximum von-misses stress is reduced to 162 MPa from 182 MPa with improvements as seen figures 5.42-5.43.
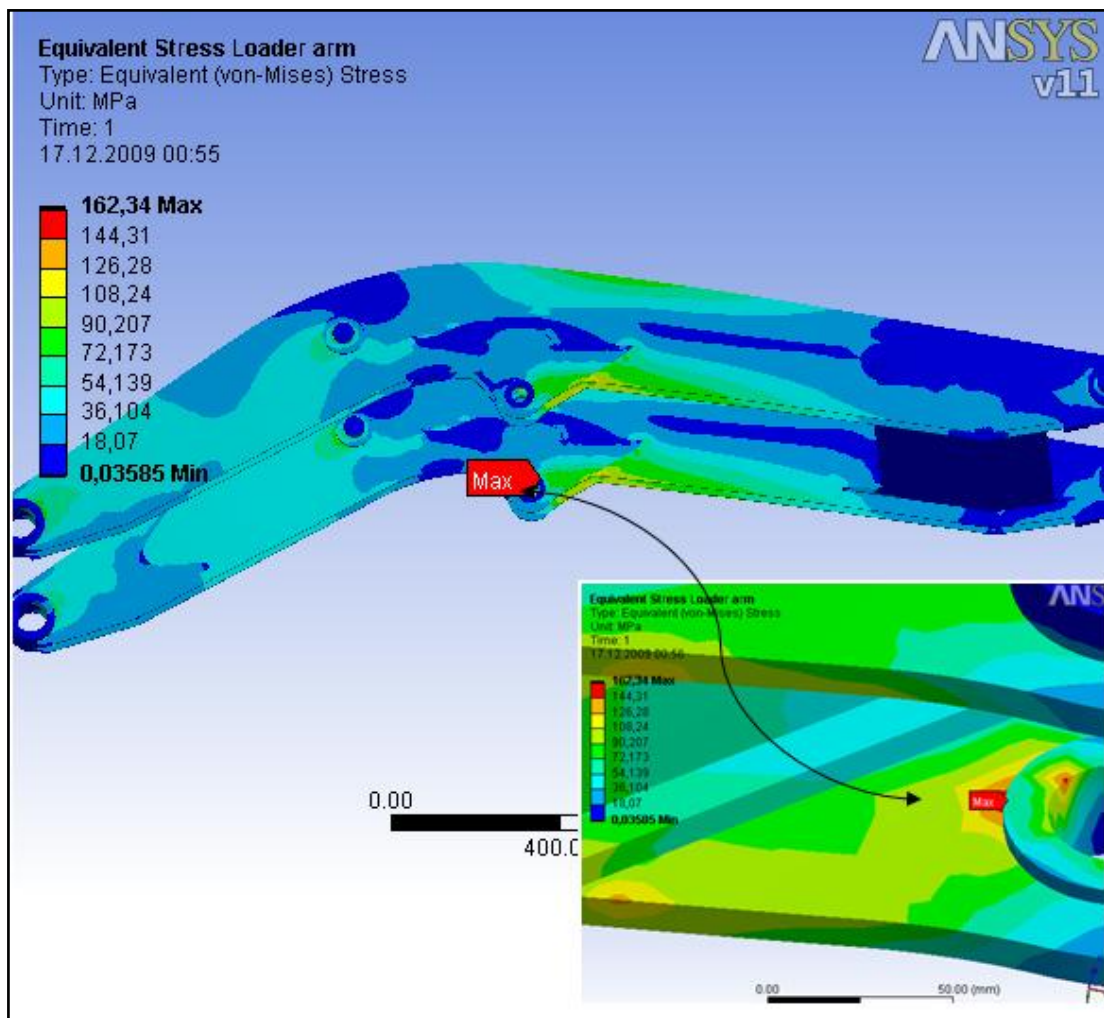
Figure 5.42 Equivalent stress distribution of loader arm
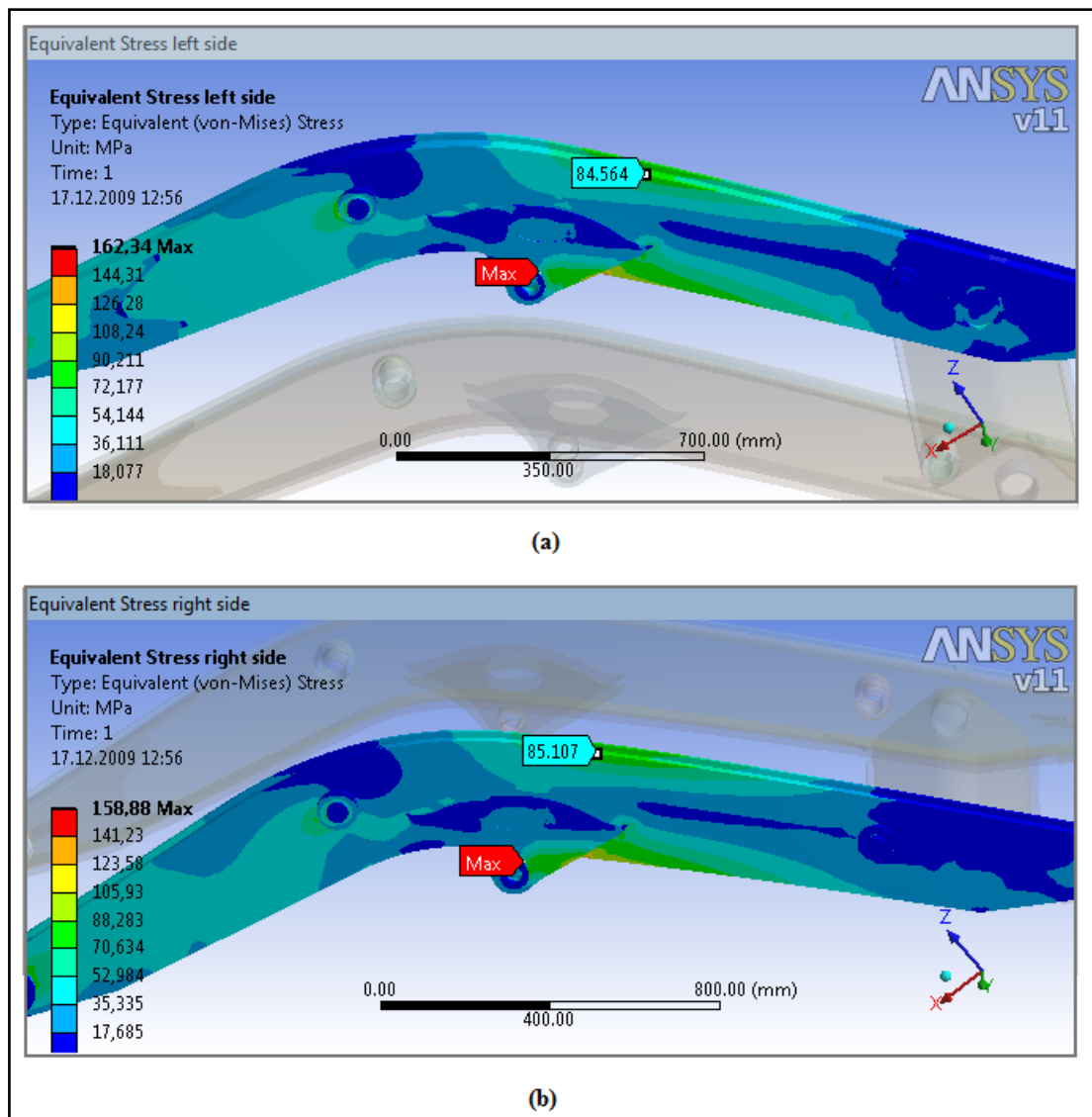
Figure 5.43 Equivalent stress distribution of **symmetrical** loading while **loader cylinder** is active and with new improvement. (a) Loader arm left side, (b) Loader arm side right side

Figure 5.43 shows the equivalent (von-misses) stress distribution of the right and left side of the loader arm with improvement. Stress distributions and values of stresses are symmetrical and maximum stress value is reduced to 162 MPa from 182 MPa.
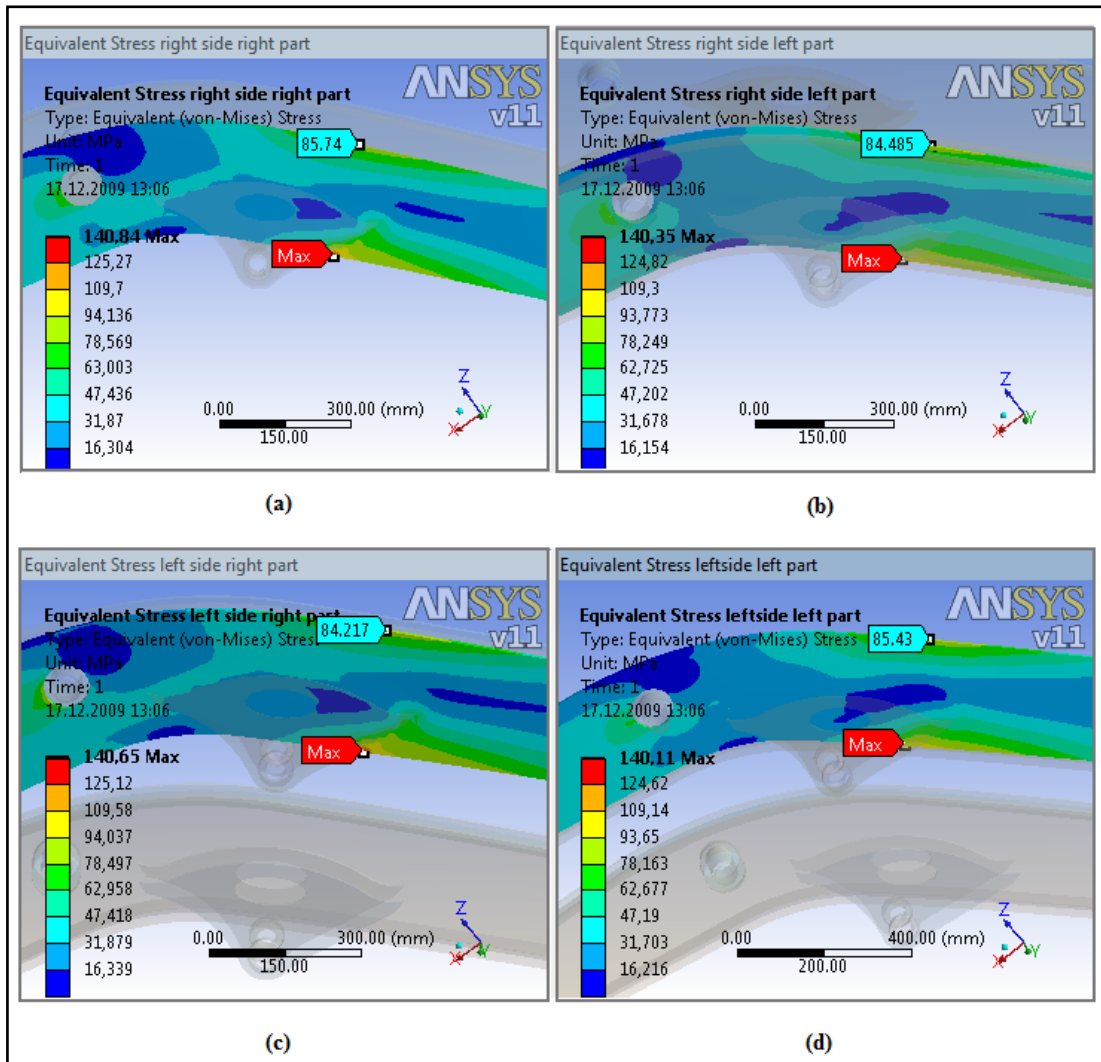
Figure 5.44 Equivalent stress distribution of **symmetrical** loading while **loader cylinder** is active with new **improvement**. (a) Loader arm right side right part, (b) Loader arm right side left part, (c) Loader arm left side right part, (d) Loader arm left side left part.

Figure 5.44 shows the equivalent (von-misses) stress distribution of the right and left parts of the loader arm with improvements.

Figure 5.45 shows the equivalent (von-misses) stress distribution of the supports for symmetrical loading with improvements. Stress distribution is symmetrical and maximum value is 162 MPa.

Figure 5.45 Equivalent stress distribution of **symmetrical** loading while **loader cylinder** is active with new improvement. (a) Loader arm right side right support, (b) Loader arm right side left support, (c) Loader arm left side right support, (d) Loader arm left side left support.

Analysis result of Unsymmetrical loading while loader cylinder is active and with improvements;

With these improvements secondly, the analysis considering unsymmetrical loading while loader cylinder is active is done and the Equivalent (von-misses) stress distribution of loader is shown in figures 5.46 -5.49. These figures show maximum stress points of the loader arm with the applied boundary conditions. Maximum von-misses stress is reduced to 262 MPa from 314 MPa with improvements.

Figure 5.46 Equivalent stress distribution of loader arm

Figure 5.47 Equivalent stress distribution of **unsymmetrical** loading while **loader cylinder** is active and with new improvement. (a) Loader arm left side, (b) Loader arm side right side

Figure 5.47 shows the equivalent (von-misses) stress distribution of the right and left side of the loader arm with improvements. For unsymmetrical loading, maximum stress is at the right side of the loader arm and its value is 262 MPa.

Figure 5.48 Equivalent stress distribution of **unsymmetrical** loading while **loader cylinder** is active with new **improvement**. (a) Loader arm right side right part, (b) Loader arm right side left part, (c) Loader arm left side right part, (d) Loader arm left side left part.

Figure 5.48 shows the equivalent (von-misses) stress distribution of the right and left parts of the loader arm with improvements. Maximum stress distribution is at the right and left part of the right side and its value is 262 MPa.

Figure 5.49 shows the equivalent (von-misses) stress distribution of the supports for unsymmetrical loading with improvements. Maximum stress distribution occurs at the right side supports and its value is 248 MPa.
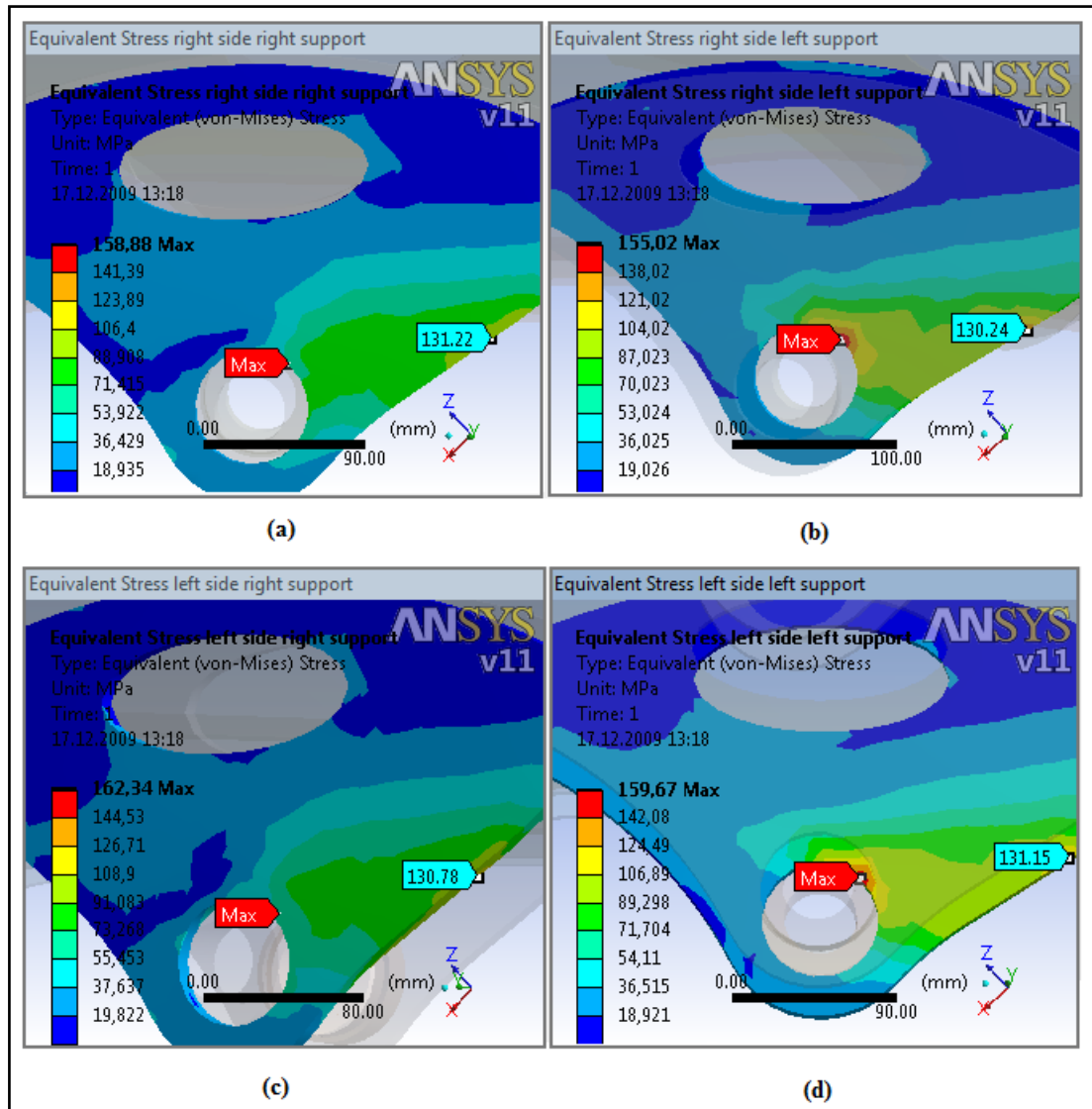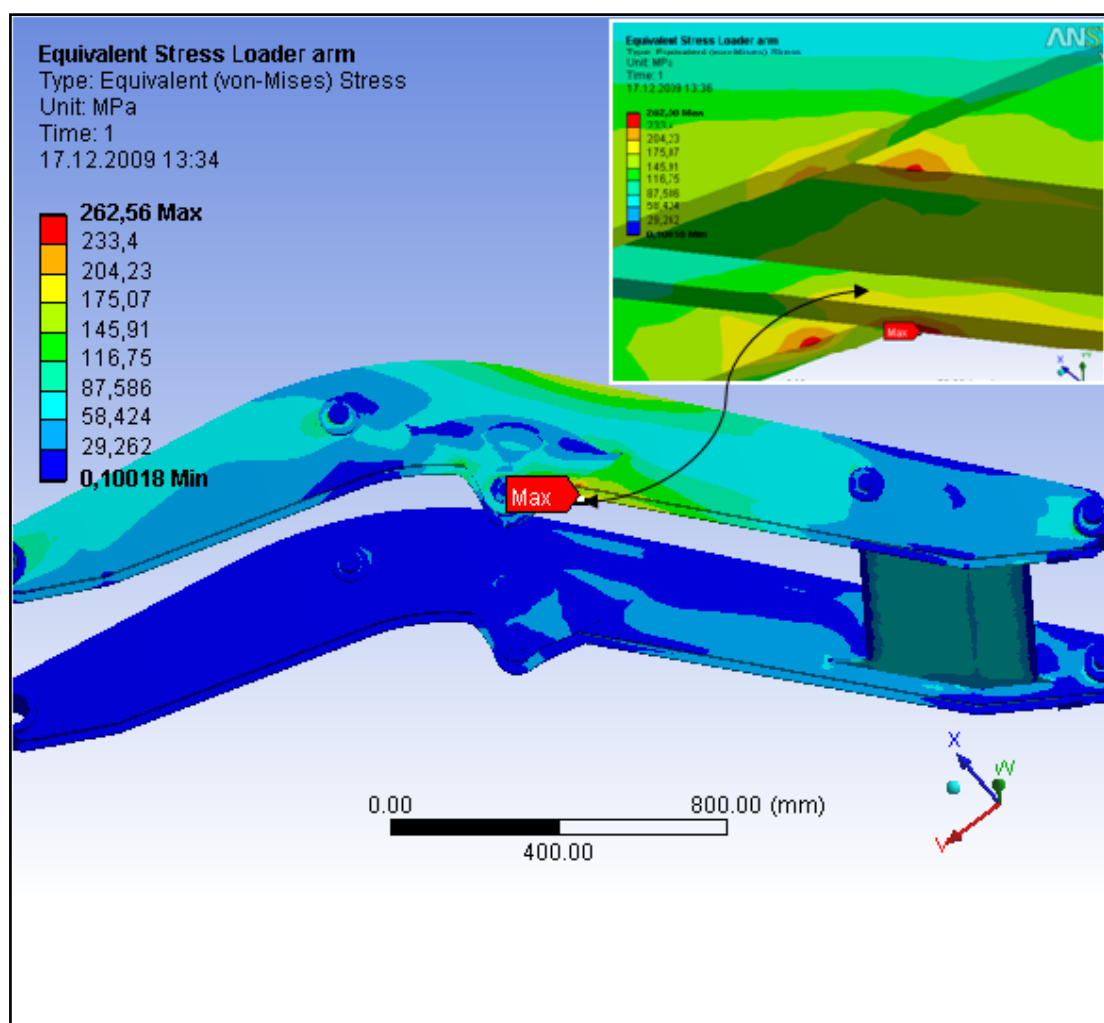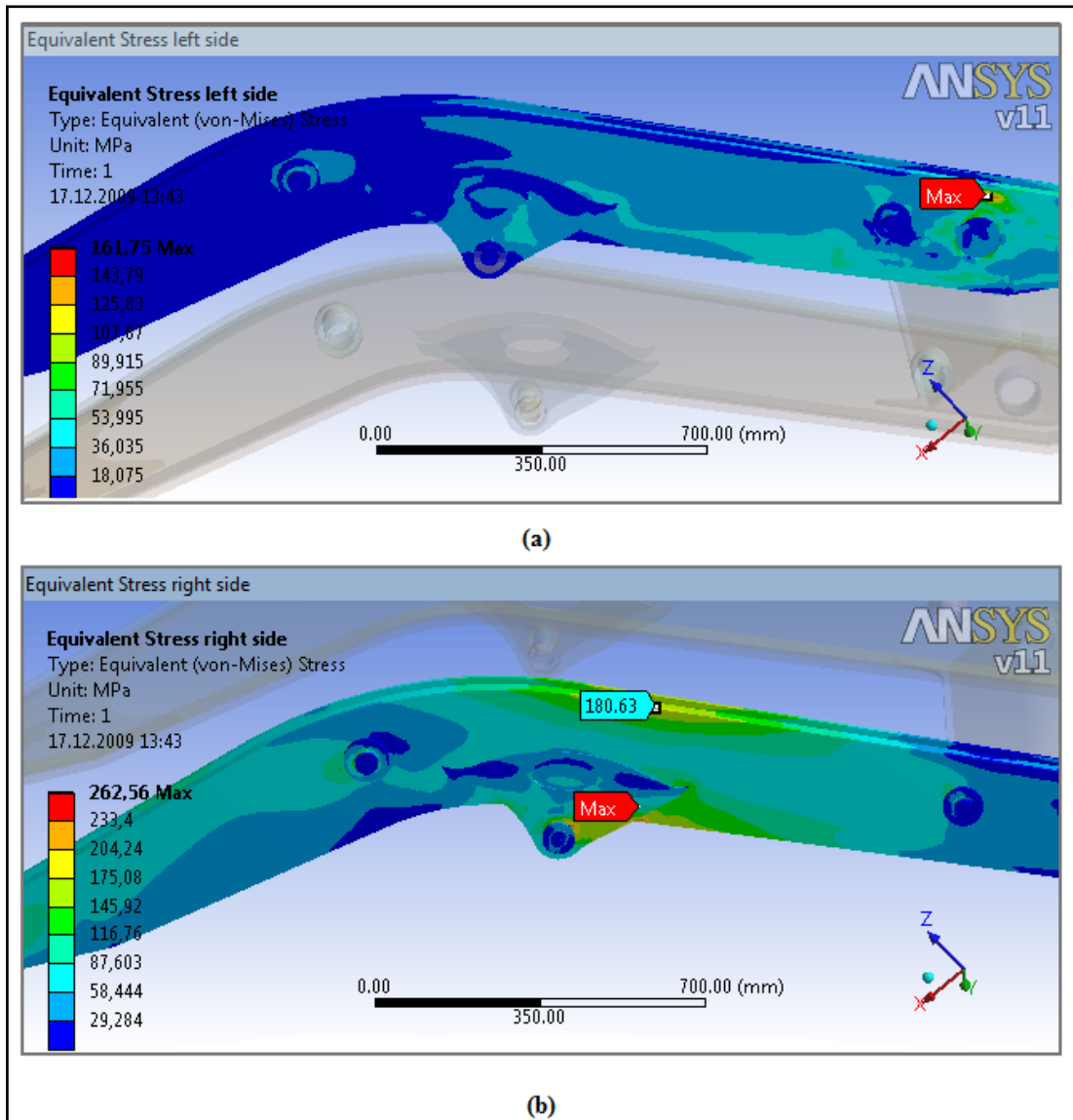
Figure 5.49 Equivalent stress distribution of **symmetrical** loading while **loader cylinder** is active with new improvement. (a) Loader arm right side right support, (b) Loader arm right side left support, (c) Loader arm left side right support, (d) Loader arm left side left support.

Analysis result of Symmetrical loading while Bucket cylinder is active and with improvements;

The analysis is done considering symmetrical loading while Bucket cylinder is active and the equivalent (von-misses) stress distribution of loader is shown in figures 5.50 -5.53. These figures show maximum stress points of the loader arm with the applied boundary conditions. Maximum von-misses stress is reduced to 144 MPa from 166 MPa with improvements.
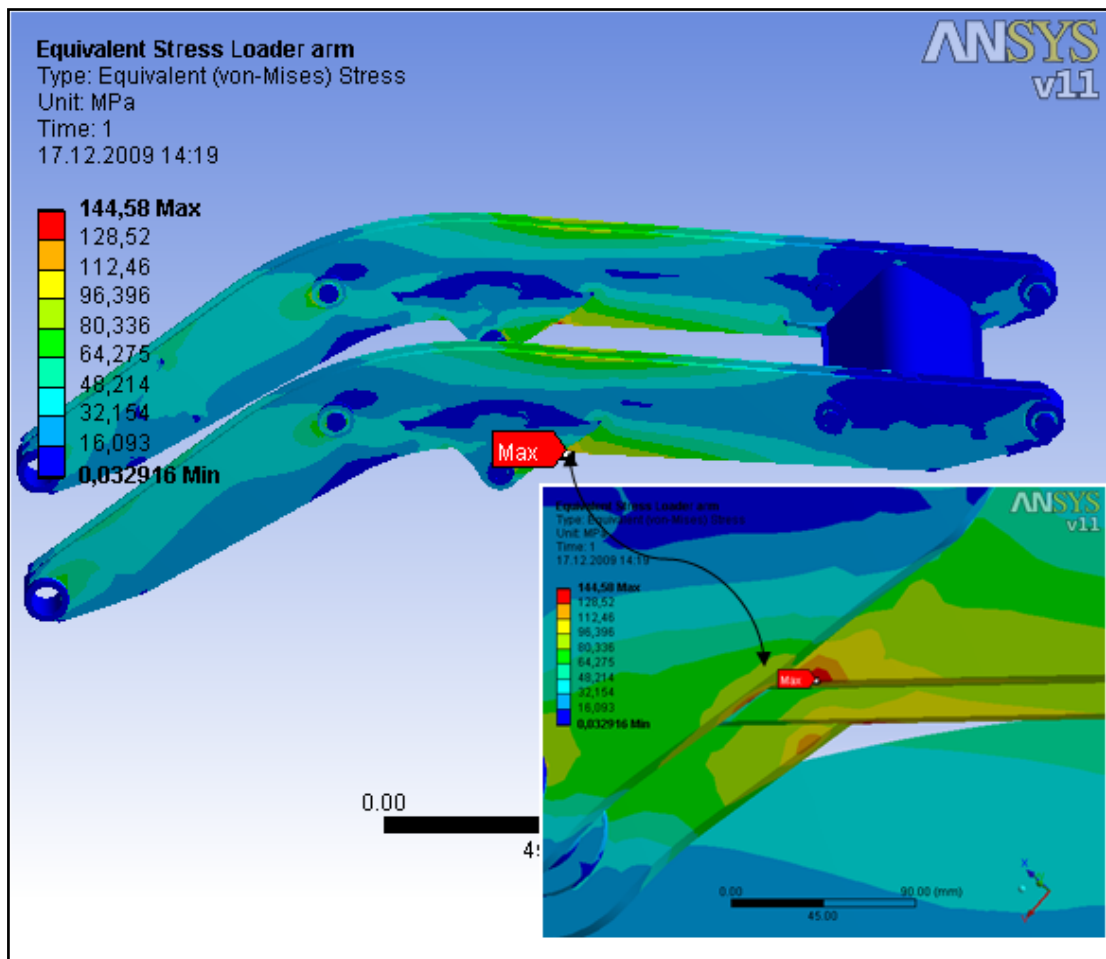
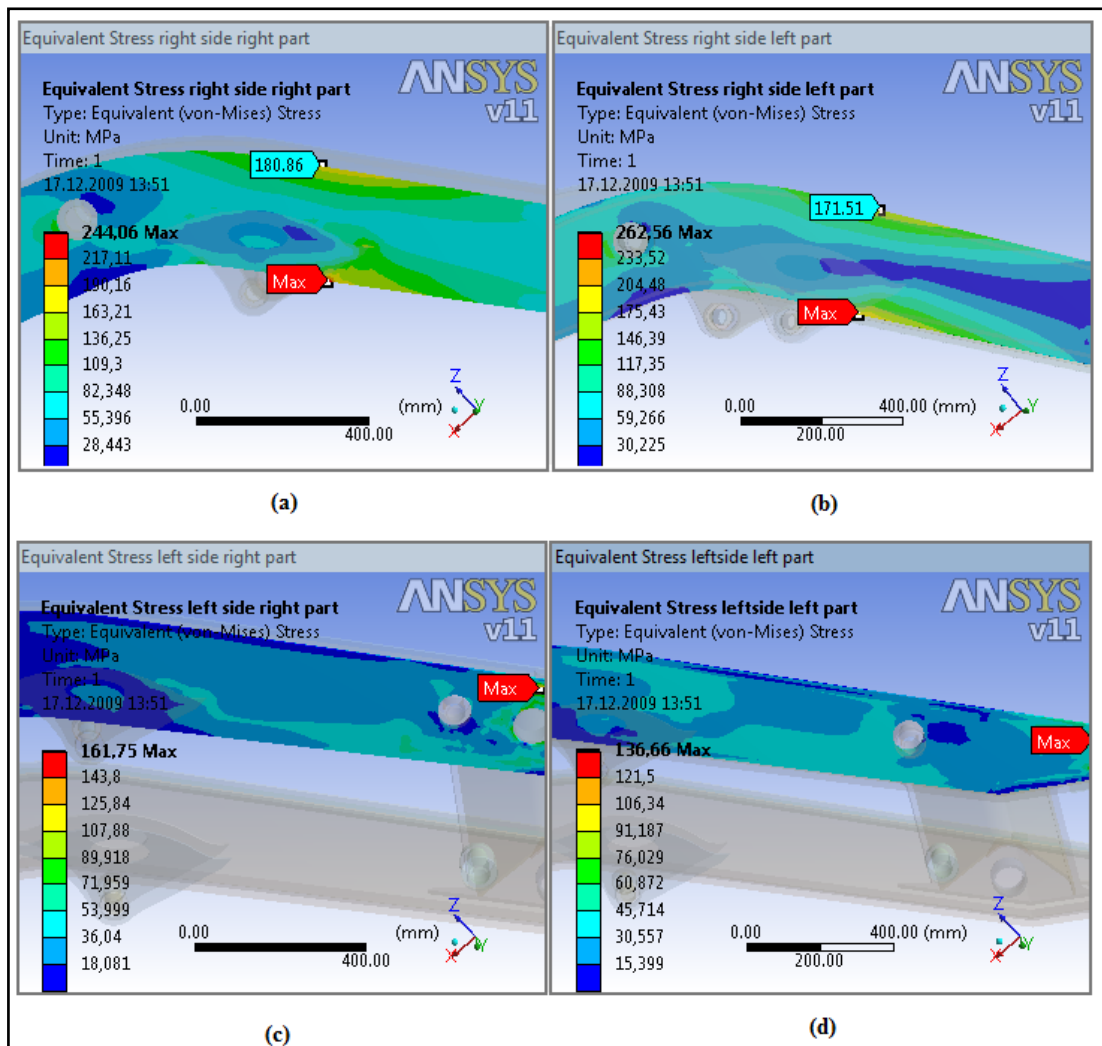**Figure 5.50** Equivalent stress distribution of loader arm

Figure 5.51 Equivalent stress distribution of **symmetrical** loading while **bucket cylinder** is active and with new improvement. (a) Loader arm left side, (b) Loader arm side right side

Figure 5.51 shows the equivalent (von-misses) stress distribution of the right and left side of the loader arm while bucket cylinder is active with improvement.
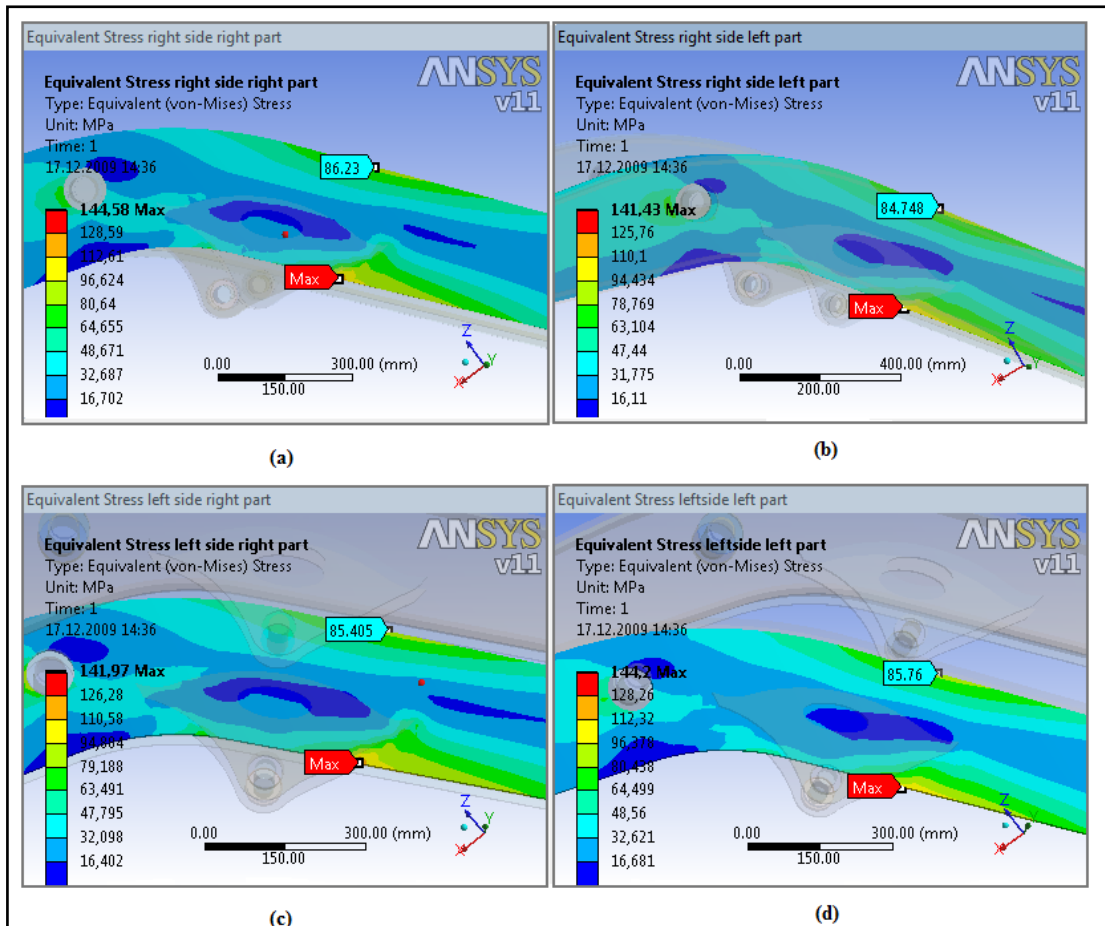
Figure 5.52 Equivalent stress distribution of **symmetrical** loading while **bucket cylinder** is active with new **improvement**. (a) Loader arm right side right part, (b) Loader arm right side left part, (c) Loader arm left side right part, (d) Loader arm left side left part.
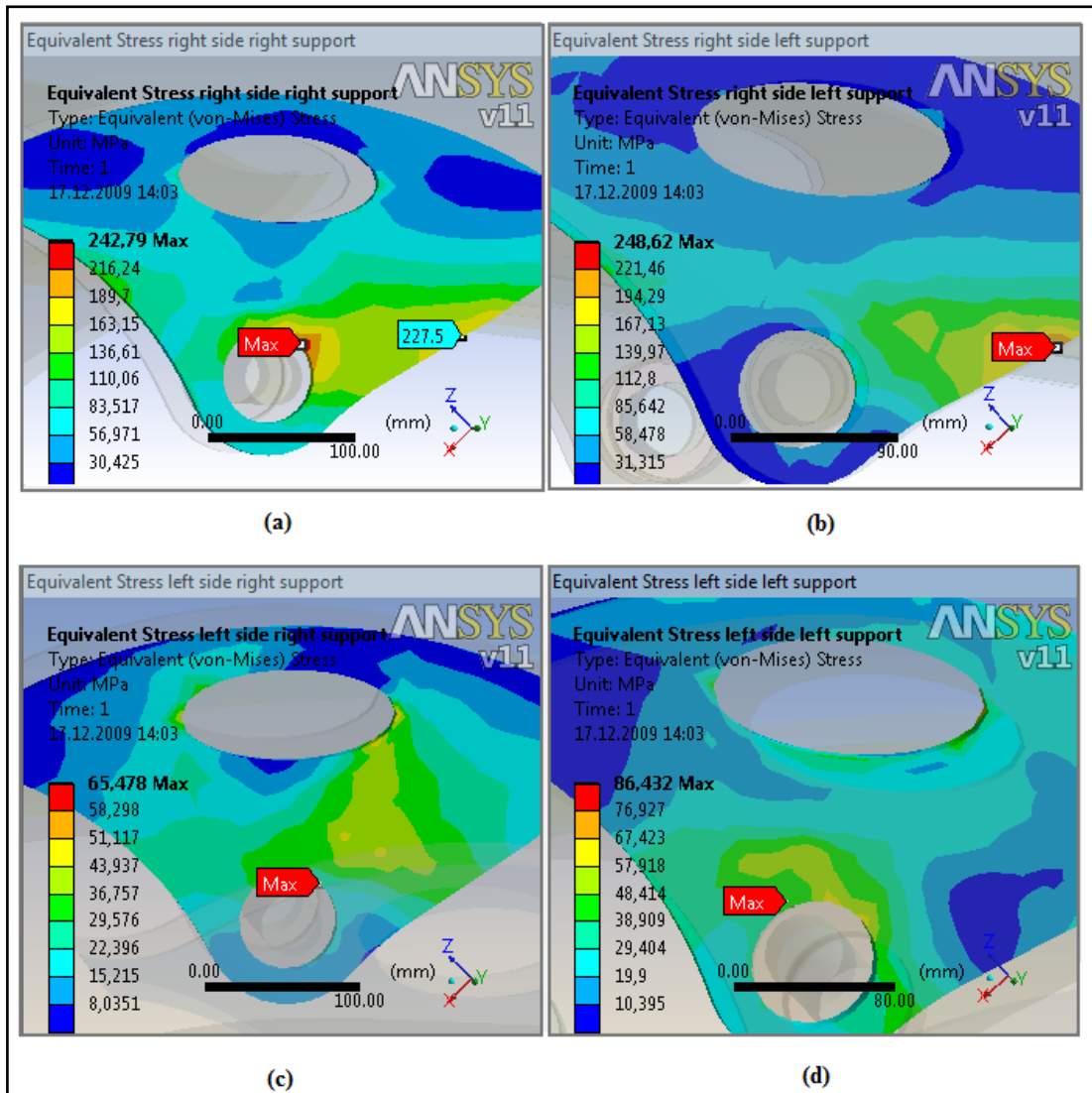
Figure 5.52 shows the equivalent (von-misses) stress distribution of the right and left parts of the loader arm with improvements.

Figure 5.53 shows the equivalent (von-misses) stress distribution of the supports for symmetrical loading with improvements. Stress distribution is symmetrical and maximum value is 133 MPa.

Figure 5.53 Equivalent stress distribution of **symmetrical** loading while **bucket cylinder** is active with new improvement. (a) Loader arm right side right support, (b) Loader arm right side left support, (c) Loader arm left side right support, (d) Loader arm left side left support.

Analysis result of Unsymmetrical loading while Bucket cylinder is active and with improvements;

The analysis is done considering unsymmetrical loading while bucket cylinder is active and the equivalent (von-misses) stress distribution of loader is shown in figures 5.54-5.57. These figures show maximum stress points of the loader arm with the applied boundary conditions. Maximum von-misses stress is reduced to 268 MPa from 322 MPa with improvements.

Figure 5.54 Equivalent stress distribution of loader arm

Figure 5.55 Equivalent stress distribution of **unsymmetrical** loading while **bucket cylinder** is active and with new improvement. (a) Loader arm left side, (b) Loader arm side right side
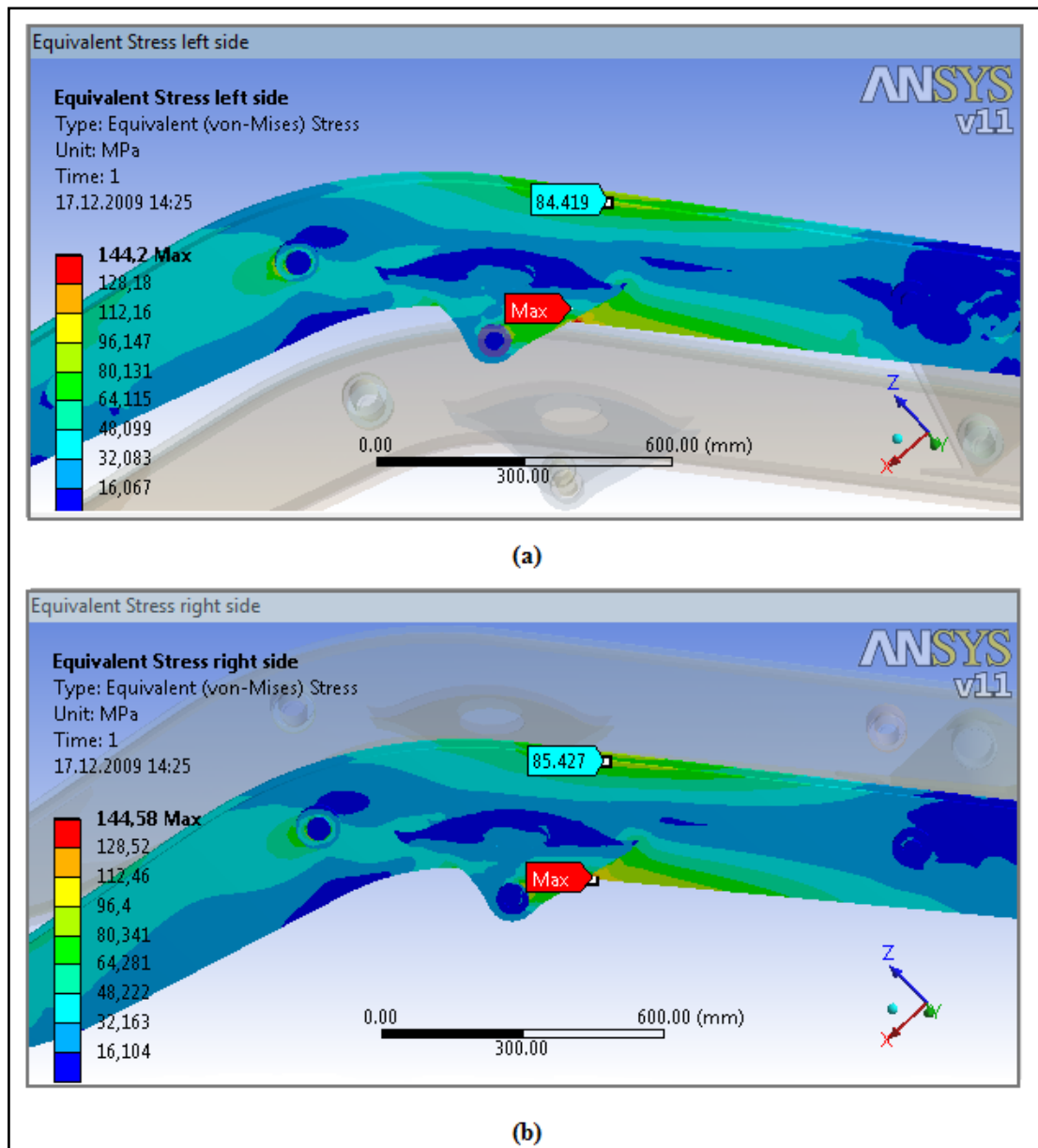
Figure 5.55 shows the equivalent (von-misses) stress distribution of the right and left side of the loader arm with improvements. For unsymmetrical loading, maximum stress is at the right side of the loader arm and its value is reduced to 268 MPa from 322 MPa.
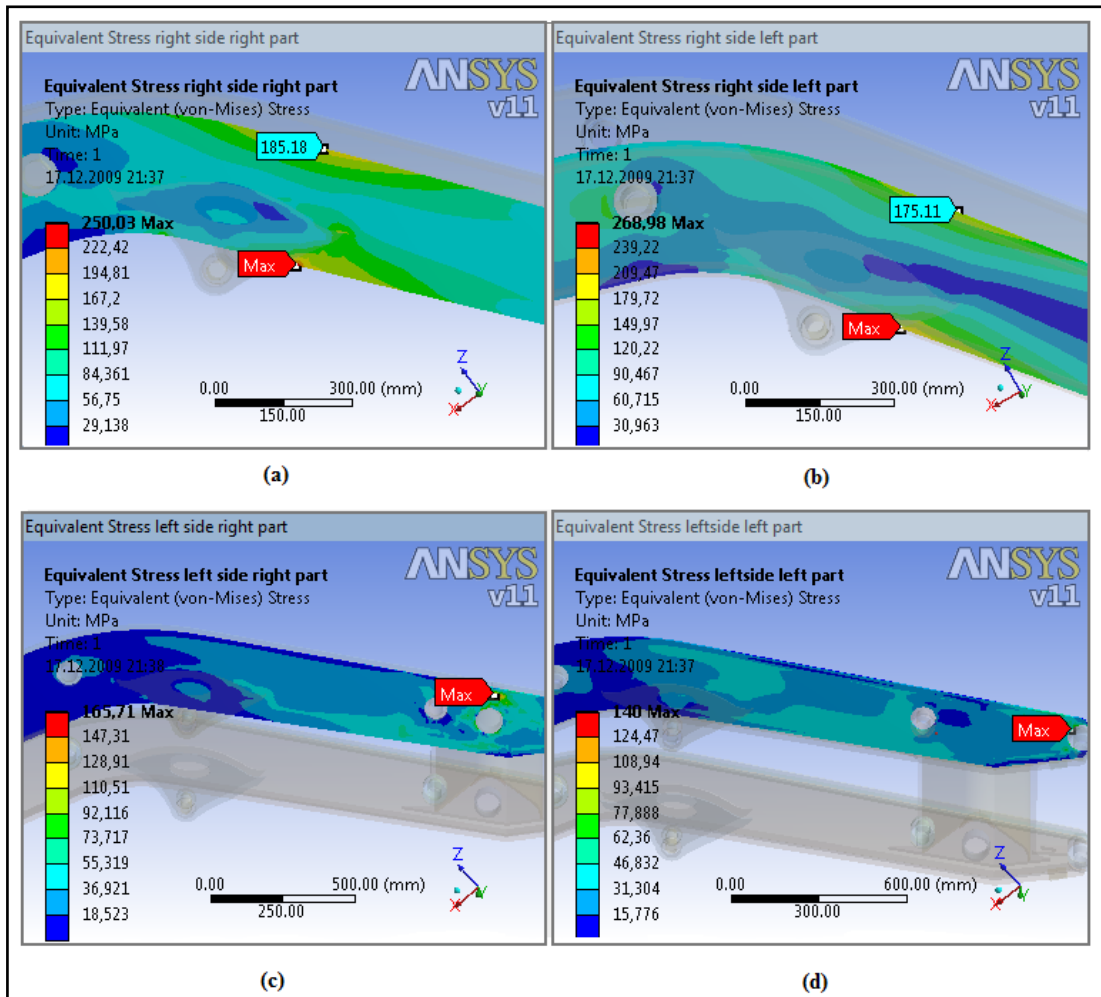
Figure 5.56 Equivalent stress distribution of **unsymmetrical** loading while **bucket cylinder** is active with new **improvement**. (a) Loader arm right side right part, (b) Loader arm right side left part, (c) Loader arm left side right part, (d) Loader arm left side left part.

Figure 5.56 shows the equivalent (von-misses) stress distribution of the right and left parts of the loader arm with improvements. Maximum stress distribution is at the right and left part of the right side and its value is 268 MPa.

Figure 5.57 shows the equivalent (von-misses) stress distribution of supports for unsymmetrical loading with improvements. Maximum stress distribution occurs at the right side supports and its value is 254 MPa.
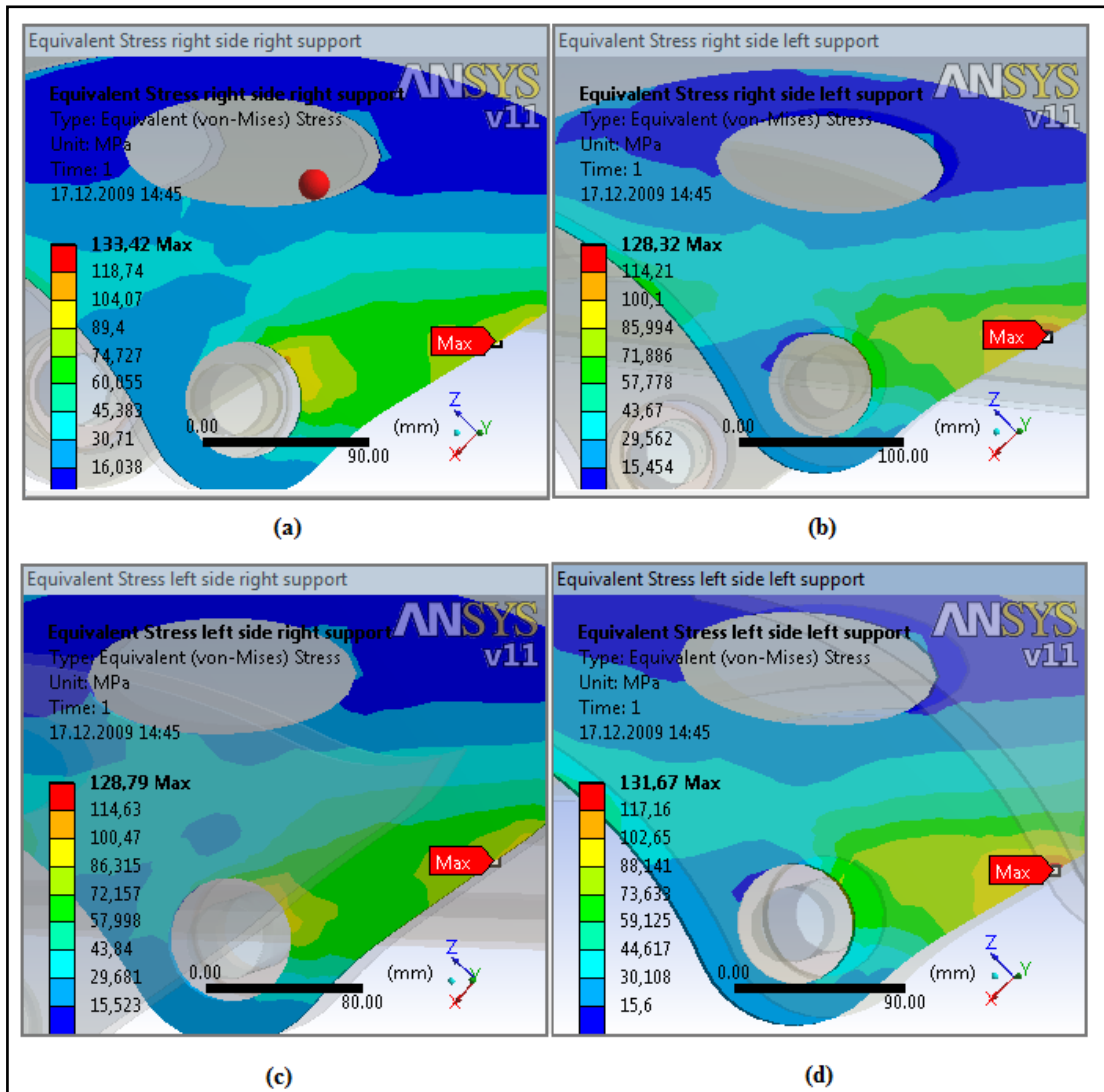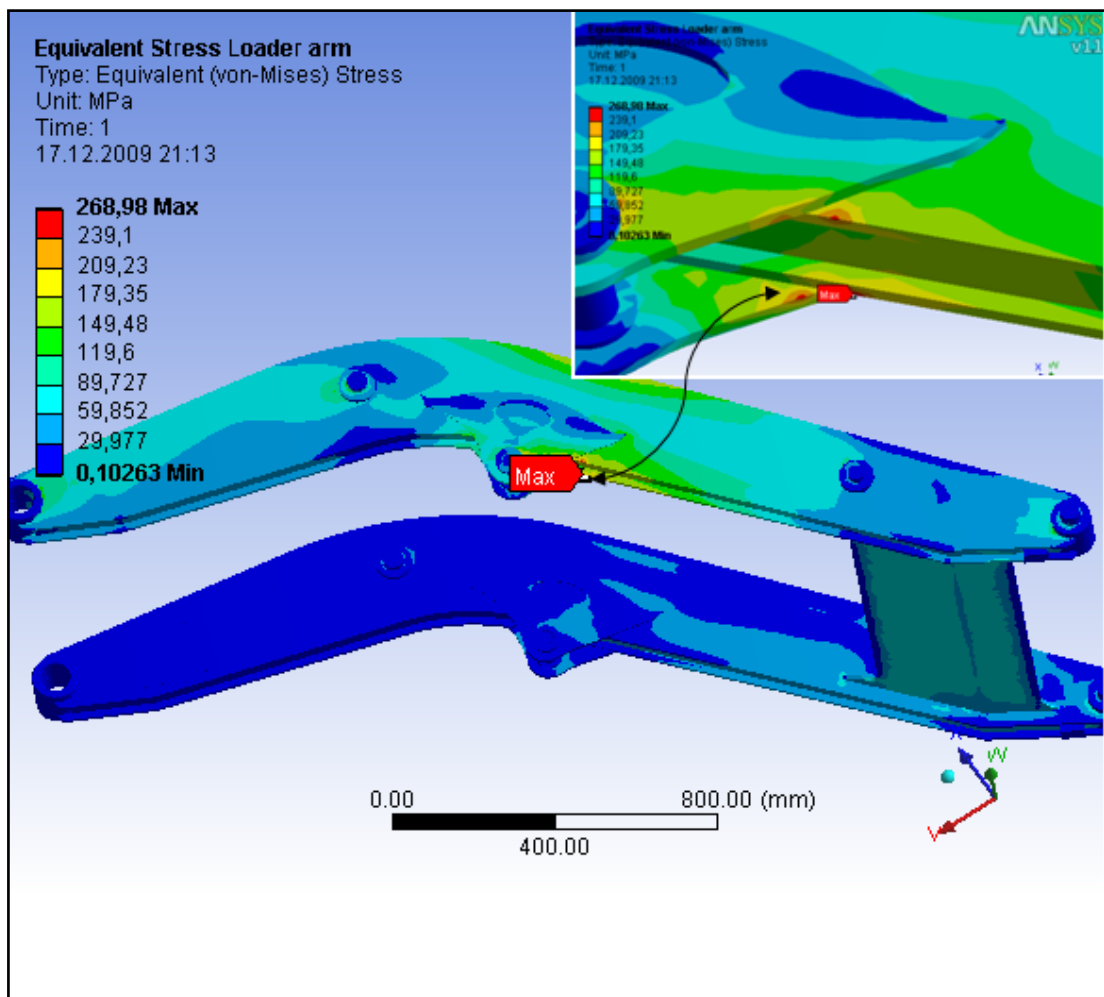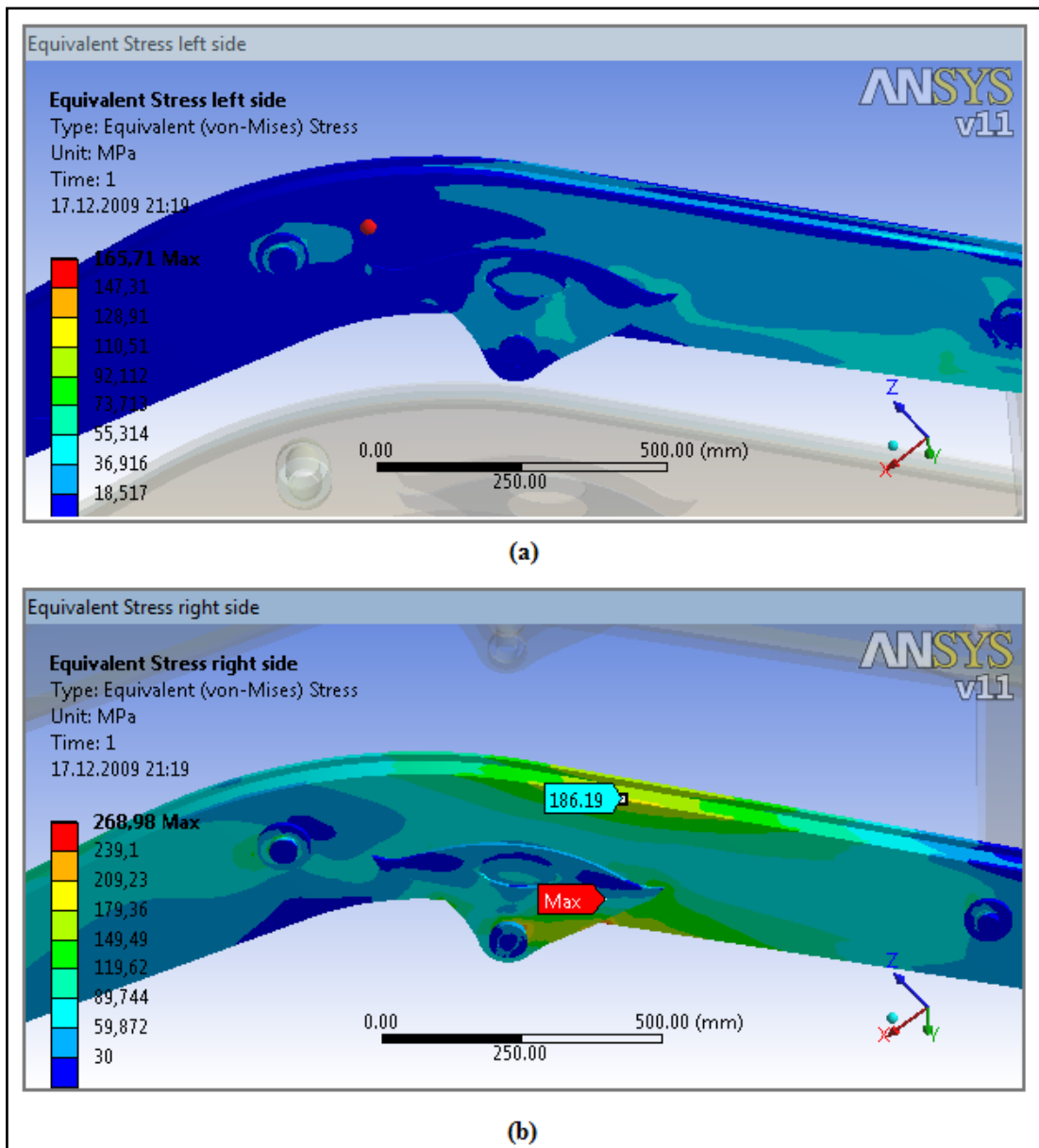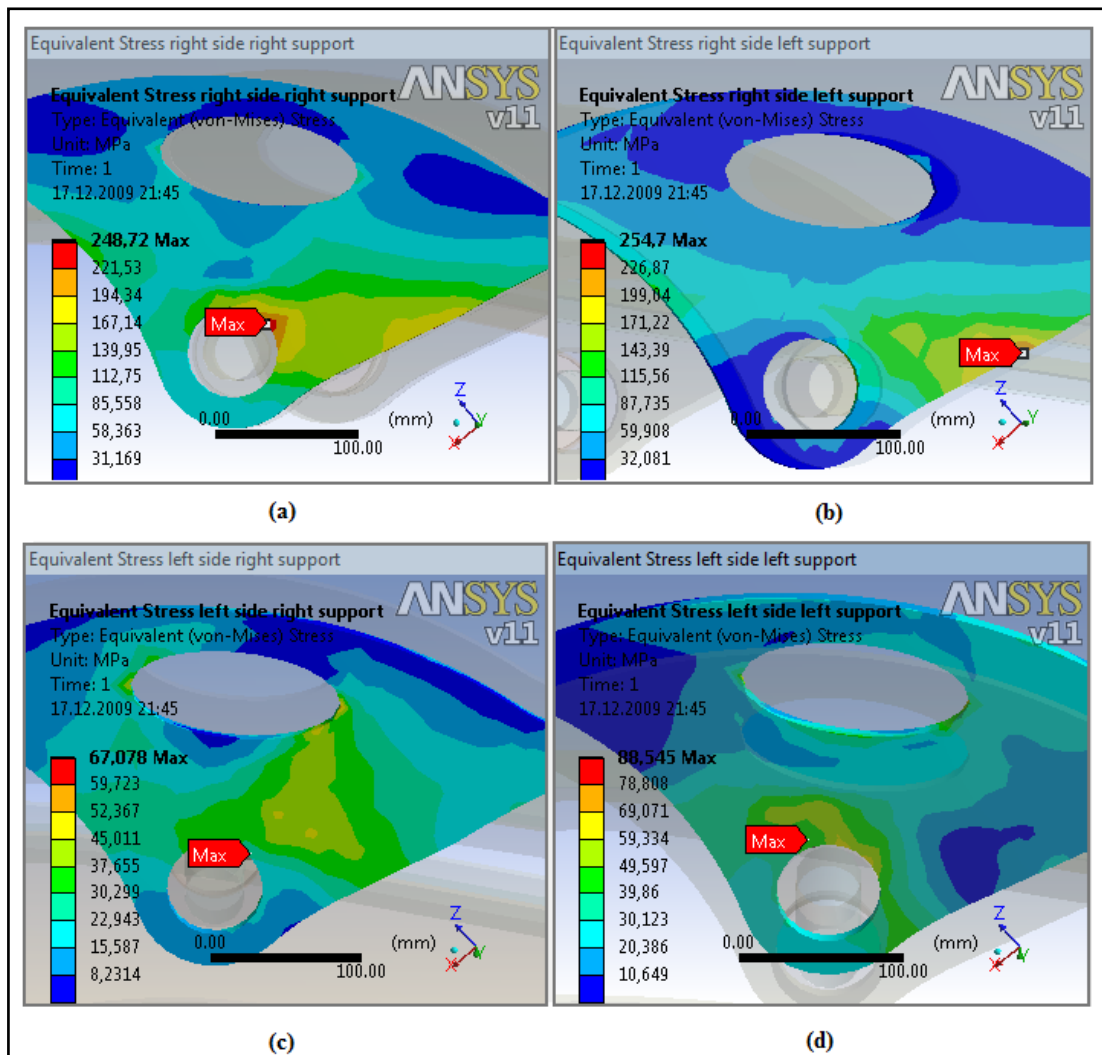
Figure 5.57 Equivalent stress distribution of **unsymmetrical** loading while **Bucket cylinder** is active with new improvement. (a) Loader arm right side right support, (b) Loader arm right side left support, (c) Loader arm left side right support, (d) Loader arm left side left support.

Maximum stress values and their locations are given in the table 5.2 for while loader cylinder is active and in the table 5.3 maximum stress values and location have been given for while bucket cylinder is active. As seen in the table 5.2, while loader cylinder is active and after improvements the maximum stress is reduced to 162.34 MPa from 182.62 MPa for symmetrical loading and reduced to 262.56 MPa from 314.69 MPa for unsymmetrical loading. While bucket cylinder is active the maximum stress is reduced to 144.58 MPa from 166.53 MPa for symmetrical loading and reduced to 268.98 MPa from 322.39 MPa for unsymmetrical loading as shown in the table 5.3.

Table 5.2 Comparisons of maximum stress points of original front arm and improved arm for each loading types while loader cylinder is active.

	While Loader Cylinder is active			
	Symmetrical	Symmetrical with **new improvements.**	Unsymmetrical	Unsymmetrical with **new improvements.**
Maximum stress (MPa)	182.62	**162.34**	314.69	**262.56**
Bodies maximum stress occurs	Arm support part shown figures(5.23 and 5.26 (d))	Arm support part shown figures(5.42 and 5.45(c))	Arm support part shown figures(5.27 and 5.30 (b))	Arm right side left part shown figures (5.46 and 5.48 (b))

Table 5.3 Comparisons of maximum stress points of original front arm and improved arm for each loading types while bucket cylinder is active

	While Bucket Cylinder is active			
	Symmetrical	Symmetrical with **new improvements.**	Unsymmetrical	Unsymmetrical with **new improvements.**
Maximum stress (MPa)	166.53	**144.58**	322.39	**268.98**
Bodies maximum stress occurs	Arm right side right part shown figures (5.31 and 5.33 (a))	Arm right side right part shown figures (5.50 and 5.52 (a))	Arm support part shown figures (5.34 and 5.38 (b))	Arm right side left part shown figures (5.54 and 5.56 (b))

5.4.7 Safety Factor

ANSYS Workbench can show contour plot of the factor of safety. Figure 5.58 shows safety factors of front arm before improvement and after improvement at the symmetrical loading while loader cylinder is active. As seen from the figure safety factor has increased to 2.18 from 1.94. Figure 5.59 shows safety factors of front arm before improvement and after improvement at the unsymmetrical loading while bucket cylinder is active. As seen from the figure safety factor has increased to 1.32 from 1.10.
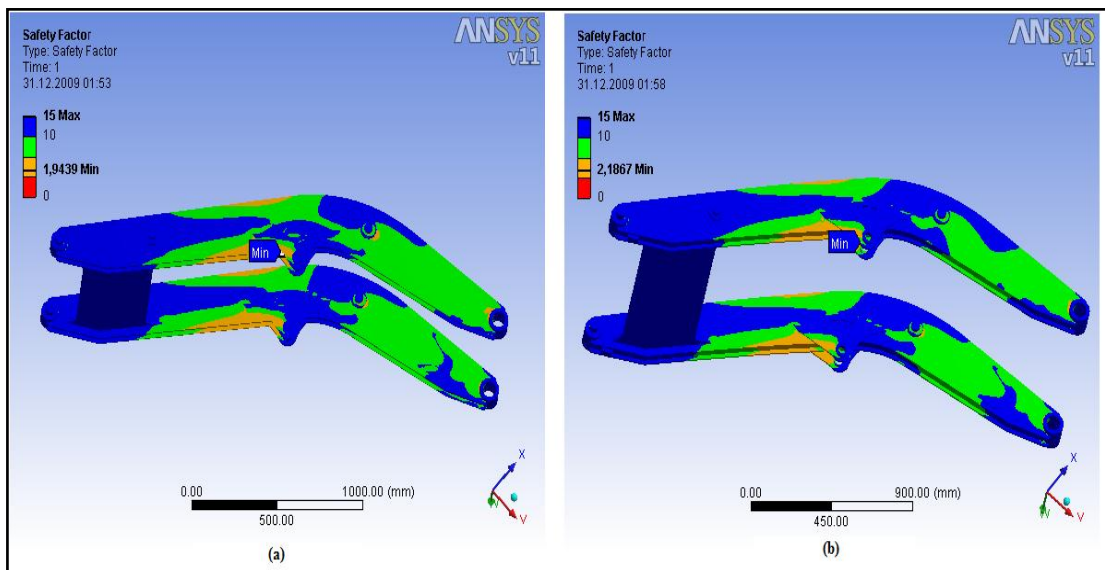
Figure 5.58 Safety Factors of symmetrical loading while loader cylinder is active with new improvement. (a) Before improvement, (b) After improvement
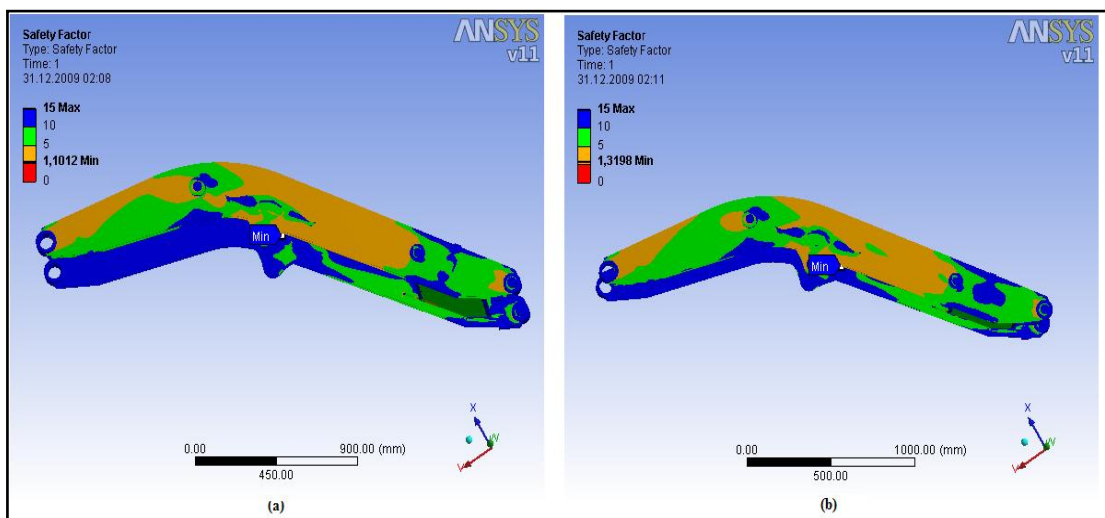
Figure 5.59 Safety Factors of unsymmetrical loading while bucket cylinder is active with new improvement. (a) Before improvement, (b) After improvement

5.4.8 Conclusion on Front Arm

In this chapter, firstly static forces calculated by doing static forces analysis. Then calculated forces used in the FEA. The front arm has been analyzed with four different conditions which are namely, symmetrical and unsymmetrical loading while loader cylinder is active and symmetrical and unsymmetrical loading while bucket cylinder is active.

Then FEA has been carried out in order to find maximum stress values and locations on front arm. Equivalent (von-misses) stress distribution of the front arm is shown in section 5.3.6.1. After improvements while loader cylinder is active, the maximum stress is reduced to 162.34 MPa from 182.62 MPa for symmetrical loading and reduced to 262.56 MPa from 314.69 MPa for unsymmetrical loading. Also while bucket cylinder is active the maximum stress is reduced to 144.58 MPa from 166.53 MPa for symmetrical loading and reduced to 268.98 MPa from 322.39 MPa for unsymmetrical loading. For front arm safety factor has been increased to 2.18 from 1.94 at the symmetrical loading while loader cylinder is active. Safety factor have been increased to 1.32 from 1.10 at the unsymmetrical loading while bucket cylinder is active.

CHAPTER 6

CONCLUSIONS

The backhoe-loader back arm and front arm have been analyzed with maximum load and boundary conditions by using FEM. ANSYS workbench FEA program has used to carry out analysis. Both for back arm and front arm firstly static force analyses have been carried out and the forces calculated as results of these analyses are used in FEA. Different loading conditions are examined in the analyses. Symmetrical and unsymmetrical boundary conditions for both loading types have been examined for front arm.

With respect to analyses results some improvement have been done and comparisons of stress results and safety factors of original arms and improved arms have been carried out both for front and back arm. Safety factor is increased 1.98 from 1.59 for back arm. Strength of the back arm has been increased in 24.5 %. For front arm safety factor has been increased to 2.18 from 1.94 at the symmetrical loading while loader cylinder is active. Strength has been increased in 12.37 %. Safety factors have been increased to 1.32 from 1.10 at the unsymmetrical loading while bucket cylinder is active. Strength of front arm has been increased in 20 %.

Also comparisons of breakout forces and reaction forces of FEA results and static force calculations have been carried out to see reasonability of the analyses. These results have been shown that the reaction forces and maximum breakout forces are nearly the same values.

These analyses and results show critical points of designed parts. FEA can be used to improve our design before doing prototypes.

FUTURE WORKS

In this study, back arm and front arm of Backhoe-loader have been analyzed with FEM. Analyses can be extended by doing analysis of other parts of Backhoe-loader such as back boom, back and front buckets and lever links. Also lateral forces which come from the swinging cylinders can be added to see its affects.

In this study, pins and links are assumed as rigid. Analyses can be repeated with deformable pins and links.

Also results should be supported by doing experimental test and analysis.

REFERENCES

[1]   Özer S., kazıcı-yükleyicilerde kazma mesafesine bağlı olarak bom-stik grubunun tasarımı, a Major Project Report for the Degree of Master of Science in Mechanical Engineering, Mersin University, 2007

[2]   Yener M., Design of Computer Interface for Automatic Finite Element Analysis of Excavator Boom, a Major Project Report for the Degree of Master of Science in Mechanical Engineering, Middle East Technical University, 2005

[3]   Dağ S., Fıçıcı F., Geniş K, İş Makinelerinde Kırılma ve Yorulma Problemlerinin Sonlu Elemanlar Yöntemiyle İncelenmesi, Mühendis ve Makina Cilt : 48 Sayı: 571

[4]   Çetin B., design of a demolition boom, a Major Project Report for the Degree of Master of Science in Mechanical Engineering, Middle East Technical University, 2007

[5]   Smolnicki T., Derlukiewicz D., Stańcoe M. StańcoE (2008), Evaluation of load distribution in the superstructure rotation joint of single-bucket caterpillar excavators, Journal of Automation in Construction, **17**, 218-223

[6]   Bosnjak S., Petkovic Z., Zrnic N., Simic G. and Simonovic A. (2009). Cracks, repair and reconstruction of bucket wheel slewing excavator platform, *Eng Fail Anal*, doi:10.1016/j.engfailanal.2008.11.009

[7]   Karamolla M., kule vinçlerin matematik modellemesi, a Major Project Report for the Degree of doctor of philosophy in Mechanical Engineering, Celal Bayar University, 2005

[8]   Bosnjak S., Petkovic Z., Zrnic N., Simic G. and Simonovic A. (2009).Cracks, repair and reconstruction of bucket wheel slewing excavator platform, journal of *Engineering Failure Analysis*, **16**, 740-750

[9]   Rusinski E., Czmochowski J., Moczki P. (2006). Numerical and Experimental Analysis of a Mine's Loader Boom Crack, Journal of *Achievements of Materials and Manufacturing Engineering*, **17**, Issue 1-2, 273-276

[10]   Çolpan A. C., Lastik Tekerlekli Yükleyicilerin taşıyıcı kol tasarımının iyileştirilmesi, a Major Project Report for the Degree of Master of Science in Mechanical Engineering, The University of Gebze Yüksek Teknoloji Enstitüsü, 2007

[11]   Karahan M., İki kademeli teleskopik vincin tasarım ve sonlu eleman analizi, a Major Project Report for the Degree of Master of Science in Mechanical Engineering, The University of Atatürk, 2007

[12]   Karlinski J., Rusinski E., Smolnicki T. (2008). Protective structures for construction and mining machine operators, Journal of *Automation in Construction* **17**, 232-244

[13]   Derlukiewicz D., Przybylek G. (2008). Chosen aspects of FEM strength analysis of telescopic jib mounted on mobile platform, Journal of *Automation in Construction*, **17**, 278-283

[14]   Bayrakceken H., Tasgetiren S., Yavuz I. (2007). Two cases of failure in the power transmission system on vehicles: A universal joint yoke and a drive shaft, journal of *Engineering Failure Analysis*, **14**, 716-724

[15]   Miralbes R., Castejon L. (July 1-3 2009). Design and Optimization of Crane Jibs for Forklift Trucks, *Proceedings of the World Congress Analysis*, **2**, London, U.K

[16]   Kalkan E., Tractor güvenlik kabini statik yükleme deneylerinin sonlu elemanlar yöntemi ile incelenmesi, a Major Project Report for the Degree of Master of Science in Mechanical Engineering, The University of Sakarya, 2007

[17]   ANSYS   workbench-platform   documentation   for   ANSYS Workbench,*www.ansys.com/assets/brochures/workbench-platform-12.0.pdf,*

 [18]   ANSYS User's Manual, Release 11.0 documentation for ANSYS Workbench.

[19]   Chunjun P., Static analysis of rolling bearings using finite element method, a Major Project Report for the Degree of Master of Science in Mechanical Engineering, Stuttgart University, 2009

[20]   ANSYS User's Manual, Release 11.0 documentation for ANSYS.